



COCORA 2013

The Third International Conference on Advances in Cognitive Radio

ISBN: 978-1-61208-267-7

April 21 - 26, 2013

Venice, Italy

COCORA 2013 Editors

Silvian Spiridon, Broadcom - Bunnik, The Netherlands

Pascal Lorenz, University of Haute-Alsace, France

COCORA 2013

Foreword

The Third International Conference on Advances in Cognitive Radio (COCORA 2013), held between April 21st-26th, 2013 in Venice, Italy, continued a series of events dealing with various aspects, advanced solutions and challenges in cognitive (and collaborative) radio networks. It covered fundamentals on cognitive and collaborative radio, specific mechanism and protocols, signal processing and dedicated devices, measurements and applications.

Most of the national and cross-national boards (FCC, European Commission) had/have a series of activities in the technical, economic, and regulatory domains in searching for better spectrum management policies and techniques, due to spectrum scarcity and spectrum underutilization issues. Therefore, dynamic spectrum management via cognition capability can make opportunistic spectrum access possible (either by knowledge management mechanisms or by spectrum sensing functionality). The main challenge for a cognitive radio is to detect the existence of primary users reliably in order to minimize the interference to licensed communications. Optimized collaborative spectrum sensing schemes give better spectrum sensing performance. Effects as hidden node, shadowing, fading lead to uncertainties in a channel; collaboration has been proposed as a solution. However, traffic overhead and other management aspects require enhanced collaboration techniques and mechanisms for a more realistic cognitive radio networking.

We take here the opportunity to warmly thank all the members of the COCORA 2013 Technical Program Committee. The creation of such a high quality conference program would not have been possible without their involvement. We also kindly thank all the authors who dedicated much of their time and efforts to contribute to COCORA 2013. We truly believe that, thanks to all these efforts, the final conference program consisted of top quality contributions.

Also, this event could not have been a reality without the support of many individuals, organizations, and sponsors. We are grateful to the members of the COCORA 2013 organizing committee for their help in handling the logistics and for their work to make this professional meeting a success.

We hope that COCORA 2013 was a successful international forum for the exchange of ideas and results between academia and industry and for the promotion of progress in the field of cognitive radio.

We are convinced that the participants found the event useful and communications very open. We also hope the attendees enjoyed the charm of Venice, Italy.

COCORA Advisory Committee:

Tomohiko Taniguchi, Fujitsu Laboratories Limited, Japan

Adrian Popescu, Blekinge Institute of Technology - Karlskrona, Sweden

COCORA 2013

Committee

COCORA Advisory Committee

Tomohiko Taniguchi, Fujitsu Laboratories Limited, Japan
Adrian Popescu, Blekinge Institute of Technology - Karlskrona, Sweden

COCORA 2013 Technical Program Committee

Anwer Al-Dulaimi, Brunel University, UK
Cornelia Badoi, Ericsson Romania, Romania
Ilham Benyahia, Université du Québec en Outaouais, Canada
Derya Çavdar, Bogazici University, Istanbul, Turkey
Malgorzata Gajewska, Gdansk University of Technology, Poland
Slawomir Gajewski, Gdansk University of Technology, Poland
Matthieu Gautier, Université de Rennes 1, IRISA, INRIA, France
Liljana Gavrilovska, Ss. Cyril and Methodius University -Skopje, Macedonia
Tien-Ke Huang, National Tsing Hua University, Taiwan
Abubakar Sadiq Hussaini, Instituto de Telecomunicações - Aveiro, Portugal/University of Bradford, UK
Insoo Koo, University of Ulsan, South Korea
Thomas D. Lagkas, University of Western Macedonia, Greece
Jia-Chin Lin, National Central University, Taiwan
Ivana Marci, Aviat Networks - Santa Clara, USA
Jean-Claude Moissinac, TELECOM ParisTech, France
Homayoun Nikookar, Delft University of Technology, The Netherlands
Sema Oktug, Istanbul Technical University, Turkey
Adrian Popescu, Blekinge Institute of Technology - Karlskrona, Sweden
Arnd-Ragnar Rhiemeier, Cassidian Electronics - Ulm, Germany
Usman Shahid, NDSU - Fargo, USA
Boyan Soubachov, University of Cape Town, South Africa
Silvian Spiridon, Broadcom - Bunnik, The Netherlands
Tomohiko Taniguchi, Fujitsu Laboratories Limited, Japan
Ba Lam To, Phare - LIP6 - UPMC (Paris 6), France
Liaoyuan Zeng, University of Electronic Science and Technology of China, China

Copyright Information

For your reference, this is the text governing the copyright release for material published by IARIA.

The copyright release is a transfer of publication rights, which allows IARIA and its partners to drive the dissemination of the published material. This allows IARIA to give articles increased visibility via distribution, inclusion in libraries, and arrangements for submission to indexes.

I, the undersigned, declare that the article is original, and that I represent the authors of this article in the copyright release matters. If this work has been done as work-for-hire, I have obtained all necessary clearances to execute a copyright release. I hereby irrevocably transfer exclusive copyright for this material to IARIA. I give IARIA permission to reproduce the work in any media format such as, but not limited to, print, digital, or electronic. I give IARIA permission to distribute the materials without restriction to any institutions or individuals. I give IARIA permission to submit the work for inclusion in article repositories as IARIA sees fit.

I, the undersigned, declare that to the best of my knowledge, the article does not contain libelous or otherwise unlawful contents or invading the right of privacy or infringing on a proprietary right.

Following the copyright release, any circulated version of the article must bear the copyright notice and any header and footer information that IARIA applies to the published article.

IARIA grants royalty-free permission to the authors to disseminate the work, under the above provisions, for any academic, commercial, or industrial use. IARIA grants royalty-free permission to any individuals or institutions to make the article available electronically, online, or in print.

IARIA acknowledges that rights to any algorithm, process, procedure, apparatus, or articles of manufacture remain with the authors and their employers.

I, the undersigned, understand that IARIA will not be liable, in contract, tort (including, without limitation, negligence), pre-contract or other representations (other than fraudulent misrepresentations) or otherwise in connection with the publication of my work.

Exception to the above is made for work-for-hire performed while employed by the government. In that case, copyright to the material remains with the said government. The rightful owners (authors and government entity) grant unlimited and unrestricted permission to IARIA, IARIA's contractors, and IARIA's partners to further distribute the work.

Table of Contents

A New Throughput Analysis in Cognitive Radio Networks Using Slotted CSMA <i>Afonso Jose de Faria and Jose Marcos Camara Brito</i>	1
Efficiency of Opportunistic Spectrum Sensing by Sequential Change Detection in Cognitive Radio <i>Karsten Husby, Arne Lie, and Jan-Erik Hakegard</i>	7
Sensing of DVB-T Signals for White Space Cognitive Radio Systems <i>Daniel Riviello, Roberto Garello, Sergio Benco, Alberto Perotti, and Floriana Crespi</i>	12
Software Defined Radio Transceiver Front-ends in the Beginning of the Internet Era <i>Silvian Spiridon</i>	18
Emerging Applications of Cognitive Radios <i>Muhammad Adnan Qureshi, Muhammad Umar Khan, and Mahmood Ashraf Khan</i>	23
On Multi-channel Opportunistic Access in Heterogeneous Cognitive Radio Networks <i>Said Rutabayiro Ngoga, Yong Yao, and Adrian Popescu</i>	29
Wireless Deterministic Medium Access: A Novel Concept Using Cognitive Radio <i>Dimitri Block and Uwe Meier</i>	35
Analytical Evaluation of Proactive Routing Protocols with Route Stabilities under two Radio Propagation Models <i>M. Umar Khan, Imad Siraj, and Nadeem Javaid</i>	39
A Quantization Scheme based on Kullback-Leibler Divergence for Cooperative Spectrum Sensing in Cognitive Radio <i>Van Hiep Vu and Insoo Koo</i>	44

A New Throughput Analysis in Cognitive Radio Networks Using Slotted CSMA

Afonso José de Faria and José Marcos Câmara Brito

Instituto Nacional de Telecomunicações - INATEL

Santa Rita do Sapucaí, Brazil

faria.afonso@mtel.inatel.br, brito@inatel.br

Abstract— Cognitive Radio Networks (CRN) are a new area of interests for researchers and a new technology for the next generation wireless networks. Multiple access protocol is an important issue to define the networks performance. In this paper, the throughput of a primary and secondary network is analyzed considering the Capture Effect in both systems and the Packet Error Rate (PER) due to the interference between primary and secondary stations, considering that the slotted Aloha protocol is proposed for the licensed network and Slotted Carrier Sense Multiple Access (CSMA) protocol is used in the secondary network.

Keywords- Cognitive Radio; Multiple Access; Throughput; Performance analysis

I. INTRODUCTION

The radio frequency spectrum is a natural resource [2] and it is partitioned into several bands that are generally attributed to licensed holders through long-term agreements [3][4]. Inside frequency spectrum there are some unlicensed portions reserved for industrial, scientific or medical (ISM) purposes and they are commonly used for data communication in smaller networks [3].

The studies and measurements performed by the Spectrum Policy Task Force (SPTF), linked to the Federal Communications Commission (FCC), concluded that certain spectrum bands are heavily used by licensed or unlicensed users (ISM users), while other spectrum fractions are used occasionally or rarely, depending on geographic location and time [2][5]. Also according to [6], in the future there could be scarcity of this precious resource due to increasing demand powered by a variety of factors, like the rapid economic growth of the telecommunications sector and the convenience offered by them, the emerging services and applications, the increasing of the human mobility and the appearance of new technologies [6].

Changes in the policy for the frequency spectrum that become more flexible the access to this resource, by using dynamic spectrum access (DSA), and the improvement in the spectrum management procedures would improve the efficiency in the using of this natural resource and would avoid its possible scarcity [2] [3] [4] [6]. According to [5], the DSA becomes viable by the emerging technology of the cognitive radio (CR). It is a new concept in the development of wireless communication systems enabling more efficient use of radio spectrum and, therefore, it is a strong candidate as a technological solution for the future wireless networks, so-called NeXt Generation (xG) networks or cognitive radio networks.

In [5], CR is defined as a radio that can change its transmission parameters based on the interaction with the operating environment and its main goals are to provide reliable and seamless communication and to enable the efficient spectrum utilization. The cognitive radios must also be able to reconfigure their communication parameters rapidly and in the real time [2].

The cognitive radio networks can be defined as “networks that can dynamically alter their functionality and/or topology in accordance with the changing needs of its users, taking into account current environmental conditions. This dynamic modification is done in accordance with applicable business rules and regulatory policies” [7].

The CRN architecture is formed by two groups: the primary network and the secondary network. These groups can coexist in the same geographic region and they can operate in the same spectrum band. According to [4], the primary network is an existing network where primary users (PU) have license to operate in a specific frequency band. Licensed users have higher priority in channel access. The secondary networks, or cognitive networks are those that do not have license to operate in the desired band [4] and the so-called secondary users (SU) operate in such network. According to [8], the secondary users have lower transmission priority and they exploit the frequency spectrum in an opportunistic fashion, through the spectrum holes and without causing harmful interference to licensed users transmissions.

According to [1], in the primary network, the protocols for medium access control (MAC) are important to organize access of the different primary users to the channels. In the secondary network, the MAC protocols are responsible for organizing access of the secondary users to the free primary network channels, avoiding or making the interference acceptable in the primary network.

The network throughput is affected by the capture effect. In [1], the performance of cognitive radio networks (CRN) is analyzed for several MAC protocols, including an analysis that considers using Slotted Aloha in the primary network and the slotted carrier sense multiple access protocol (CSMA) in the secondary network. In these analyzes the Capture Effect is also taken into account in primary and secondary networks: if the difference between the power level of a concerned packet signal in relation to others interfering packets is higher than a threshold called capture ratio (R), then the concerned packet can be detected by the receiver, whereas all others fail in medium access [9].

However, the analysis introduced in [1] does not consider the possible errors due to interference during the packet detection. In this paper, we extend the analysis of [1], taking

into account the packet error rate due to multiple access scheme and their effects on the networks throughput.

The remainder of this paper is organized as follows. In Section II, we present the original model used in [1] for performance analysis; a new system model is introduced in Section III and the networks throughput is evaluated considering the PER; Section IV introduces and compares the analytical results for both models; and our conclusions are shown in Section V.

II. THE ORIGINAL SYSTEM MODEL AND ITS PERFORMANCE ANALYSIS

The Fig. 1 shows the network architecture analyzed in [1]. The primary network uses Slotted Aloha as multiple access protocol to access the medium and in the unlicensed network is considered Slotted-CSMA protocol. The primary access point (PAP) and the secondary access point (SAP) provide services for primary and secondary networks respectively. All primary users can be viewed by SAP and vice versa. In the primary network there are N_p primary users (PU) and among these, I_p stations are attempting to transmit their data packets during a time slot. On other hand, the secondary network has N_s secondary users (SU). During a time slot, there are J_s unlicensed users attempting to send their packets [1].

The primary users have priority to transmit their data packets and, therefore, the SUs sense the channel to avoid interference with PUs and to identify clearly the spectrum holes that occur when a time slot of slotted aloha is idle.

The Fig. 2 shows the structure of time slot for slotted aloha and slotted CSMA. In the primary network, each time slot can be busy or idle, depending on transmission states of PUs during a time slot. If there is no primary user attempting to transmit packets at the beginning of a time slot, then it is considered idle. This spectrum opportunity can be exploited by the secondary users [1].

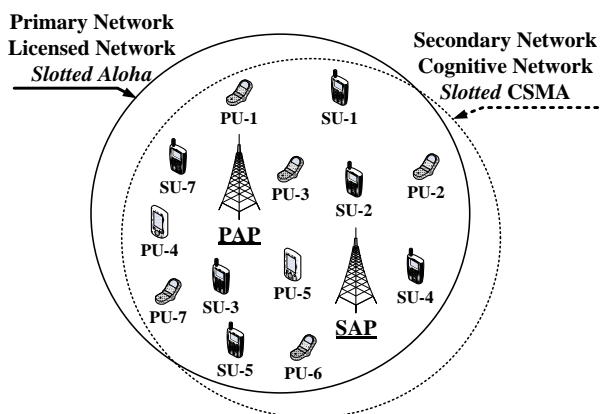


Figure 1. Original model architecture; Slotted Aloha in the primary network and Slotted CSMA in the cognitive network

Primary network BUSY (slotted Aloha)	Primary network IDLE Secondary network Slotted CSMA	...	Primary network IDLE Secondary network Slotted CSMA	Primary network BUSY (slotted Aloha)	...
1	2	...	t-2	t-1	t

Figure 2. Slots structure of Slotted Aloha for primary users and Slotted CSMA for secondary users

A. Primary Network Analysis

According to the traffic model introduced in [1], any PU that is not in a retransmission state can generate a new packet with probability σ_p . Therefore, the probability that a PU does not generate any packet is $(1-\sigma_p)$. If a new packet is generated in the network, it is transmitted immediately in the next time slot. If the packet is not successfully transmitted during a time slot, it is retransmitted with probability σ_p in the following time slots until that packet is successfully transmitted. Users in the retransmission state cannot generate new data packets [1].

1) *Fading Model in the Primary Networks:* let x_p be the instantaneous power of a concerned packet signal in the primary network and be y_i the instantaneous power of the interfering packets signals generated by the others PUs during a time slot. The fading model considered in [1] is a Rayleigh fading channel with the following exponential distributions,

$$p_x(x_p) = \frac{1}{X_p} e^{-x_p/X_p} \quad (1)$$

$$p_y(y_i) = \frac{1}{Y_i} e^{-y_i/Y_i} \quad (2)$$

where X_p and Y_i are the average power of concerned and interfering packet signals, respectively. In [1], $X_p=Y_i$.

2) *Capture Effect in the Primary Network:* according to [1] and [9], the signals arriving at the receiver have different power levels due to transmission power practiced by the user, fading or shadowing. In this case, whether the power of the concerned data packet from a PU is greater than the sum of the powers levels of all interfering packets in this network and satisfies a given threshold, so-called capture ratio (R), the concerned packet can be detected by PAP and all others interfering users fail in access medium. Thus, the probability of capture ($P_{cap \rightarrow PAP}$) can be calculated as [1],

$$P_{pcap \rightarrow PAP}(I_p) = \Pr \left(\frac{x_p}{\sum_{i=1}^{I_p-1} y_i} > R \right) = \left(\frac{1}{R+1} \right)^{I_p-1} \quad (3)$$

Where I_p represents the total numbers of simultaneous transmitting primary users at a given time slot [1].

3) *Primary Network Throughput:* according to [1], the primary network throughput, S_{po} , can be calculated as below,

$$S_{po} = \sum_{i_p=0}^{N_p} i_p \binom{N_p}{i_p} \sigma_p^{i_p} (1 - \sigma_p)^{N_p - i_p} \left(\frac{1}{R+1} \right)^{i_p - 1}. \quad (4)$$

B. Cognitive Network Analysis for the original model

In this network, Slotted CSMA protocol is used for medium access and its proposed slot structure is presented in the Fig. 3 [1].

In the Fig. 3, the first and third time slots of the primary network are busy, i.e., they are used by PUs. The second and fourth ones represent spectral opportunities and they can be exploited by SUs. Each of idle time slots of Slotted Aloha is subdivided into mini-slots. So, the channel is time slot based for primary network and mini-slot based for secondary users. The duration of each mini slot is equal to the maximum propagation delay (p) found in the primary and secondary networks and corresponds to the distance from point a to b in the Fig. 3 [1].

There are two kinds of mini-slots: (1) few are designed for carrier sensing period (S_{mi}), and (2) the most are aimed for packet transmissions (T_{mi}) of the SUs [1]. According to the Fig. 3, the maximum sensing period allowed is from point a , i.e., the beginning of an idle time slot, to point c and the sensing point is set to happen at the beginning of each mini-slot. The distance between point c and point e is specified as the maximum length of the data packets (T_{mi}) from the secondary network in terms of the number of mini-slots. Therefore, the packet length of the secondary network is shorter than the packet length of the primary network due to the carrier sensing period [1].

1) *Traffic model for the secondary network*: in the secondary network, using Slotted CSMA as protocol to access the channel, each SU can generate a new packet with probability (σ_{mi}) during a mini-slot. Consequently, the probability of a SU does not generate a new packet is $(1 - \sigma_{mi})$. Whether an unlicensed user is in the retransmission state, it cannot generate a new packet [1].

During an idle or busy time slot in the primary network, if a new packet is generated by a SU within carrier sensing period of a mini-slot, it senses the channel in the following sensing point of the carrier sensing period. If the channel is idle, its packet is transmitted immediately. If the channel is busy, the SU gives up and starts sensing the channel with probability σ_{mi} during each sensing point of the remaining carrier sensing period in the current time slot, i.e., the point c in Fig. 3. And whether the channel remains busy during this carrier sensing period, the process continues with probability σ_{mi} during each sensing point in the following time slots until the channel is idle and the packet is successfully transmitted. If a new packet is generated outside the designated carrier sensing period, the new packet is stored and the station begins to sense the channel with probability σ_{mi} during each sensing point in the following carrier sensing periods until the channel becomes idle and the new packet is successfully transmitted. According to [1], a packet transmission of a SU can start from any sensing point of the carrier sensing period that channel is sensed idle [1].

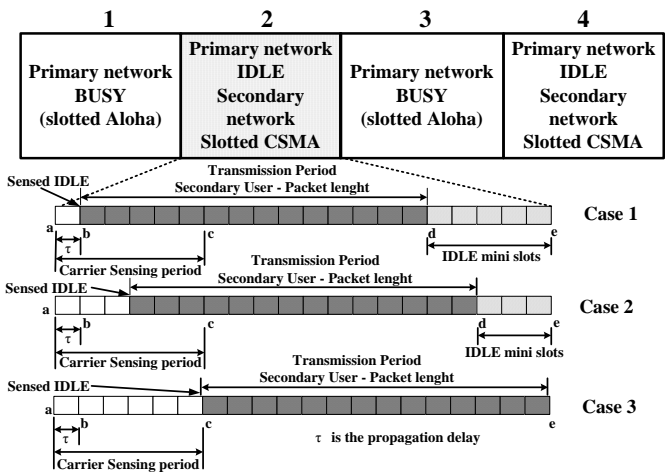


Figure 3. Time slot structure of Slotted CSMA for secondary users

Observing the cases (1) and (2) in the Fig. 3, one can observe that if the channel is sensed idle before the end of the carrier sensing period in the current time slot (point c in the Fig. 3), then after the end of packet transmission remains some unused mini-slots [1]. Finally, in the model proposed in [1], SU should be able to sense the channel and determine if it is busy or not. The idle time slots represent spectral opportunities that are disputed by the secondary users within an environment for cooperation between themselves.

2) *Fading Analysis and Capture Effect for the Secondary Network*: let x_s and z_j be instantaneous power level of the concerned packet signal and the interfering packet signals originated in this network, respectively. In [1] is considered a Rayleigh fading channel with the following exponential distributions [1],

$$P_x(x_s) = \frac{1}{X_s} e^{-x_s/X_s} \quad (5)$$

$$P_z(z_j) = \frac{1}{Z_j} e^{-z_j/Z_j} \quad (6)$$

where X_s and Z_j are the mean power level of that signals. In Slotted CSMA, the capture probability can also be calculated as below [1],

$$P_{scap \rightarrow SAP}(J_s) = \Pr \left[\frac{z_j}{\sum_{j=1}^{J_s-1} z_j} > R \right] = \left(\frac{1}{R+1} \right)^{J_s-1}. \quad (7)$$

Where J_s denotes the number of SUs are attempting packet transmission during an idle time slot and R is the Capture Ratio [1].

3) *The Secondary Network Throughput*: according to [1], the secondary network throughput is defined as the packet length in terms of number of mini-slots divided by the total number of mini-slots that are spent in the process of packet transmission, including in this case both busy and idle slots. Then, the secondary network throughput, S_{so} , is computed by [1],

$$S_{so} = \frac{(1 - \sigma_p)^{N_p} T_{mi}}{(T_{mi} + S_{mi})} \sum_{s=1}^{S_{mi}} \left((1 - \sigma_{mi})^{N_s} \right)^{s-1} \times \sum_{j_s=0}^{N_s} j_s \binom{N_s}{j_s} \sigma_{mi}^{j_s} (1 - \sigma_{mi})^{N_s - j_s} \left(\frac{1}{R+1} \right)^{j_s - 1}. \quad (8)$$

C. Overall Networks Throughput

The overall networks throughput, S_{oto} , is the sum of primary network throughput and secondary network throughput, as calculated below [1],

$$S_{oto} = S_{po} + S_{so}. \quad (9)$$

III. THE PROPOSED NEW SYSTEM MODEL

In this section, we propose an extension to the original model considering the influence of PER in the calculation of throughput. Transmission errors occur during the packet detection due to the network interfering signals. This approach becomes a more realistic model, since the packets received with errors are discarded and retransmitted in the most of data communication applications.

The system architecture shown in Fig. 1 is also used for the new model, as well as the structure of time slots and mini-slots introduced in the Fig. 2 and Fig. 3 in the original model.

In this new model, the USs also use Slotted CSMA protocol to access the medium and they can sense the channel. Thus, during a packet transmission in a given network, primary or secondary, in the SIR calculating are considered only the interfering signals generated by users of that network, i.e., SUs cannot transmit packets when there are PUs attempting to transmit their packets. The Users from cognitive network only can transmit packets when a time slot of the primary network is idle.

A. Packet Error Rate

The knowledge of the packet error rate in communication systems is important, since in most of these systems, data are transmitted in packets rather than bit streams. Moreover, their performance is determined by PER instead of bit error rate (BER) or symbol error rate (SER) [10]. The PER is dependent of the signal-to-interference plus noise ratio (SNIR) in the considered channel. However, as in [11], the additive noise is negligible in interference-limited channels. Therefore the model called signal-to-interference ratio (SIR) is used in this paper.

References [12], [13], [14], [15], [16] and [17] introduce empirical or approximate methods for PER calculating. Their conclusion is that such calculation is quite complex, imprecise and cannot be generalized to the real applications. All proposed methods above to calculate or estimate the PER model the communication channels according to a Markov chain, where the signal-to-noise ratio (SNR) is partitioned into a finite number of states that can range between two and several. The difficulties of working with Markovian models are in to set the transition probabilities of states to reflect the real channel behavior. In [18], [19] and [20] methods for PER calculating are analyzed and is proposed to study such

behavior by collecting the real statistical information or even by using suitable simulation tools on computers.

Due to the exposed above, in this paper, we choose to work with the methodology introduced in [10], which allows the calculation of PER as a function of SIR, in a direct and simple fashion by using a highly accurate upper bound for the system analyzed.

Considering that the SUs can listen the channel and they cannot cause interference to PUs, we can obtain the expected value for SIR in the primary network, Δ_p , as below,

$$\Delta_p = \frac{X_p}{(I_p - 1)Y_i} = \frac{1}{(I_p - 1)}. \quad (10)$$

Taking into account that the SUs compete for idle time slots from the primary network, then the average SIR for the unlicensed network, Δ_s , is given by,

$$\Delta_s = \frac{X_s}{(J_s - 1)Z_j} = \frac{1}{(J_s - 1)}. \quad (11)$$

Now, let $f(\delta)$ be a function that links the PER with the instantaneous SIR at reception (δ) in a channel with additive white Gaussian noise (AWGN) and $p(\delta)$ is the probability density function of SIR in the receiver, with exponential distribution. According to [10], the average PER, represented by $P_{ave}(\Delta)$, can be calculated by the following integrals,

$$P_{ave}(\Delta) = \int_0^{\infty} f(\delta) p(\delta) d\delta \quad (12)$$

$$P_{ave}(\Delta) = \frac{1}{\Delta} \int_0^{\infty} f(\delta) e^{-\delta/\Delta} d\delta. \quad (13)$$

Considering the modulation techniques employed, packet lengths and the coding schemes used, the resolution of (13) for the general cases is quite difficult. Then in [10] an approximation to calculate the PER by upper bound is proposed, according to the following inequality,

$$P_{ave}(\Delta) \leq 1 - e^{-w_0/\Delta}. \quad (14)$$

The successfully transmitted packets rate (PSR) is then given by the equation below,

$$PSR \geq e^{-w_0/\Delta}. \quad (15)$$

Where w_0 is a constant value for the Rayleigh fading channel and can be obtained through the integral below [10],

$$w_0 = \int_0^{\infty} f(\delta) d\delta. \quad (16)$$

And $f(\delta)$ can be obtained as follows [10],

$$f(\delta) = \{1 - [1 - b(\delta)]^n\}. \quad (17)$$

Where $b(\delta)$ is the BER in AWGN channels. For a modulation technique as the binary phase shift keying (BPSK) with coherent detection, without using the channel coding scheme and considering packets of n bits, $b(\delta)$ can be calculated according to the equation given below [10],

$$b(\delta) = \frac{1}{2} \operatorname{erfc}(\sqrt{\delta}). \quad (18)$$

Reference [10] presents an analytical resolution of the upper bound and the corresponding simulations for the expected values for PER as a function of average SNR. From the results presented in [10], we can observe that the upper

bound provides an accurate value for the PER under some assumptions, e.g., when coherent BPSK is employed as a technique for modulation, with or without a channel coding scheme and by using some packet lengths (greater than or equal to 127 bits when channel coding is not used). In our analysis we assume coherent BPSK modulation without a channel coding scheme and with packets length of 127 [bits]. According to the considerations above, in this paper, we consider that the PER and the PSR are obtained in an approximate fashion by the equations presented below,

$$P_{ave}(\Delta) \cong 1 - e^{-w_0/\Delta} \tag{19}$$

$$PSR(\Delta) \cong e^{-w_0/\Delta}. \tag{20}$$

Using MATLAB and comparing to the results presented in [10], the values obtained for w_0 are shown in the Table I.

B. The Primary Network Throughput for the New model

The primary network throughput is defined as the total number of packets transmitted by the licensed users and received correctly by PAP during a time slot [1].

In the new system model, a packet is considered successfully transmitted when it is captured by the receiver and it does not have any errors due to interference present in the networks. In this case, the primary network throughput, S_{pn} , is approximately given by:

$$S_{pn} = S_{po} \times PSR(\Delta_p) \cong S_{po} \times e^{-w_0(I_p-1)}. \tag{21}$$

Where S_{po} is the primary network throughput for the original model and $PSR(\Delta_p)$ is the successfully transmitted packet rate.

C. The Secondary Network Throughput for the New Model

Referring to the secondary network, the throughput is defined as the length of packet in terms of mini-slots divided by the total number of mini-slots used in the transmission process, including both busy and idle slots [1]. When one considers only the packets received without errors due to interference of the networks, the secondary network throughput, S_{sn} , is given approximately by,

$$S_{sn} = S_{so} \times PSR(\Delta_s) \cong S_{so} \times e^{-w_0(I_s-1)}. \tag{22}$$

Where S_{so} is the secondary network throughput for the original model and $PSR(\Delta_s)$ is the successfully transmitted packet rate.

D. The Overall Networks Throughput for the New Model

The overall throughput for the new system model, S_{om} , is the sum of the primary and secondary networks throughput, as below:

$$S_{om} = S_{pn} + S_{sn}. \tag{23}$$

IV. NUMERICAL RESULTS

The Fig. 4, Fig. 5 and, Fig. 6 shown the analytical results obtained for throughput of primary and secondary network throughput and overall throughput system. To compare the results between the new model and the original model, in the following graphics are used the same parameters introduced

in [1], i.e., $N_p = 20$ (users), $N_s = 20$ (users), $R = 3$ (dB), $\gamma = 10$, $S_{mi} = 10$ (mini slots), $T_{mi} = 100$ (mini slots) e $\sigma_p = \sigma_{mi}$.

TABLE I. VALUES OF w_0 CONSIDERING COHERENT BPSK MODULATION

Packet length in n (bits)	w_0
Uncoded 127 (bits)	3.4467
Uncoded 1023 (bits)	5.3361

The graphs of Fig. 4, Fig. 5 and, Fig. 6 show that the effect of the PER on the primary and secondary networks transmissions, due to interference caused by their stations, cannot be disregarded. When one considers the PER, there is a significant reduction in the primary and secondary network throughput and also in the overall network throughput.

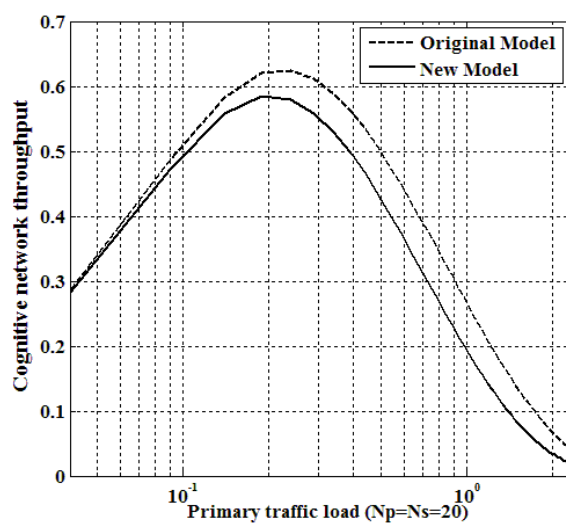


Figure 4. Cognitive network throughput ($N_p=N_s=20$, $S_{mi}=10$, $R=3$ dB)

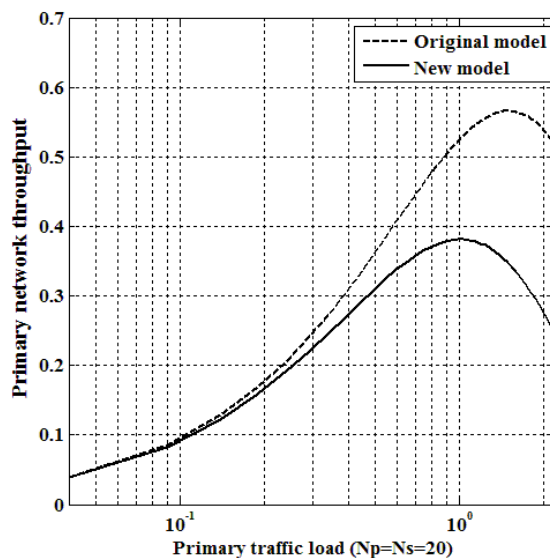


Figure 5. Primary network throughput ($N_p=N_s=20$, $S_{mi}=10$, $R=3$ dB)

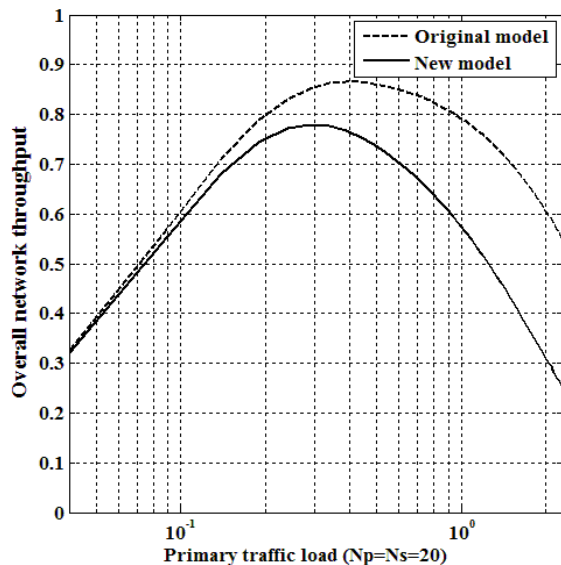


Figure 6. Overall network throughput ($N_p=N_s=20$, $S_{mi}=10$, $R=3$ dB)

V. CONCLUSION

In this paper, we propose a new model to compute the throughput in a cognitive radio network, considering Slotted Aloha in the licensed network and Slotted CSMA in the cognitive network. This proposed model is an extension of the model analyzed in [1].

The new model proposed considers the interference between the stations of the networks and their effects over the throughput of each network. It is verified that the interference increases the packet error rate and reduces the primary network throughput, the secondary network throughput and overall networks throughput. Therefore, it is concluded that the PER, due to interference between radio stations of both networks, cannot be neglected, as happens in [1].

As suggestion for future study, it is proposed to investigate mechanisms to reduce the packet error rate on the networks and thereby improve the throughput of each network and the overall throughput.

REFERENCES

- [1] Z. Yang, "Investigations of multiple access protocols in cognitive radio networks," Ph.D. dissertation, Dept. of Elect. and Comput. Eng., Stevens Inst. of Technology, Hoboken, NJ, 2010.
- [2] S. Haykin, "Cognitive radio: brain-empowered wireless communications," *IEEE J. Sel. Areas Commun.*, vol. 23, no. 2, Feb. 2005, pp. 201-220.
- [3] E. Hossain, D. Niyato, and Z. Han, "Introduction to cognitive radio," in *Dynamic Spectrum Access and Management in Cognitive Radio Networks*, 1st ed., New York, NY: Cambridge University Press, 2009, ch.2, pp.39-73.
- [4] I.F. Akyildiz, W.Y. Lee, M.C. Vuran, and S. Mohanty, "A survey on spectrum management in cognitive radio networks," *IEEE Commun. Mag.*, vol. 46, issue:4, Apr. 2008, pp. 40-48.
- [5] I.F. Akyildiz, W.Y. Lee, M.C. Vuran, and S. Mohanty, "NeXt generation/dynamic spectrum access/cognitive radio wireless networks: a survey," *Comput. Networks*, vol. 50, issue:13, May 2006, pp. 2127-2159.
- [6] P. Kolodzy et al, "Spectrum Policy Task Force seeks public comment on issues related to commission's spectrum policies," The Federal Communications Commission (FCC), Indianapolis, IN, ET Docket No. 02-135, 2002.
- [7] J. Strassner, "The role of autonomic networking in cognitive networks," in *Cognitive Networks: Towards Self-Aware Networks*, 1st ed., New York, NY: Wiley, 2008, ch. 2, pp. 23-52.
- [8] T. Yucek and H. Arslan, "A survey of spectrum sensing algorithms for cognitive radio applications," *IEEE Commun. Surveys & Tutorials*, vol. 11, no. 1, Mar. 2009, pp. 116-130.
- [9] Y. Onozato, J. Liu, and S. Noguchi, "Stability of a slotted Aloha system with capture effect," *IEEE Trans. on Veh. Technology*, vol. 38, no. 1, Feb. 1989, pp. 31-36.
- [10] Y. Xi, A. Burr, J. Wei, and D. Grace, "A general upper bound to evaluate packet error rate over quasi-static fading channels," *IEEE Trans. on Wireless Commun.*, vol. 10, no. 5, May 2011, pp. 1373-1375.
- [11] S. Kucera, S. Aissa, and S. Yoshida, "Adaptive channel allocation for enabling target SINR achievability in power-controlled wireless networks," *IEEE Trans. on Wireless Commun.*, vol. 9, no. 2, Feb. 2010, pp. 833-843.
- [12] H. Bai and M. Atiquzzaman, "Error modeling schemes for fading channels in wireless communication: a survey," *IEEE Commun. Survey & Tutorials*, vol. 5, no. 2, Dec 2003, pp. 2-9.
- [13] J.R. Yee and E. J. Weldon, "Evaluation of the performance of error-correcting codes on a Gilbert channel," *IEEE Trans. on Commun.*, vol. 43, no. 6, Aug. 1995, pp.2316-2323.
- [14] J.P. Ebert and A. Willy, "A Gilbert-Elliott bit error model and the efficient use in packet level simulation," *TKN Techn. Rep.*, Tech. University Berlin, Berlin, rep. 99-002, 1999.
- [15] H. Bischl and E. Lutz, "Packet error rate in the non-interleaved Rayleigh channel," *IEEE Trans. on Commun.*, vol. 43, no. 2/3/4, Feb./Mar./Apr. 1995, pp. 1375-1382.
- [16] G. Sharma, A. Dholakia, and A. Hassan, "Simulation of error trapping decoders on a fading channel," In. *Proc IEEE Veh. Technology Conf. 1996, Atlanta, GA*, vol. 2, pp. 1361-1365.
- [17] H. Labiod, "Performance of Reed Solomon error-correcting codes fading channels," in *1999 IEEE Int. Conf. on Personal Wireless Commun., Jaipur, India*, pp. 259-263.
- [18] B.D. Fritchman, "A binary channel characterization using partitioned Markov chains," *IEEE Trans. on Inform. Theory*, vol. 13, no. 2, Apr. 1967, pp. 221-227.
- [19] J. Arauz, P. Krishnamurthy, and M.A. Labrador, "Discrete Rayleigh fading channel modeling," *Wireless Commun. and Mobile Computing*, vol. 4, issue:4, Jun. 2004, pp. 413-425.
- [20] C.C. Tan and N.C. Beaulieu, "On first-order Markov modeling for the Rayleigh fading channel," *IEEE Trans. on Commun.*, vol. 41, no. 12, Dec. 2000, pp. 2032-2040.

Efficiency of Opportunistic Spectrum Sensing by Sequential Change Detection in Cognitive Radio

Karsten Husby, Arne Lie, Jan-Erik Håkegård
 Communication Systems
 SINTEF ICT
 Trondheim, Norway
 karsten.husby@sintef.no

Abstract—A critical point in cognitive radio spectrum sensing is the ability to detect presence and absence of primary users as fast as possible at very low SNR. In this paper, sequential power detection by cumulative sum and recursive generalized likelihood ratio test is used to detect free spectral slots of opportunity. The benefits of these change detection algorithms are the adaptive sensing window, the low processing burden and the optimality in sense of maximum likelihood. A spectrum utilization efficiency metric is proposed that put a cost on late detections as well as on false alarms that might give rise to harmful interference into the primary system. The efficiency metric is then simulated versus the size of the free slot of opportunity and for different SNR. The detectors presented are found useful for cognitive radio.

Keywords—Cognitive radio; CUSUM; GLRT; Hypothesis testing; Maximum likelihood estimation;

I. INTRODUCTION

Algorithms for quick detection under noisy conditions have been in use since the 1920s. The first control chart originated from Bell Labs, where Dr. Shewhart set up control limits based upon the Bell curve to find out if a process was in control or out of control.

Later, an improved method based on an intuitive cumulative sum was proposed [1]. This method is now named CUSUM, and is closely related to the Neyman-Pearson test that tries to distinguish between two hypotheses [2][3][4] when the probability density function (PDF) for both is known in advance.

Another popular, but often regarded as a high complexity test, is the generalized likelihood ratio test (GLRT), where unknown parameters are part of the PDF of the process. Because this test is based on maximum likelihood estimation (MLE), it is asymptotically optimal for a large number of applications. However, for systems requiring a low false alarm probability, a huge amount of data needs to be stored and processed before an optimal decision can be made [8][9][10][11][12][13]. This is particularly troublesome in high bandwidth systems.

For cognitive radio spectrum sensing, high performance and low processing burden detectors are wanted. Recursion is often an efficient processing method, and in this paper, focus is put on low processing burden recursive change detection algorithms that also offer certain optimality in the maximum likelihood (ML) sense. One useful recursive algorithm is the CUSUM detector, which is optimal for a

given signal to noise ratio (SNR). Structures of parallel CUSUM detectors that are optimal for several SNRs may be implemented and lead to GLRT type of detectors. One particularly useful detector is the recursive GLRT detector called R-GLRT [5].

In cognitive radio secondary users need to detect when to transmit or not. This involves both power turn-off and power turn-on detection. All knowledge about the primary user transmit timing and the free window of opportunity W is also important. If this window is unknown it becomes important to estimate W or at least transmit packets short enough not to interfere with the primary user at power turn-on. Detectors both for on and off detection are presented but estimation of W is considered outside the scope of the paper.

This paper contributes in the area of spectrum sensing for opportunistic cognitive radio networks using the well-known CUSUM detector and the novel R-GLRT detector at very low SNR where the processing burden of other GLRT type detectors is significant. Both CUSUM and R-GLRT are very efficient algorithms that do not saturate when the amount of collected data grows. Due to their optimality, these detectors give increased spectral utilization. An efficiency metric is presented to quantify the performance offered by these detectors.

This paper is organized as follows. After a system introduction in Section II, the CUSUM detector and R-GLRT detector are presented in Section III. In Section IV both algorithms are simulated, and in Section V their impact when used in a cognitive radio system is found based on the spectrum efficiency metric.

II. MULTIPLE HYPOTHESES SYSTEM MODEL

The detector operates on an increasing number of n input samples $x(i)$, $i=1:n$ supplied from any sensor circuitry such as a bandpass filter, a FFT processor, a cyclostationary feature processor, or a Kalman filter matched to the parameter whose change is to be detected. The samples are assumed to be independent and identically distributed although such a limitation is not always required according to [16]. Without loss of generality $x(i)$ is assumed normal distributed with mean value μ and standard deviation σ ; i.e.,

$$p(x(i);\theta) = N(\theta) = N(\mu, \sigma) \quad (1)$$

Immediately after an unknown sample number m the primary user either turns off or on its transmitter. This is defined as the change point

$$m \in [0 : n] \quad (2)$$

Before and at the change point m , we have $x(i) \sim N(\theta_0)$. After the change point for $i > m$, we have $x(i) \sim N(\theta_1)$. It is necessary to handle all possible $n + 1$ different change points m as separate hypotheses H_m meaning that the m first samples belong to $N(\theta_0)$ and the rest to $N(\theta_1)$. In [5] it is established that CUSUM and R-GLRT are detectors that solves this multiple hypotheses problem.

III. CUSUM AND R-GLRT CHANGE DETECTION

It has been proven [7] that the CUSUM test only needs to investigate the sequential sum of the log likelihood ratio (LLR) between two probabilities to reach asymptotic optimal performance as long as both θ_0 and θ_1 are known in advance. It has also been proven that CUSUM is optimal for all finite thresholds γ [4]. The LLR is

$$LLR(i) = \ln(p(x(i); \theta_0)) - \ln(p(x(i); \theta_1)) \quad (3)$$

which in case of the normal distribution is

$$LLR(i) = \ln\left(\frac{\sigma_1}{\sigma_0}\right) - \frac{(x(i) - \mu_0)^2}{2\sigma_0^2} + \frac{(x(i) - \mu_1)^2}{2\sigma_1^2} \quad (4)$$

The sum LLR is very efficiently implemented in recursive form. The cumulative sum C is started from an initial value $C(0)$ that affects the transient response of the CUSUM. It is possible to improve the performance if $C(0)$ is increased to balance out the transient. This is called fast initial response (FIR) CUSUM [14][15]. In this paper, $C(0) = 0$, even though the R-GLRT algorithm also will benefit from FIR. The CUSUM recursive programming step is

$$C(i) = C(i-1) + LLR(i) \quad (5)$$

for $i = 1 : n$. For the traditional single sided CUSUM algorithm, only the final value $C(n)$ is stored for later use. In addition, the maximum value of C at the change point is stored as

$$M = \max(C(i)) \quad (6)$$

The CUSUM stopping time becomes

$$T = \min\{n : M - C(n) > \gamma\} \quad (7)$$

The average run length ARL_1 is the average stopping time when all samples are $N(\theta_1)$. ARL_0 is the average stopping time when all samples are $N(\theta_0)$ and is equivalent to the mean duration between false alarms.

The R-GLRT detector simultaneously runs parallel CUSUMs

$$C_{u,s} = L_{0,u} + L_{1,s} \quad (8)$$

indexed by u to adapt to different prior statistics $\theta_{0,u}$ for $i = 1 : n$

$$L_{0,u}(i) = L_{0,u}(i-1) + \ln(p(x(i); \theta_{0,u})) \quad (9)$$

and indexed by s to adapt to different $\theta_{1,s}$ statistics after the change point.

$$L_{1,s}(i) = L_{1,s}(i-1) - \ln(p(x(i); \theta_{1,s})) \quad (10)$$

The ML solution, which is already inherently part of the traditional CUSUM [5] is then solved recursively in multiple dimensions that includes the unknown statistics before and after the change point as well as the MLE of the change point itself \hat{m} .

$$[\hat{u}, \hat{s}, \hat{m}] = \arg \max (M_{u,s} - L_{1,s}(n)) \quad (11)$$

The stopping time under these constraints becomes

$$T = \min\{n : M_{\hat{u},\hat{s}} - L_{0,\hat{u}}(n) - L_{1,\hat{s}}(n) > \gamma_{\hat{u},\hat{s}}\} \quad (12)$$

IV. CHANGE DETECTION SIMULATIONS

Simulations are done in MATLAB by a flexible R-GLRT detector that handles any number of pre change parameter sets $\theta_{0,u}$ and any number of post change parameter sets $\theta_{1,s}$. If the number of possible pre change parameter sets and post change parameter sets are only one then the R-GLRT algorithm collapse into the traditional CUSUM algorithm.

The simulations show how well these detectors are able to detect a sudden shift in variance. The signal to noise ratio generating the change is defined as

$$SNR = \frac{(\mu_0 - \mu_1)^2 + |\sigma_1^2 - \sigma_0^2|}{\min(\sigma_0^2, \sigma_1^2)} \quad (13)$$

For detection of a change in variance, the mean values are disregarded by setting $\mu_0 = \mu_1 = 0$. To detect primary user power turn-on, $\sigma_0^2 = 1$ and $\sigma_1^2 = \sigma_0^2 + \sigma_p^2$, where the primary user power is represented by σ_p^2 . To detect primary user turn-off, $\sigma_1^2 = 1$ and $\sigma_0^2 = \sigma_1^2 + \sigma_p^2$. In both cases the primary user power is swept.

Results from a simulation of ARL for detection of sudden power turn-on and turn-off are given in Fig. 1. ARL_0 should be as high as possible and ARL_1 should be as low as possible. Note that the power turn-on detection is slightly better than the power turn-off detection both with regard to detection speed and false alarm at the optimum SNR which in this example is -3dB. It is important to note that the detection of primary user power turn-on or the detection of primary user power turn-off leads to different ARL although the algorithm is almost the same.

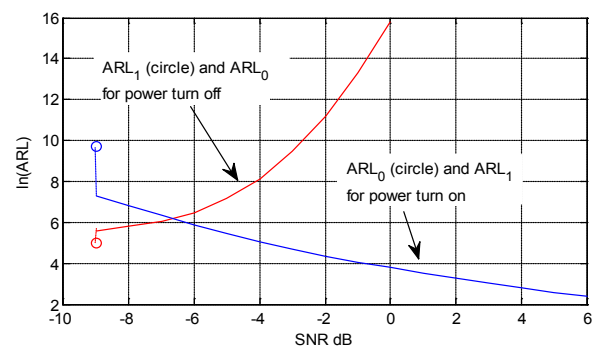


Figure 1. ARL for unknown power turn-on and off of two CUSUM detectors with $\gamma=6$ running equal but swapped sets of parameters θ .

One obvious difference for CUSUM is that detecting an unknown power turn-on gives improved detection speed if the power (SNR) is increased. Opposite, while detecting an unknown power turn-off the detection speed is almost constant independent of the apriori SNR.

A. The SNR wall problem

The CUSUM detector needs knowledge about θ_0 and θ_1 for optimal performance. The R-GLRT detector is able to pick the most likely θ_0 and θ_1 when they are not known in advance. Therefore unknown power levels both before and after the change point can be controlled. However, if the system noise floor is not properly calibrated it is impossible to distinguish between the power from an actual primary user or the unknown power from the detector itself. This eventually leads to the so-called SNR wall problem [17]. It is therefore obvious that some kind of automatic noise floor calibration is needed to prepare the detectors for accurate operation. In such a setting the R-GLRT detector is not only capable of giving stopping information but also valuable tracking information to refresh any estimate of the detector set noise σ_0 . While important, this topic is anyway outside the scope of this paper.

B. Primary user turn-on detection

The ARL for an unknown power turn-on is presented in Fig. 2. As illustrated, the two CUSUMs are quite robust to SNR offsets from their most optimal design points. Therefore the discretization of the continuous parameter space can be done by a relatively small number of parallel CUSUMs when setting up the R-GLRT algorithm. The simulation shows that this R-GLRT algorithm reaches almost identical stopping times compared to each of the single CUSUMs at their best SNR.

C. Primary user turn-off detection

Fast and reliable turn-off detection is considered very important for cognitive radio applications. One complicating factor is the presence of multiple primary users at different power level turning off their transmitters at unknown change points.

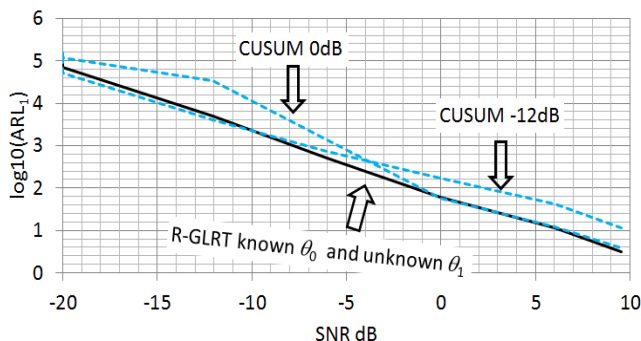


Figure 2. ARL_1 for unknown power turn-on of two CUSUM detectors optimal at -12dB and 0 dB compared with ARL_1 from R-GLRT containing three CUSUM detectors each optimal at -12, -6 and 0dB. ARL_0 for no shift equals 132000 for all.

It turns out that it is more complicated to detect the last (and sometimes the weakest) primary user power turn-off than the first primary user power turn-on. For example, assume 2 primary users, one strong and the other one at weak power. They transmit both for a long time. During this period the R-GLRT integrate prior statistics for all different $\theta_{0,u}$. The algorithm is however not capable of collecting any useful information about the weaker transmitter. If the stronger primary user turns off its carrier, the assumption of a constant (but unknown) θ_0 no longer holds, and the R-GLRT will have to trust the stopping condition from the CUSUM running on the weak power setting independent of the potential higher likelihood and faster stopping times from other CUSUMs. The R-GLRT detector is therefore not very well adapted to the task of detecting all primary users power turn off.

The CUSUM detector is on the other hand well adapted for such a task. In this case the mean detection speed versus different SNR becomes constant while the false alarm probability is reduced when the power is increased as illustrated in Fig. 1. This kind of detector behavior is conservative and not far from the wanted behavior. While it is possible to achieve faster detection speeds for higher SNR using the R-GLRT detector, the detection of power off has to be given with a certain confidence for the power being below a certain level. One single CUSUM is in fact capable of doing this task in ML optimal manner for all γ . Therefore we entirely focus on the CUSUM detector for power off detection.

The CUSUM power off detector is simulated for three different SNR as depicted in Fig. 3, Fig. 4 and Fig. 5. In these Figs interpolated ARL values are fitted based on

$$\begin{aligned} ARL_0 &\approx k_0 e^\gamma \\ ARL_1 &\approx k_1 \gamma \end{aligned} \tag{14}$$

Closed form expressions of ARL are difficult to derive. It is however obvious that the mean likelihood growth is linear for constant θ . Therefore ARL_1 becomes asymptotically linear to γ . Our simulations also strongly indicate that ARL_0 is asymptotically linear to e^γ .

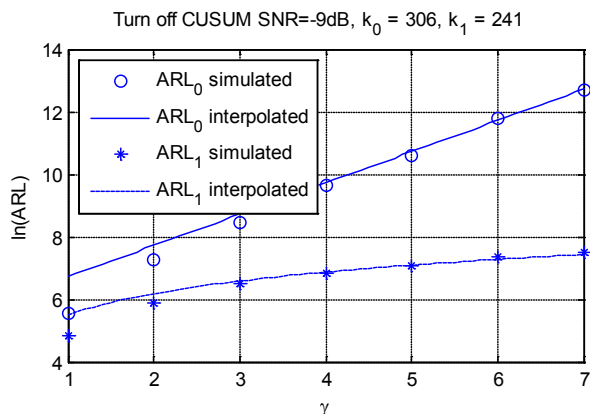


Figure 3. ARL for power turn off versus γ .

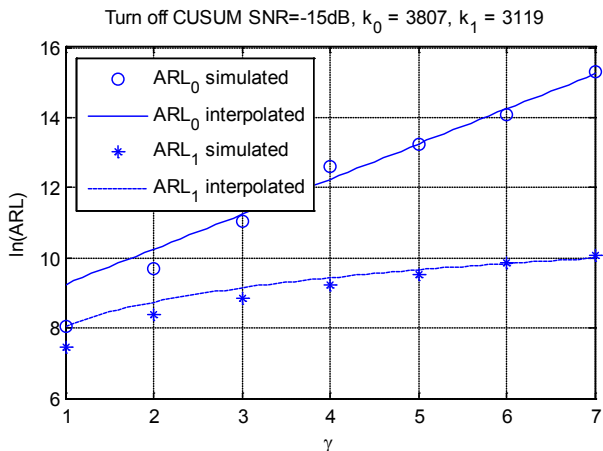


Figure 4. ARL for power turn off.

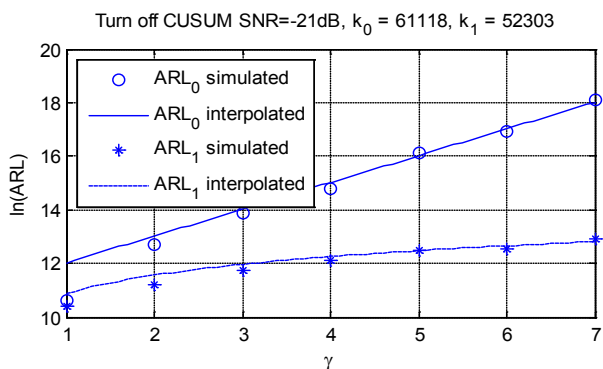


Figure 5. ARL for power turn off.

The empirical asymptotic solutions (14) are therefore well suited to find ARL at larger thresholds where simulations are cumbersome

V. COGNITIVE RADIO SENSING EFFICIENCY

In this chapter the sequential change detection algorithms are linked to cognitive radio opportunistic spectrum utilization. A spectral efficiency metric is defined that express how well the available spectrum is utilized. There are two terms that contribute to this metric. They are the correct transmissions factor η_c and the faulty transmissions penalty η_f . η_f is also to be understood as the maximum interference ratio into the primary system if a primary user is doing a continuous transmit operation. The total spectrum efficiency metric is defined by subtracting these two terms after weighting them equally

$$\eta = \eta_c - \eta_f \tag{15}$$

Correct transmissions are defined as transmissions done when the channel is idle during a free window of W consecutive samples. The utilization of this window is

$$\eta_c = \frac{W - ARL_1}{W} \tag{16}$$

where the length of the secondary user transmission is $W-ARL_1$. If ARL_1 approaches zero, the utilization approaches

unity which is the highest possible. If $ARL_1 \geq W$, no mean successful utilization is possible. The second term of the spectral efficiency is the penalty when interfering into the primary user spectrum

$$\eta_f = \frac{W - ARL_1}{W - ARL_1 + ARL_0} \tag{17}$$

where $W-ARL_1+ARL_0$ is the average length between each faulty transmission. The efficiency metric η approaches its optimal value unity if $ARL_1 \ll W \ll ARL_0$. Note that the idle window size W is assumed either known or estimated by the secondary users. Once the primary user turn-off change point \hat{m} is detected at the stopping time instant T , the secondary user is assumed to be capable of transmitting a packet with duration $W + \hat{m} - T$ before the free slot of opportunity closes after W samples. If in doubt about the size of W and the accuracy of \hat{m} , the secondary user may decide to turn off early to allow itself to search for the primary user turn-on to update estimates of W . The cognitive radio spectral efficiency in case of correct knowledge of W and negligible variance of \hat{m} becomes

$$\eta \approx \frac{W - k_1\gamma}{W} - \frac{W - k_1\gamma}{W - k_1\gamma + k_0e^\gamma} \tag{18}$$

From this equation it is possible to find the maximum efficiency for a given SNR and W by varying γ . The result is given in Fig. 6. It is thinkable to utilize short windows of opportunity if the SNR from all primary users is known to be high. However, at an SNR of -21 dB, at least 12,000,000 free samples are needed to give an utilization higher than 95%. All different CUSUMs, independent of SNR optimality set point, surprisingly need the same threshold γ for a given efficiency. For example at 95% efficiency a threshold of 10.8 is needed. At 97.5% efficiency the threshold has to be increased to 12.4 regardless of CUSUM SNR setting.

It is also important to check out η_f versus η . This is given in Fig. 7. With a total efficiency of 95% the maximum interference ratio into the primary system becomes 0.43%.

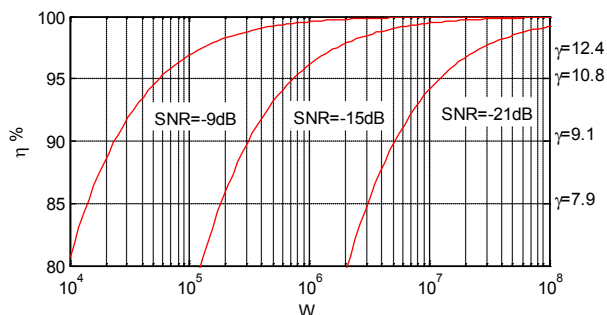


Figure 6. Maximum spectrum efficiency utilization η versus W for three different CUSUMs and their individual SNR at optimal γ .

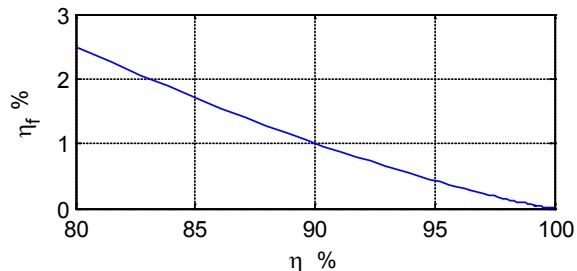


Figure 7. Primary system interference η_f versus total spectral efficiency η in percent at optimal γ .

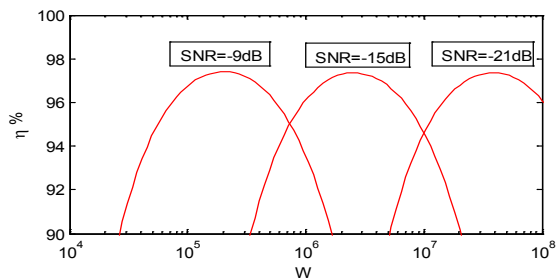


Figure 8. Spectrum efficiency utilization η versus W and SNR for three different CUSUM having equal thresholds $\gamma=10.8$.

If on the other hand the thresholds of all CUSUMs are frozen to for example 10.8, then the spectrum efficiency versus W becomes modified as shown in Fig. 8. Because the threshold now is constant, the efficiency will begin to drop when W increase above a certain maximum length. In this situation the penalty η_f due to longer faulty transmissions starts to increase. To avoid this burden for the primary user system, an adaptive threshold setting versus W is necessary.

The spectral efficiency found here is close to the results given in [6] using a predefined fixed window length. The main difference and the benefit of recursive sequential detection compared to block based sensing is that the sensing window length is not chosen in advance but rather is decided by the algorithm itself as soon as the predefined likelihood is reached. As a consequence, sequential detection is more robust to variable conditions. Another complicating factor of block based sensing is the need for synchronization or sliding window techniques to maintain an optimum start with respect to the unknown change point.

VI. CONCLUSION

Two algorithms for ML optimal change detection have been presented and compared for cognitive radio application. The R-GLRT achieves as expected better performance under unknown SNR conditions particularly for power on detection. Power off detection is very well handled by the traditional CUSUM detector. For 95% spectrum efficiency utilization a free window of 50,000 samples is needed at SNR=-9dB, 700,000 free samples is needed for SNR=-15dB and 12,000,000 free samples is needed for SNR=-21dB. It is shown that the interference level against the primary users in this case is 0.43%

independent of SNR.

The processing burden of the R-GLRT as simulated in this paper, is about 20 additions per input sample and unlike traditional GLRT completely independent of observation window size and threshold setting. Therefore both the traditional CUSUM and the R-GLRT algorithm are particularly useful in cognitive radio when doing lengthy estimations at low SNR and low probability of false alarm.

REFERENCES

- [1] E.S. Page, "Continuous inspection schemes," *Biometrika*, 1954, vol. 41, pp.100-115.
- [2] S. M. Kay, *Fundamentals of statistical signal processing Volume II Detection theory*, Prentice hall, 2009.
- [3] M. Basseville, I. V. Nikiforov, *Detection of Abrupt Changes: Theory and Application*, Previously published by Prentice-Hall Inc.
- [4] H. Vincent Poor and O. Hadjiladis, *Quickest Detection*, Cambridge University Press, 2009.
- [5] K. Husby, A. Lie, and J. E. Håkegård, "Quickest recursive GLRT Maximum Likelihood change detection," 2012, unpublished.
- [6] A. M. Wylinski, M. Nekovee, and Y. T. Hou, *Cognitive radio communications and networks, Principles and Practice*, Academic Press, 2010.
- [7] G. Lorden, "Procedures for reacting to a change in distribution," *The Annals of Mathematical Statistics* 1971, vol. 42, No. 6, 1897-1908.
- [8] G. J. Ross, D. K. Tasoulis, and N. M. Adams, "Sequential monitoring of a Bernoulli sequence when the pre-change parameter is unknown," *Comput Stat*, doi: 10.1007/s00180-012-0311-7, Springer-Verlag, 2012.
- [9] H. Li, C. Li, and H. Dai, "Quickest Spectrum Sensing in Cognitive Radio," 42nd Annual Conference on Information Sciences and Systems, doi: 10.1109/CISS.2008.4558521, pp. 203-208, 2008.
- [10] L. Lai, Y. Fan, and H. Vincent Poor, "Quickest Detection in Cognitive Radio: A Sequential Change Detection Framework," doi: 10.1109/GLOCOM.2008.ECP.567, pp. 1-5, IEEE GLOBECOM, 2008.
- [11] G. Verdier, N. Hilgert, and J. P. Vila, "Optimality of CUSUM Rule Approximations in Change-Point Detection Problems: Application to Nonlinear State-Space Systems," *IEEE Transactions on information theory*, vol. 54, No. 11, pp. 5102-5112, November 2008.
- [12] F. Gustafsson, "The marginalized likelihood ratio test for detecting abrupt changes," *Automatic Control*, *IEEE Transactions on* 41(1): pp. 66-78, 1996.
- [13] T. Kerr, "Decentralized Filtering and Redundancy Management for Multisensor Navigation," *Aerospace and Electronic Systems*, *IEEE Transactions on* AES-23(1): pp. 83-119, 1987.
- [14] J. M. Lucas and R. B. Crosier, "Fast Initial Response for CUSUM Quality-Control schemes: Give your CUSUM a head start," *Technometrics*, vol. 24, NO. 3, August 1982
- [15] J. Lee, S. Pullen, and P. Enge, "Sigma-mean monitoring for the local area augmentation of GPS," *Aerospace and Electronic Systems*, *IEEE Transactions on* 42(2): pp. 625-635, 2006.
- [16] G. V. Moustakides, "Quickest detection of abrupt changes for a class of random processes," *Information Theory*, *IEEE Transactions on* 44(5): pp. 1965-1968, 1998.
- [17] R. Tandra and A. Sahai, "SNR Walls for Signal Detection," *IEEE Journal of selected topics in signal processing*, vol. 2, NO. 1, pp. 4-17, doi: 10.1109/JSTSP.2007.914879, Feb 2008.

Sensing of DVB-T Signals for White Space Cognitive Radio Systems

Daniel Riviello, Roberto Garello
Dipartimento di Elettronica e Telecomunicazioni
Politecnico di Torino
Torino, Italy
Email: daniel.riviello@studenti.polito.it,
roberto.garello@polito.it

Sergio Benco, Floriana Crespi, Alberto Perotti
Networks and Wireless Communications
CSP-ICT Innovation
Torino, Italy
Email: {sergio.benco, floriana.crespi, alberto.perotti}@csp.it

Abstract—In cognitive radio networks, systems operating in digital television white spaces are particularly interesting for practical applications. In this paper, we consider single-antenna and multi-antenna spectrum sensing of real DVB-T signals under different channel conditions. Some of the most important algorithms are considered and compared, including energy detection, eigenvalue based techniques and methods exploiting OFDM signal knowledge. The obtained results show the algorithm performance and hierarchy in terms of ROC and detection probability under fixed false alarm rate, for different channel profiles in case of true DVB-T signals.

Keywords—Cognitive radio; spectrum sensing; DVB-T; OFDM; white spaces.

I. INTRODUCTION

The increasing demand for higher data rates in wireless communications is a strong driver for research and development of new communication technologies able to exploit transmission opportunities wherever licensed channels are not employed by primary users. One of most relevant developments in this context aims at exploiting the so called TV white spaces in order to provide internet access through broadband wireless communications.

Cognitive radio networks and systems [1] are based on an efficient *spectrum sensing* unit [2] in order to gain awareness of the available transmission opportunities through the observation of the surrounding electromagnetic environment. Such unit's ultimate goal consists in providing an indication on whether a primary transmission is taking place in the considered channel. Such indication is determined as the result of a binary hypothesis testing experiment wherein hypothesis \mathcal{H}_0 (\mathcal{H}_1) corresponds to the absence (presence) of the primary signal. Thus, the sensing unit collects samples of kind

$$y(n)|_{\mathcal{H}_0} = w(n) \quad (1)$$

$$y(n)|_{\mathcal{H}_1} = x(n) + w(n). \quad (2)$$

where $x(n)$ are samples of the primary transmitted signal and $w(n)$ are noise samples.

Given the vector y of all samples, the sensing algorithm builds a test statistics $T(y)$ and compare it against a predefined threshold θ . The performance of each detector is usually assessed in terms of *probability of detection* and

probability of false alarm

$$P_d = \mathbb{P}(T(y) > \theta | \mathcal{H}_1) \quad (3)$$

$$P_{fa} = \mathbb{P}(T(y) > \theta | \mathcal{H}_0) \quad (4)$$

as a function of the signal-to-noise ratio (SNR) ρ , defined as

$$\rho = \frac{\mathbb{E}\|x(n)\|^2}{\mathbb{E}\|w(n)\|^2}. \quad (5)$$

Several methods have been proposed for the computation of the test statistics: a comprehensive description can be found in [3] and references therein. In this paper, we consider the most important of these algorithms, including energy detection, multi-antenna eigenvalue based techniques under both known and unknown noise variance, and techniques exploiting the signal characteristics.

The added value of this paper is that the algorithms are applied to real DVB-T signals generated by a transmitter implemented on a DSP board and applied to different realistic channel profiles. This way, the algorithms performance are evaluated and compared in realistic conditions, providing useful results for practical realizations.

This paper is organized as follows: Section II describes the main characteristics of the DVB-T standard OFDM signal and the considered channel models. Section III describes the sensing algorithms employed in this investigation. Finally, in Section IV the obtained results are shown and commented.

II. PRIMARY SIGNAL

The DVB-T standard [4] specifies a set of coded OFDM transmission schemes to be used for broadcasting of multiplexed digital television programs.

The transmitted signal consists of a sequence of fixed-duration OFDM symbols. A cyclic prefix (CP) is prepended to each symbol in order to avoid inter-symbol interference over frequency-selective fading channels. The most relevant parameters of DVB-T signals are shown in Table I.

The signal bandwidth is approximately 7.61 MHz, with an intercarrier frequency spacing of 8MHz. A subset of the available 2048 subcarriers (in 2k mode) or 8192 subcarriers (in 8k mode) are used to carry higher layer data and PHY-layer signalling information. The latter consists

Table I
MAIN PARAMETERS OF DVB-T.

	2k mode	8k mode
Symbol duration (T_U)	224 μ s	896 μ s
Guard interval duration (Δ)	7 – 56 μ s	28 – 224 μ s
Number of active subcarriers	1705	6817
Subcarrier spacing (approx.)	4464Hz	1116Hz
CP duration ratio (Δ/T_U)	1/4, 1/8, 1/16, 1/32	
Constellations	QPSK, 16-QAM, 64-QAM	
Code rate	1/, 2/3, 3/4, 5/6, 7/8	

of pilot sequences, either allocated to fixed subcarriers (continual pilots) or scattered throughout OFDM symbols according to a periodic pattern, which are used for channel estimation at the receiver side, and Transmission Parameter Signaling (TPS) information, wherein encoded information about the current transmission parameters used on data subcarriers is delivered.

OFDM symbols with CP are grouped into frames and superframes: each frame consists of 68 symbols and each superframe consists of 4 frames.

In our study, we used a real encoded and modulated MPEG transport stream (TS) with code rate 5/6, 64-QAM constellation and CP ratio 1/4. The resulting bit rate is approx. 24.88 Mbits/s. At the sensing unit, the DVB-T signal was sampled at the nominal rate of 64/7 Msamples/s.

A. DVB-T signal characteristics

As a common assumption in the literature on spectrum sensing, the primary signal is modeled as a Gaussian process. Fig. 1 shows that, in the case of DVB-T signals, this assumption is well motivated. In fact, Fig. 1(a) shows the *pdf* of the real and imaginary parts of the DVB-T signal's complex envelope. Clearly, the Gaussian distribution is very well approximated. A more accurate evaluation is provided in Fig. 1(b), where the *quantile-quantile* plot of the DVB-T distribution vs. a zero-mean Gaussian distribution with same variance is shown.

Let us assume that the primary signal is detected through K sensors (receivers or antennas). Typically, a flat Rayleigh fading channel is considered in the literature. In such case, the received signal can be modeled as a linear mixture model of the kind

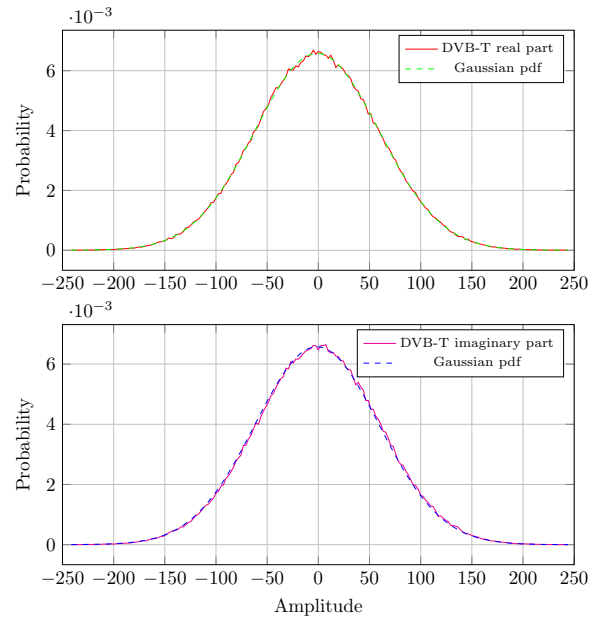
$$\mathbf{y}(n) = \mathbf{h}x(n) + \mathbf{v}(n) \quad (6)$$

where \mathbf{h} is the K -element channel vector of size $K \times 1$ whose elements $h_i \sim N_{\mathbb{C}}(0, \sigma_h^2)$ are mutually independent. Moreover we apply the following normalization:

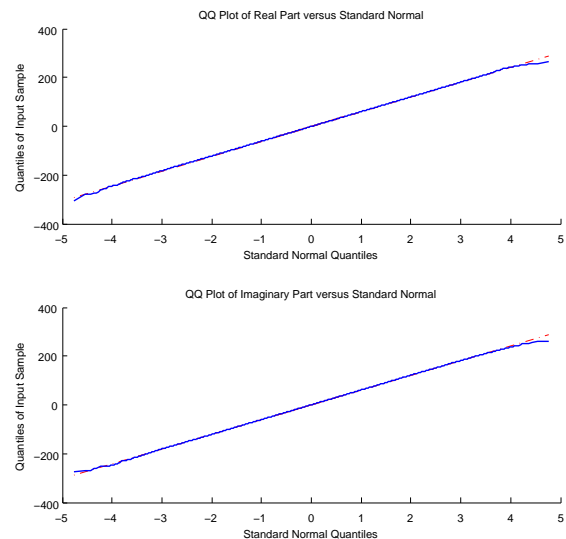
$$\sum_{n=1}^K h_n h_n^* = K. \quad (7)$$

Moreover, $\mathbf{v}(n)$ is the additive white Gaussian noise distributed as $N_{\mathbb{C}}(\mathbf{0}_{K \times 1}, \sigma_v^2 \mathbb{I}_{K \times K})$.

In order to assess the performance of the considered algorithms in a more realistic case, we used a frequency- and time-selective channel model, the 6-path Typical Urban (TU6) mobile radio propagation model developed by



(a) Estimated probability density function.



(b) Quantile-quantile plot.

Figure 1. Statistics of the DVB-T signal.

the COST 207 European project [5]. The Doppler spread has been set to 10Hz.

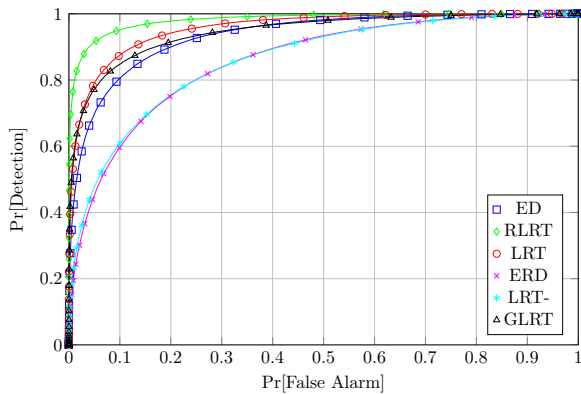
III. TEST STATISTICS

Let us suppose that the detector sensing algorithm builds its test statistic from K sensors (receivers or antennas) and N time samples. Let $\mathbf{y}(n) = [y_1(n) \dots y_k(n) \dots y_K(n)]^T$ be the $K \times 1$ received vector at time n , where the element $y_k(n)$ is the n -th discrete baseband complex sample at receiver k .

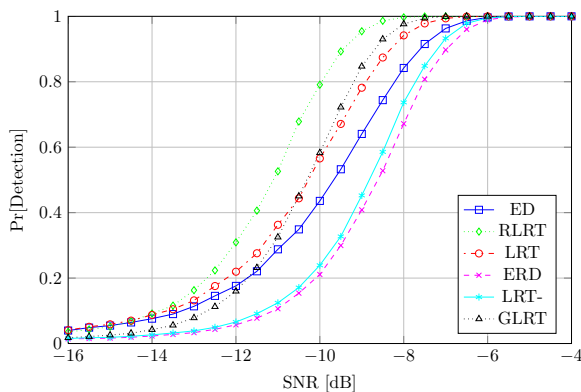
The noise is modeled as an additive white Gaussian noise process with zero mean and variance $\sigma_v^2 = N_0/2$, N_0 being the two-sided power spectral density of noise.

The received samples are stored in a $K \times N$ matrix:

$$\mathbf{Y} \triangleq [\mathbf{y}(1) \dots \mathbf{y}(N)]. \quad (8)$$



(a) Receiver operating curves (SNR = -10dB).



(b) Detection probability.

Figure 2. DVB-T signal through flat-fading channel.

The sample covariance matrix \mathbf{R} is:

$$\mathbf{R} \triangleq \frac{1}{N} \mathbf{Y} \mathbf{Y}^H \quad (9)$$

We will denote by $\lambda_1 \geq \dots \geq \lambda_K$ the eigenvalues of \mathbf{R} , sorted in decreasing order.

Many spectrum sensing algorithms have been proposed in the literature. Reviews and comparisons can be found, for example, in [3], [6] and [7]. In this paper, we consider some of the most popular tests, with the aim of comparing them against true DVB-T signals. The considered tests are divided in three classes.

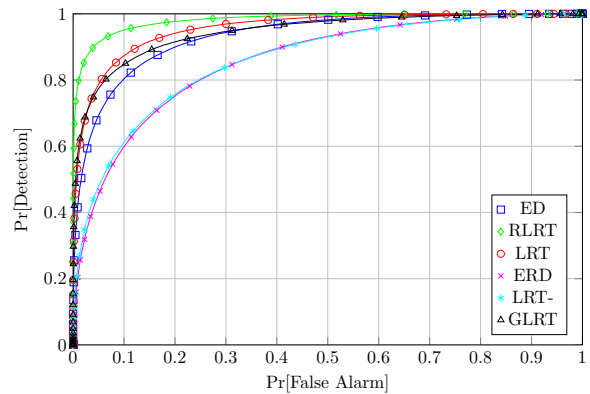
A. Non-parametric tests, known noise variance

These tests are non-parametric, i.e., do not exploit the knowledge of the signal characteristics. An excellent estimation of the noise variance σ_v^2 is supposed (obtained, for example, during a long training phase).

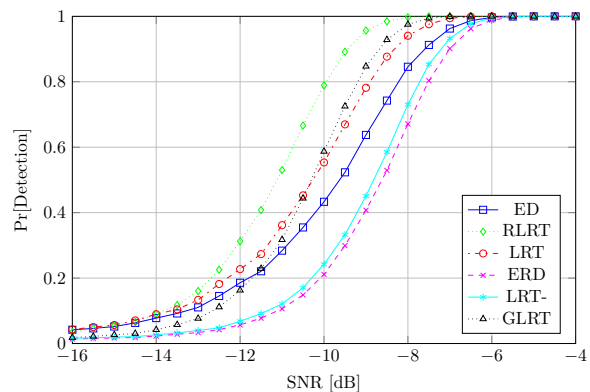
Energy Detection (ED): the test statistic is the average energy of the received samples, normalized by the noise variance:

$$T_{ED} = \frac{1}{KN\sigma_v^2} \sum_{k=1}^K \sum_{n=1}^N |y_k(n)|^2 \quad (10)$$

The energy detection method is probably the most popular technique for spectrum sensing, also thanks to



(a) Receiver operating curves (SNR = -10dB).



(b) Detection probability.

Figure 3. Gaussian signal through flat-fading channel.

its simplicity. Analytical performance expressions for this detector are well-known in the literature (e.g., [8]).

Roy's Largest Root Test (RLRT): this method tests the largest eigenvalue of the sample covariance matrix against the noise variance. The test statistic is

$$T_{RLRT} = \frac{\lambda_1}{\sigma_v^2} \quad (11)$$

The RLRT was originally developed in [9]. Performance analysis can be found, for example, in [10], [11], and [7]. For Gaussian signals and not too low signal-to-noise ratio, the RLRT is the best test statistics in this class.

Likelihood Ratio Tests (LRT): different LRT-based detectors were given in [6]. The complete, noise-dependent, log-likelihood ratio test statistic is given by

$$T_{LRT} = 2(N-1) \left[\log \left(\frac{\sigma_v^{2K}}{\det \mathbf{R}} \right) + \left(\frac{\text{tr} \mathbf{R}}{\sigma_v^2} - K \right) \right] \quad (12)$$

Performance analysis for this test can be found, for example, in [6].

B. Non-parametric tests, unknown noise variance

These tests are again non-parametric, but the noise variance is supposed unknown.

Generalized Likelihood Ratio Test (GLRT): this method uses as test statistic the ratio

$$T_{GLRT} = \frac{\lambda_1}{\frac{1}{K} \text{tr}(\mathbf{R})} \quad (13)$$

Performance analysis can be found for example in [12].

It is interesting to note that the GLRT is equivalent (up to a nonlinear monotonic transformation) to [7]:

$$T_{GLRT'} = \frac{\lambda_1}{\frac{1}{K-1} \sum_{i=2}^K \lambda_i}. \quad (14)$$

The denominator of $T_{GLRT'}$ is the maximum-likelihood (ML) estimate of the noise variance assuming the presence of a signal, hence the GLRT can be interpreted as a largest root test with an estimated $\hat{\sigma}_v^2$ instead of the true σ_v^2 .

Eigenvalue Ratio Detector (ERD): the test statistic (also called maximum-minimum eigenvalue, or condition number test) is the ratio between the largest and the smallest eigenvalue of \mathbf{R}

$$T_{ERD} = \frac{\lambda_1}{\lambda_K} \quad (15)$$

Performance analysis can be found, for example, in [13], [14].

Noise-independent LRT (LRT-): an alternative log-likelihood ratio was derived in [6], under the assumption of unknown noise variance:

$$T_{LRT-} = 2(N-1) \left[\frac{\frac{1}{K} \sum_{i=1}^K \lambda_i}{\left(\prod_{i=1}^K \lambda_i \right)^{1/K}} \right]^K \quad (16)$$

In statistics, this method has been known for many years as the *sphericity test* [15], [16]. Performance analysis for cognitive radio applications can be found, for example, in [6].

C. Parametric tests

Primary OFDM signal detection is considered. Primary signal detectors that exploit the presence of the CP in OFDM transmissions have been proposed. In [17] the detectors based on CP correlation described in [18] have been improved, applied to a real scenario and implemented using a software-defined radio platform.

As previously stated, DVB-T signal consists of OFDM modulated symbols of which a-priori parameter knowledge is assumed, such as: the number of subcarriers, cyclic prefix length, constellation type or the code rate. The aim of parametric test statistics is to exploit signal parameter knowledge (i.e., signal features) in order to enable primary signals detection with high sensitivity.

The algorithm implemented in [19] using SDR is the well known CP-based spectrum sensing. Assuming $N_s = N_c + N_d$ as the samples in a captured OFDM symbol (cyclic prefix plus data samples respectively), the correlation function (3) in [17], reproduced in (17) for clarity, provides the analysis of $2N_d + N_c$ samples coherently averaged over K symbols.

$$R_{xx}^{(CP)}[n, \tau] = \frac{1}{KN_s} \left| \sum_{k=0}^{K-1} \sum_{n=\tau+kN_s}^{\tau+(k+1)N_s-1} x^*[n]x[n+N_d] \right| \quad (17)$$

where τ represents the synchronization mismatch between our capture and the symbol start. It can be modelled as uniformly distributed over the interval $[0, N_c + N_d - 1]$, that defines the minimum period in which one correlation maximum occurs.

The coherent averaging before taking the absolute value allow us to improve sensitivity, in presence of AWGN noise, at the cost of a larger capturing interval. Moreover, to enable the implementation of these algorithms, it is necessary to define a noise estimation algorithm to set a threshold that guarantees certain detection performance in terms of probability of false alarm (P_{FA}) and probability of detection (P_D).

In this paper, a slight improvement in terms of noise estimation accuracy (i.e., correlation noise) with respect to [17] is presented. In fact, without any a-priori assumption, the correlation noise estimation should be performed by analyzing the received samples when the H_0 hypothesis is true. Hence training periods with only noise samples must be performed periodically (e.g., to track system temperature changes). To avoid dedicated training, we observed that noise samples can be gathered in between two consecutive correlation maxima. The correlation function \tilde{R} used to estimate the average correlation noise level, correspond to the function R excluding $2N_c$ samples around the detected maxima. Our optimized CP-based algorithm can thus be resumed as following:

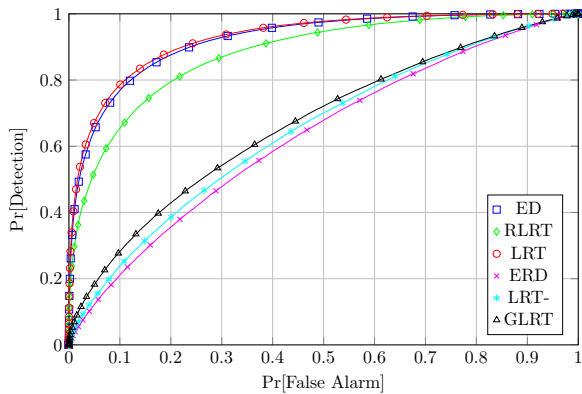
- 1) Receive $K(N_c + N_d) + N_d$ samples
- 2) Perform (17) over captured samples
- 3) Record the correlation maximum and its index i
- 4) Copy only correlation noise values from function in 2. by excluding values that have index in the range $i - N_c < i < i + N_c$
- 5) Decide if channel is occupied by evaluating the following metric:

$$\frac{\max R_{xx}^{(CP)}[n, \tau]}{\tilde{R}_{xx}^{(CP)}[n, \tau]} \underset{\leq}{\geq} \gamma \quad (18)$$

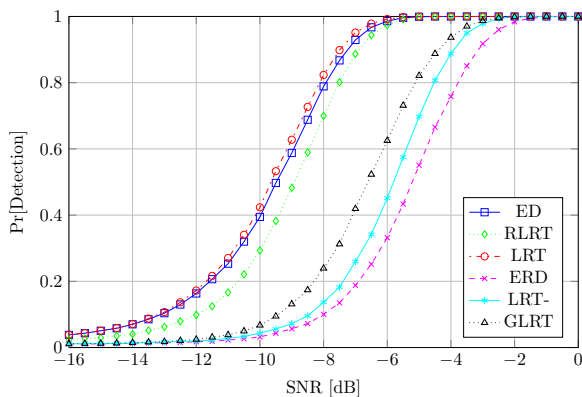
In order to obtain the curve plotted in Fig. 5, we firstly have calculated the threshold γ . To reproduce H_0 , white Gaussian distributed input noise samples were considered. In this way the γ value at which the $P_{FA} = 10^{-2}$ can be evaluated. We used a Monte Carlo approach over 1000 repetitions for $K=1$ (1 symbol). Once the threshold γ has been set, we varied the input SNR during H_1 tests to plot the corresponding P_D function.

IV. RESULTS

The results obtained for the DVB-T signal under linear mixture models provided by flat fading Rayleigh channel are reported in Fig. 2. First, we report the ROC (Receiver Operating Characteristic) curve obtained by plotting the detection probability versus the false alarm one. Then by fixing the false alarm rate to 0.01, we plot the detection probability as a function of the signal-to-noise ratio. By fixing the detection probability, this allows to evaluate the differences in terms of SNR between the algorithms, at the parity of detection and false alarm probability.



(a) Receiver operating curves (SNR = -10dB).



(b) Detection probability.

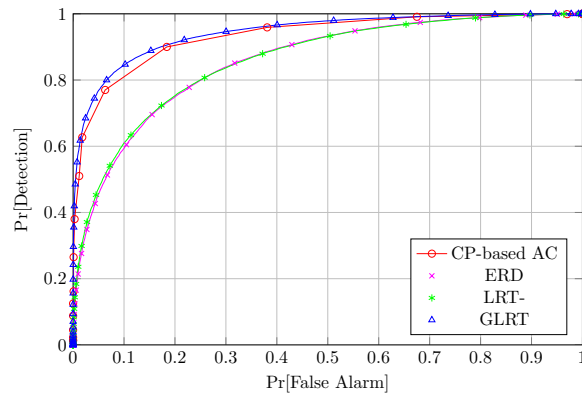
Figure 4. DVB-T signal through TU6 channel.

Simulations have been performed assuming $K = 10$ antennas and an observation interval corresponding to $N = 50$ samples. For the CP correlation method, an interval corresponding to one OFDM symbol has been considered. Moreover, in such case, the signal was sampled at 12.5 Msamples/s.

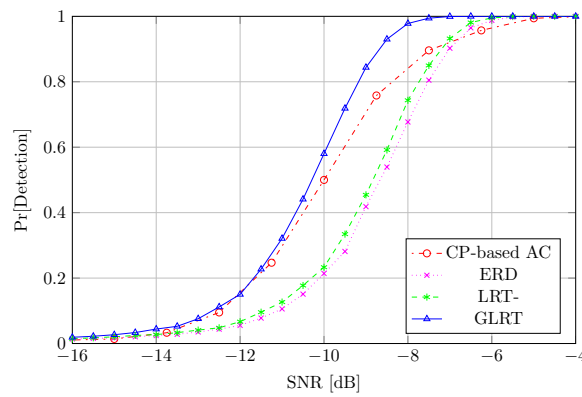
By looking at Fig. 2 we can observe that the best algorithm for known noise variance is the RLRT, while GLRT is the best under unknown variance. It is interesting to note that these results are in agreement with the results providing in the literature for Gaussian signals. As a reference, results for the same algorithms obtained by simulating Gaussian signal samples are reported in Fig. 3 and are essentially identical to the previous one (as expected after verifying the Gaussian properties of the DVB-T signal).

Under a more realistic model, the TU6 channel, the performance of the algorithms are different, as can be observed in Fig. 4. We can see how both GLRT and RLRT lose their predominant position when the received model is different from the linear mixture one: simple energy detection becomes highly competitive in this case. The difference between algorithms with known and unknown noise variance is larger, too.

It is important to note that in this work we have supposed a perfect known noise variance for RLRT, LRT and energy detection. Further analysis will be applied to



(a) Receiver operating curves (SNR = -10dB).



(b) Detection probability.

Figure 5. Comparison with the CP correlation method [17], [18].

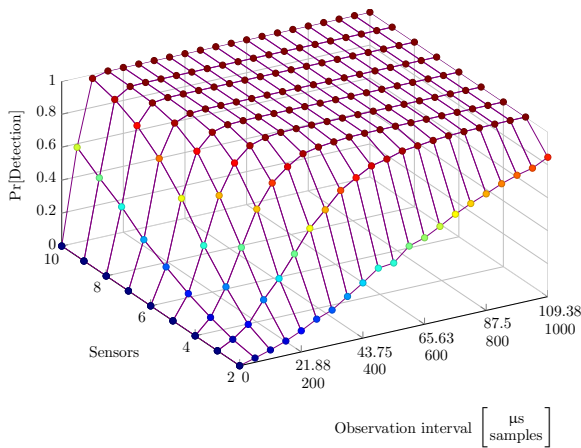
study their performance under imperfect noise variance knowledge, and address its impact for real DVB-T signals (analysis for Gaussian signals can be found, for example, in [19] for energy detection and [7] for RLRT).

Furthermore, we compare the algorithms for unknown noise variance against the technique exploiting the cyclic prefix autocorrelation of the received signal [17], [18] described before. Here, the AWGN channel model is adopted. In this case we can observe that the performance of this algorithm is similar to that of the GLRT. This single-antenna algorithm does not require the computation of the sample covariance matrix eigenvalues, but resorts to a precise knowledge of the signal characteristics.

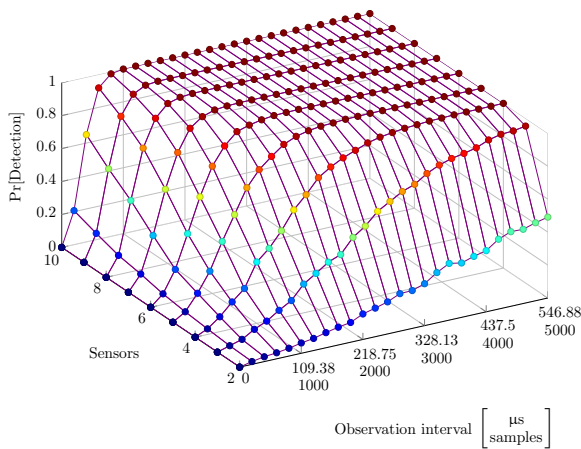
Finally, in Fig. 6 we plot the detection probability of GLRT as a function of the observation interval (expressed both in time units and number of received samples per sensor) and the number of sensors for a specific SNR value of -10dB and -15dB, while the false alarm probability remains fixed to 10^{-2} . The channel is Rayleigh flat-fading. As shown, it is possible to obtain the same performance achieved in Fig. 2 using $N = 10$ sensors even with a lower and hence more realistic number of antennas.

V. CONCLUSIONS

Some of the most important sensing algorithms have been applied to real DVB-T signals and their performance has been assessed considering different channel profiles. The flat fading channel analysis confirms the results



(a) SNR = -10dB, $P_{fa} = 0.01$.



(b) SNR = -15dB, $P_{fa} = 0.01$.

Figure 6. GLRT detection probability as a function of time (samples) and sensors through flat-fading channel.

previously obtained by simulation using linear mixture models of Gaussian signals. Under a more realistic multipath channel model, the performance and hierarchy of the algorithms completely change with respect to the flat-fading case. The obtained results are very useful for the implementation of cognitive systems and networks operating in the digital television white spaces.

REFERENCES

[1] J. Mitola, III, "Cognitive radio - an integrated agent architecture for software defined radio," Ph.D. dissertation, Royal Institute of Technology (KTH), May 2000.

[2] S. Haykin, D. J. Thomson, and J. H. Reed, "Spectrum sensing for cognitive radio," *Proceedings of the IEEE*, May 2009, pp. 849-877

[3] Y. Zeng, Y.-C. Liang, A. T. Hoang, and R. Zhang, "A review on spectrum sensing for cognitive radio: Challenges and solutions," *EURASIP Journal on Advances in Signal Processing*, Jan. 2010, pp. 1-15

[4] European Telecommunications Standards Institute, "ETSI EN 300 744, digital video broadcasting (DVB); framing structure, channel coding and modulation for digital terrestrial television," Jan. 2009.

[5] COST207, "Digital land mobile radio communications (final report)," Commission of the European Communities, Directorate General Telecommunications, Information Industries and Innovation, Tech. Rep., 1989.

[6] Q. Zhang, "Advanced detection techniques for cognitive radio," in *Proc. of International Conference on Communications (ICC 2009)*, Jun. 2009, pp 1-5.

[7] B. Nadler, F. Penna, and R. Garello, "Performance of eigenvalue-based signal detectors with known and unknown noise level," in *Proc. of International Conference on Communications (ICC 2011)*, Jun. 2011, pp. 1-5.

[8] H. Urkowitz, "Energy detection of unknown deterministic signals," *Proceedings of the IEEE*, Apr. 1967, pp. 523-531.

[9] S. N. Roy, "On a heuristic method of test construction and its use in multivariate analysis," *Annals of Mathematical Statistics*, Jun. 1953, pp. 220-238.

[10] L. Wei and O. Tirkkonen, "Cooperative spectrum sensing of ofdm signals using largest eigenvalue distributions," in *IEEE International Symposium on Personal, Indoor and Mobile Radio Communications (PIMRC 2009)*, Sep. 2009, pp. 2295-2299.

[11] S. Kritchman and B. Nadler, "Non-parametric detections of the number of signals: Hypothesis testing and random matrix theory," *IEEE Transactions on Signal Processing*, Oct. 2009, pp. 3930 -3941.

[12] P. Bianchi, J. Najim, G. Alfano, and M. Debbah, "Asymptotics of eigenbased collaborative sensing," in *Proc. IEEE Information Theory Workshop (ITW 2009)*, Oct. 2009, pp. 515-519.

[13] Y. H. Zeng and Y.-C. Liang, "Eigenvalue based spectrum sensing algorithms for cognitive radio," *IEEE Transactions on Communications*, Jun. 2009, pp. 1784-1793.

[14] F. Penna, R. Garello, and M. A. Spirito, "Probability of missed detection in eigenvalue ratio spectrum sensing," in *5th IEEE International Conference on Wireless and Mobile Computing, Networking and Communications (WiMob)*, Oct. 2009, pp. 117-122.

[15] W. J. Krzanowski, *Principles of Multivariate Analysis: A User's Perspective*. Oxford University Press, 2000.

[16] J. W. Mauchley, "Significance test for sphericity of a normal n-variate distribution," *Annals of Mathematical Statistics*, Jun. 1940, pp. 204-209.

[17] S. Benco, F. Crespi, A. Ghittino, and A. Perotti, "Software-defined white-space cognitive systems: implementation of the spectrum sensing unit," in *The 2nd Workshop of COST Action IC0902*, Oct. 2011, pp. 1-3.

[18] D. Danev, E. Axell, and E. G. Larsson, "Spectrum sensing methods for detection of DVB-T signals in AWGN and fading channels," in *Proc. IEEE 21st International Symposium on Personal Indoor and Mobile Radio Communications (PIMRC)*, Sep. 2010, pp. 2721-2726.

[19] R. Tandra and A. Sahai, "SNR walls for signal detection," *IEEE Journal of Selected Topics in Signal Processing*, Feb. 2008, pp. 4-17.

Software Defined Radio Transceiver Front-ends in the Beginning of the Internet Era

Silvian Spiridon^{1,2}

¹POLITEHNICA University of Bucharest, Electronics, Telecommunication and Information Technology Department

²Now with Broadcom Corporation, Bunnik, The Netherlands

silvian.spiridon@gmail.com

Abstract— A mobile terminal today embeds a large number of technologies that maximize its interconnection capabilities. Regardless it is long or short range communication, the wireless terminal is definitely enabled to communicate efficiently over a large number of wireless standards. Nonetheless, the ideal candidate for such a mobile terminal radio front-end is the Software Defined Radio (SDR). This paper overlooks the key features required for a SDR in the beginning of the internet era and brings light on what is the best way to approach the SDR receiver design.

Keywords—Software defined radio transceiver; multi-standard radio receiver

I. INTRODUCTION

Communication is an intrinsic part of the human nature. Through communication information is conveyed. Today's communication is driven by the Internet.

The Internet foundations were laid in 1960s by the USA military research projects aimed at building distributed computer networks. The internet mass global spread was delayed due to lack of networking infrastructure and limited number of PC users. But, in mid 1980s the PC market boomed due to IBM's Personal Computer based on Intel 80286 microprocessor and operated by Microsoft's Disk Operating System (MS-DOS). This combination formed the template for all PC developers and vendors.

Hence, during the 1990s, it was estimated that the number of Internet users doubled each year, with a brief period of explosive growth in 1996 and 1997. By end of 2011, the Internet reached 32.5 users per 100 inhabitants worldwide, see Fig. 1, [1].

In order to show the strong relation between the IT industry and the communication sector, Fig. 1 plots the number of worldwide subscribers of fixed and mobile telephone networks and Internet users. The Internet access connects the two sectors.

The Internet was initially developed as a "wired" network. Nevertheless, as Fig. 1 reveals the latest trends show the communication sector is strongly going mobile, as today the mobile subscribers number surpasses the fixed telephony ones by a factor of five.

Therefore, radio circuits designers need to account this trend and focus on the development of efficient solutions that maximize the mobile's terminal wireless interconnectivity.

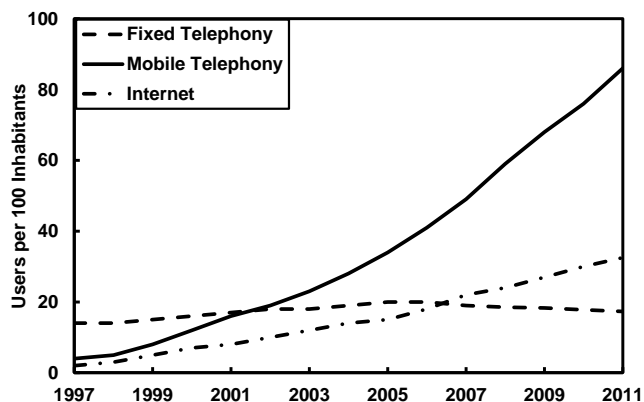


Figure 1. Internet usage – the driving force behind the need for SDRs

Section II overviews the historical development of wireless transceivers and defines the need for SDRs as the next step in the optimization process of wireless front-ends.

Section III overviews the generic SDR structure that is implemented in today's Systems on a Chip (SoCs), while in Section IV a designed receipt is proposed for the SDR receiver (SDRR) front-end.

Finally, the paper is concluded by Section V, which also overlooks the future developments.

II. THE NEED FOR SOFTWARE DEFINED RADIOS

A basic modern communication system is comprised by a large array of mobile equipment connected into wireless networks.

The communication between all these equipment is regulated by various communication standards, depending on the type of wireless network in which they operate.

Our lives today are bounded by the Internet. As presented in Section I, Internet access is possible over a wide array of wireless standards.

Hence, purely on the communication side, the present mobile equipment requires compatibility with all the standards maximizing its interaction capabilities: GSM/GPRS, UMTS, LTE, Bluetooth, Wireless LAN, LTE, WiMAX or DVBH.

Unifying the various communications standards is not a real possibility, given the huge number of users dedicated to a given wireless standard.

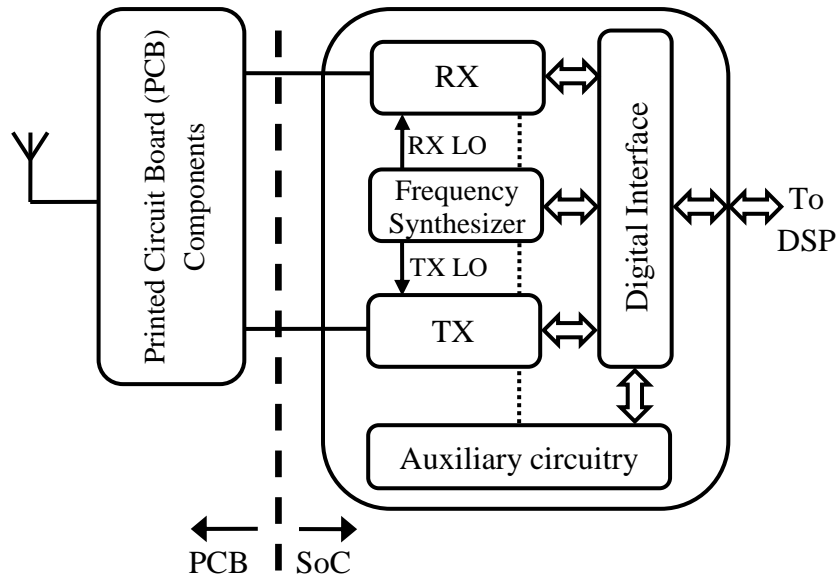


Figure 2. Software Defined Radio Transceiver Generic Block Schematic.

Therefore, there is a need of mobile equipment that enables wireless communication across the various wireless environments.

The first obvious solution was to incorporate for each standard a separate dedicated IC or Application Specific Integrated Circuit (ASIC) into the mobile device. One still has to have in mind the first Nokia mass production GSM mobile phone. The Nokia 1011 developed in the early '90s, was built from more than two dozen separate ICs and weighted about half a kilo [2]. By mid 2000's, solutions offering fully integrated quad-band GSM SoCs, [3] were already available.

A first step in reducing the cost for radio frequency (RF) front-end chips was enabled by the CMOS technology scaling. It opened the possibility of building "combo" ASICs, combining two or more SoCs on the same IC (e. g., BCM2071 [4] that integrates Bluetooth, GPS and FM radio or BCM4325 [5] that incorporates W-LAN, Bluetooth and FM radio). However, these circuits still contain one RF front-end per communications standard.

Moving forward, the natural step in the development of multi-standard communication is building a reconfigurable ASIC, able to ensure compatibility with the wide array of communication standards in use today. Such an approach is efficient from two main reasons [6]:

- One "universal" design is required; thus design, packaging and testing costs are minimized, and
- As the "universal" ASIC is compatible with a wide array of wireless communication standards the previous various ASICs can be merged; thus the overall area of ASICs comprised in a mobile terminal is minimized.

In the "digital" realm the first step on this path is the development of the new multi-core Digital Signal Processor (DSP) architectures [7]. Such processors optimally leverage

the power consumption with the IC cost, or equivalently its die area.

The idea behind it is to enforce as much parallel processing as possible to maintain a maximum "usage" of the chip die area during operation.

In this context, it is required to develop an RF transceiver capable to interface such a DSP. This RF transceiver is the Software Defined Radio (SDR).

III. TODAY'S SOFTWARE DEFINED RADIO TRANSCEIVER FRONT-ENDS

The RF transceiver SDR must employ a versatile architecture, able to change its characteristics dynamically given the particularities of each wireless standard and communication burst it has to handle.

The software driven System-on-a-Chip (SoC) combining such a re-configurable RF front-end and a multi-core DSP represents the Software Defined Radio (SDR). The block schematic of such a system is depicted in Fig. 2.

The four main blocks comprising the SDR RF front-end of Fig. 2 are:

- the frequency synthesizer (FS),
- the receiver (RX),
- the transmitter (TX), and
- the auxiliary circuitry (AUX)

The transceiver acts as a signal conditioning block. It either prepares the received signal for digital demodulation or it shapes the digitally modulated signal for the wireless transmission.

The DSP drives the RF front-end via the digital interface. By dynamically changing the transceiver settings, its performance can be adjusted depending on the requirements (e. g., noise or linearity performance, output power level) of the particular communication burst.

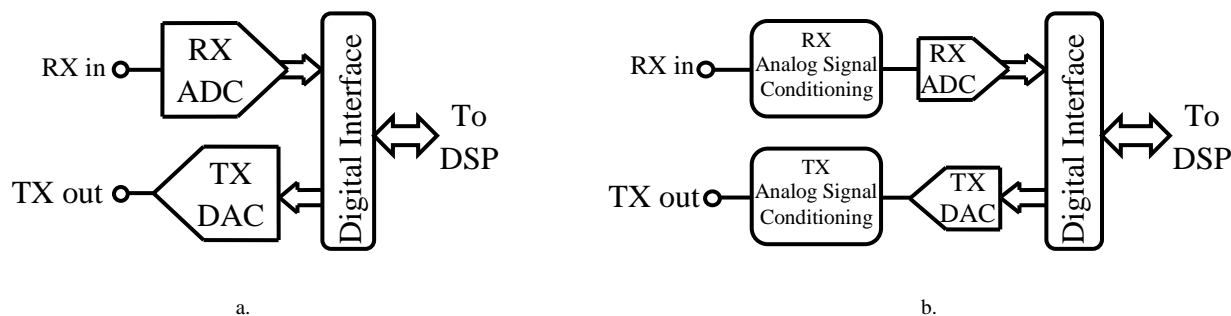


Figure 3. Software Defined Radio Simplified Block Schematic (FS and AUX not shown):
a. Mitola's Concept; b. SDR embedding analog signal conditioning.

The FS is the RF transceiver “heart”. Its beat is represented by the generation of the local oscillator (LO) signals which drive the receiver (RX LO), respectively the transmitter (TX LO).

The task of any wireless receiver is to condition the incoming wanted signal such as it can be properly demodulated.

Oppositely to the RX, the TX chain must ensure the up conversion on the RF frequency of the digitally modulated baseband signal. In the transmitter case the accent is placed on avoiding the disturbance of adjacent radio frequencies and maintaining a good signal integrity.

The auxiliary circuitry is mainly formed by the front-end's biasing block.

Fig. 6.a reveals the optimal choice from system level perspective for the TX and RX implementation. This multi-standard RF transceiver concept was coined by Mitola in [8]. Basically the RX is only an Analog-to-Digital Converter (ADC) and the TX is a Digital-to-Analog Converter (DAC). Of course, the transceiver requires a FS system to generate the ADC and DAC clocks.

In reality, due to practical implementation constrains, today's SDRs require analog signal conditioning blocks in between the antenna and the ADC and in between the DAC and the antenna (e. g., [6], [9-11]). The SDR concept shown in Fig. 6.b relaxes the ADC and DAC electrical specifications by ensuring for the wanted signal the frequency translation and additional selectivity and amplification.

IV. A DESIGN RECEIPT:

THE SOFTWARE DEFINED RADIO RECEIVER FRONT-END

In order to enhance the wireless system robustness and maximize the link budget, the latest wireless standards are very flexible (e. g, the IEEE 802.11g W-LAN uses BPSK, QPSK, QAM-16 and QAM-64 modulations on OFDMA carrier support).

Considering the abovementioned trend, as previously discussed it results the SDR is the natural solution for the radio front-end. For the receive side, the software re-

configurable hardware solution is the Software Defined Radio Receiver (SDRR).

As in-depth analyzed in [12], given the huge amount of information the SDRR designer(s) need to handle, a *structured approach* of the design process is the enabling factor in finding and implementing the optimal circuit design.

First the most suited architecture for the SDRR front-end needs to be identified. The homodyne architecture stemmed out as the best choice that matches very well the high level of integration of the current deep sub-micron CMOS processes [13, 14]. Fig. 4 presents the re-configurable homodyne radio receiver [6].

The incoming RF signal is picked-up by the receiver's antenna and is amplified by one of its LNAs. Multiple LNAs can be integrated, depending on the envisaged use. The amplified RF signal is then converted to current in the mixer input gm-stage and down-converted directly to baseband by mixing with a local oscillator signal of equal frequency. Hence, at the mixing stage output the signal has a spectrum spanning from DC to a maximum frequency that is dependent on the wireless communication standard [15].

After mixing, the signal is conditioned by a low pass filter (LPF) and a variable gain amplifier (VGA), before its conversion to digital spectrum by an analog-to-digital converter (ADC).

Second the designer has to be enabled to handle efficiently the large amount of information comprised in the wireless standards. The most effective way to do so is based on simple and efficient models suited for manual analysis.

In [16], the author introduces the SDRR *generic blockers diagram* as a very efficient tool in evaluating, in a standard independent approach, the filter partitioning for channel selection in multi-standard radio receivers. By mapping all blockers and interferers arriving at the receiver's antenna, the *generic blockers diagram* enables the designer to evaluate proficiently the trade-off between the analog low pass filter order and the ADC specifications of resolution and speed, or equivalently the trade-off between its area and power consumption. Thus the optimal analog low pass filter order is determined.

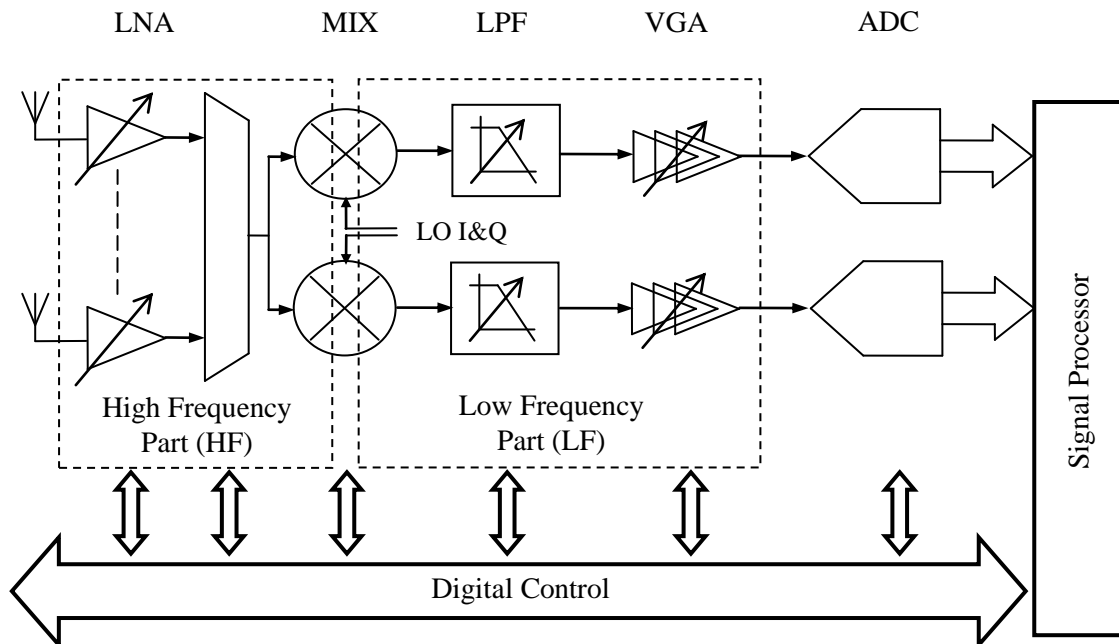


Figure 4. Software Defined Radio Transceiver Block Schematic [6].

In [17], the author introduces the *smart gain partitioning strategy* for multi-standard radio receivers. The strategy aims to aid the designer in identifying the optimal leverage between the receiver noise and linearity performance. Depending on the received signal strength, the receiver can change its noise or linearity characteristics accordingly (e. g., for large signal inputs the receiver will require a highly linear response, while it can tolerate more noise).

In the analysis from [17], the receiver gain thresholds at which the changes are triggered are calculated for various commercial standards. Thus, the designer is enabled to optimally handle the gain-noise-linearity partitioning. Of course, in order to enhance the model accuracy all these results should subsequently be completed by CAD simulations.

Third the designer needs to develop the SDRR front-end design strategy from both the system level and transistor level perspectives and to use this strategy to design the front-end's building blocks. As described in [18], the strategy needs to ensure the SDRR building blocks have the following characteristics:

- high linearity and low noise,
- immunity to particular technology characteristics and
- easiness of the design porting.

Basically, these targets are achieved by building *modular RF*, respectively *baseband circuits*, based on differential or pseudo-differential transistor pairs [18], respectively low power feedback amplifiers [19, 20].

V. CONCLUSIONS AND FUTURE TRENDS

This paper presented an overview of the key feature of software defined radio transceivers front-ends in the beginning of the internet era. The need for mobile equipment able to maximize its interconnection capabilities in conjunction with the VLSI integration have open the door for the SDR approach. Multi-core digital signal processors interfaced by flexible analog front-ends represent today's SDR.

Their transceiver front-ends employ a versatile architecture, able to change its key parameters dynamically (i. e., gain, noise, linearity performance and power consumption) based on the particular characteristics of the radio burst it handles.

Today's SDR front-ends are embedding analog signal conditioning blocks. Nevertheless, looking into the future and considering the rate at which the CMOS technology scales down, more and more signal processing is translated from the analog into the digital domain.

By making use of the relative inexpensive digital gates the modern transceivers analog circuits content is reduced [21]. This will impact the architecture of choice for all of the three key functional building blocks of the Fig. 5 SDR.

ACKNOWLEDGMENT

The author would like to acknowledge Prof. M. Bodea, and Dr. F. Op't Eynde for the fruitful discussions on the topic.

REFERENCES

- [1] Intl. Telecom. Union – Telecommunication Sector Statistics, Available on-line at:
<http://www.itu.int/ITU-D/ICTEYE/Indicators/Indicators.aspx>.
- [2] Nokia 1011, Wikipedia – the free encyclopedia, Dec 2012. Available on-line at:
http://en.wikipedia.org/wiki/Nokia_1011
- [3] K. Muhamad et al, The First Fully Integrated Quad-Band GSM/GPRS Receiver in a 90-nm Digital CMOS Process, IEEE Journal of Solid State Circuits, August 2006, vol. 41, Issue 8, pp. 1772-1783.
- [4] Broadcom BCM2071 – Bluetooth + GPS + FM Combination ('Combo') Chip Solution, Data-sheet available on-line at: <http://www.broadcom.com/products/Bluetooth/Bluetooth-RF-Silicon-and-Software-Solutions/BCM20751>
- [5] Broadcom BCM4325 – Low-Power 802.11a/b/g with Bluetooth 2.1 + EDR and FM, Data-sheet available on-line at: <http://www.broadcom.com/products/Bluetooth/Bluetooth-RF-Silicon-and-Software-Solutions/BCM4325>
- [6] S. Spiridon, Analysis and Design of Monolithic CMOS Software Defined Radio Receivers, PhD Thesis, Ed. Tehnică, 2011.
- [7] Multi-core processor, Wikipedia – the free encyclopedia, Dec 2012. Available on-line at:
http://en.wikipedia.org/wiki/Multi-core_processor
- [8] J. Mitola, Software radios – survey, critical evaluation and future directions, IEEE Nat. Telesystems Conf., 1992, pp. 13/15 – 13/23.
- [9] J. Craninckx et. al, “A Fully Reconfigurable Software-Defined Radio Transceiver in 0.13 μ m CMOS,” Digest of Technical Papers of the International Solid State Circuit Conference ISSCC 2007, pp. 346-347 and 607.
- [10] M. Ingels et. al, “A CMOS 100 MHz to 6 GHz software defined radio analog front-end with integrated pre-power amplifier,” Digest of Technical Papers of the European Solid State Circuit Conference ESSCIRC 2007, pp. 436-439.
- [11] M. Ingels et. al, “A 5mm² 40nm LP CMOS 0.1-to-3GHz multistandard transceiver,” Digest of Technical Papers of the International Solid State Circuit Conference ISSCC 2010, pp. 458-459.
- [12] S. Spiridon, C. Dan and M. Bodea, “Overcoming the challenges of designing CMOS Software Defined Radio Receivers front-ends embedding analog signal conditioning,” Proc of the 13th Intl. Conf. on Optimization of Electrical and Electronic Equipment, OPTIM 2012, pp. 1207-1210.
- [13] T. H. Lee, *The Design of CMOS Radio-Frequency Integrated Circuits*, Cambridge University Press, 2nd Ed., 2004, pp. 710-713.
- [14] S. Spiridon, C. Dan and M. Bodea, Defining the Optimal Architecture for Multi-Standard Radio Receivers Embedding Analog Signal Conditioning, Intl. Journal on Advances in Telecommunications, vol 5, no. 1&2, 2012, pp. 33–41.
- [15] S. Spiridon et. al., “Deriving the Key Electrical Specifications for a Multi-standard Radio Receiver,” Proc. Of the First Intl. Conf. on Advances in Cognitive Radio COCORA 2011, April 2011, pp. 60-63.
- [16] S. Spiridon, C. Dan, M. Bodea, “Filter partitioning optimum strategy in homodyne multi-standard radio receivers,” Proc. of the 7th Conf. on Ph.D. Research in Microelectronics and Electronics, PRIME 2011, July 2011, pp.9-13.
- [17] Spiridon et. al, “Smart gain partitioning for noise – linearity trade-off optimization in multi-standard radio receivers,” *Proceedings of the 18th International Conference Mixed Design of Integrated Circuits and Systems*, MIXDES 2011, June 2011, pp. 466-469.
- [18] S. Spiridon et al., “An Analysis of CMOS Re-configurable Multi-standard Radio Receivers Building Blocks Core,” *Revue Roumaine des Sciences Techniques, serie Electrotechnique et Énergétique*, tome 56, nr. 1, 2011, pp. 99-108.
- [19] V. Giannini et. al, “Flexible baseband analog circuits for software-defined radio front-ends,” *Journal of Solid State Circuits*, vol. 42, no. 7, July 2007, pp. 1501-1512.
- [20] S. Spiridon, F. Op’t Eynde, “An optimized opamp topology for the low frequency part of a direct conversion multi-standard radio transceiver,” *Proceedings of the First International Symposium on Electrical and Electronics Engineering*, ISEEE 2006, October 2006, pp. 11-16.
- [21] F. Op’t Eynde, “Maximally-Digital RF Front-end Architectures,” Invited paper at the European Microwave Week, EuMW 2010.

Emerging Applications of Cognitive Radios

Muhammad Adnan Qureshi, Muhammad Umar Khan, Mahmood Ashraf Khan
Centre for Advanced Studies in Telecommunication (CAST), COMSATS
Islamabad, Pakistan

{muhammad_adnan , umar_khan, mahmoodashraf} @comsats.edu.pk

Abstract— As per recent Federal Communications Commission (FCC) report, it has been observed that licensed spectrum bands are not being fully utilized by licensed users. Instead of exploring new spectrum bands at higher Giga hertz range, white spaces in existing frequency bands can be utilized for communication. Recently, cognitive radios have been introduced as being capable of increasing the spectral efficiency by opportunistically access both the licensed and unlicensed spectrum bands. In this literature, we have targeted some important applications of cognitive radios and surveyed the challenges facing by cognitive users in these applications.

Keywords- *cognitive radios; cognitive radio applications; CR emerging application*

I. INTRODUCTION

Cognitive radios are one of the computer-intensive systems which are also called to be “radio with a computer inside or a computer that transmits” [1]. Due to increasing use of wireless systems and scarce of the conventional static spectrum, policies have been formulated for unlicensed wireless devices by the Federal Communications Commission to opportunistically use spectrum holes in licensed bands, most importantly, the void spectrum spaces of TV band spectrum [2]. The expanding Cognitive Radio (CR) technology has proved itself a reliable technique of enhancing the spectral efficiency by employing the features of time, frequency, and space domains having harmless interference with previous systems.

The CR technology has equipped wireless radios and has given them a new dimension, they have the capacity to alter and modify several parameters to work with more intelligence and take decisions [3]. Cognitive radios are fully capable of choosing its own frequency in bandwidth rather than using predefined channels in accordance with the spectrum and network needs at hand. CRs are capable of cooperating very efficiently towards the possible use of the frequency band, as well with the presence of several cognitive radios and old system, non-cognitive, radios.

CR technology plays a major part in coming up with the appropriate use of the limited frequency band. It turns to help in contributing the ever increasing facilities for growing wireless appliances, like the TV spectrum through a smart grid, citizen safety, GSM network and body area network band for medical equipment. To take greater advantage of newly born opportunities, several standards, like “IEEE 802.22, IEEE 802.11af, ECMA 392, IEEE SCC41, and ETSI RRS)” are either in the development phase or are being finalized [7]. CR technology can use both licensed and unlicensed frequency bands for communication. The FM/AM, TV, GSM and satellite band spectrum, HAP control spectrums are a few examples of licensed frequency bands. License holder has the power to control the given

spectrum; therefore he can independently monitor and control noise factors present in the way of user equipment to ultimately achieve the quality of service (QoS).

Improvement in overall spectrum utilization for cognitive radios is achieved through active adjustment and adaptation to localized band availability [8]. It equips the secondary users (unlicensed users) to utilize the unused frequency band possessed by the primary users (licensed users) in the interference range which is below a certain threshold level. The Cognition Cycle (CC) plays a central role in making each SU to observe and learn, and will help to make the right decision at the right time for optimal performance of the network or close to optimal at all time. In particular, the network wide performance is significantly enhanced because of the cognition cycle as it enables the secondary users to use under-utilized spectrum opportunistically while maintaining the interference levels to a minimum for primary users.

In recent years, many advancements in CR technology have been evolved, for example, in addition to the licensed frequency band the unlicensed portions of the spectrum has also been reserved which could be used without any license by radios following a predefined set of rules. There can be a number of parameters to define that rule, one of that might be maximum power radiated per hertz (power spectral density) [6]. The prime advantage of utilizing the unlicensed spectrum is twofold, first to minimize the cost of purchasing licensed bands through auctioning which ultimately builds the burden on consumer end and hence the use of technology is finally discouraged. The other big gain is that it promotes innovation as the designers have the inherent constraint to use the same band for their cognitive radio architectures. These unlicensed bands have been shown to play an important role in wireless communications. This is reflected in the 2.4 GHz unlicensed systems such as Bluetooth, cordless phones and Wi-Fi-802.11b/g/n. Despite all the benefits of unlicensed bands, there is a limit to which we can further use them as if all the devices start using these bands then there would be too much interference that no communication would be possible.

Cognitive radios can be categorized into three main network paradigms: underlay, overlay, and interweave [6]. In case of underlay network paradigm, cognitive users are only allowed to operate if and only if the level of interference caused towards non-cognitive users is below a threshold. In overlay systems, cognitive radio uses excellent signal processing and coding to maintain or improve the communication of non-cognitive radios and at the same time get some extra bandwidth for their own communications. Finally, for interwoven systems, cognitive radio uses cunning strategy for exploiting spectral holes opportunistically without interfering with other transmissions.

The paper is structured as follows; Section II will cover the trending applications of cognitive radios and it is the core section of the paper. The applications which have been covered are; application of cognitive radios in wifi scenario, TV band devices, wireless broadband access, medical body area networks, smart grid networks, cellular networks, military applications and public safety networks. Finally, at the end, Section III will draw the paper conclusion.

II. COGNITIVE RADIO APPLICATION AREAS

Even though there is sound assurance of the fact that cognitive radio is an intelligent, smart and self-conscious technology, a variety of other interesting applications are also sprouting up stretching from commercial to health related; from Dynamic Spectrum Access (DSA) to interoperability applications towards the concept of universal transportable devices. However, the most preferred and favorite for technology developers right now is Dynamic Spectrum Access (DSA) and they see it as an extremely important application of CR technology [5].

A. Improvement in Spectrum Utilization for Wifi

CR techniques provide an appealing as well as fascinating strategy to dynamic spectrum allocation (DSA) [5]. As shown in Figure 1 a surprisingly simple and straightforward scenario exhibits 20 dB SINR betterment for wireless LAN (WLAN) employing cognitive radio strategies in an interference atmosphere setup over that offered by the existing IEEE 802.11a physical layer standard.

The experiment [5] narrows down to the license-free band 5.8 GHz ISM (industrial, scientific, and medical) to make the assessment of technique effectiveness with reference to frequency-band utilization of IEEE 802.11a/g PHY- layer with the CR model of such a WLAN radio. Through the proposed experimental setup, a typical standardized OFDM physical layer of 802.11a/g WLAN was developed and afterwards simulation was successfully done to assess the exploitation of the spectrum for both the cases; fixed channel assignment strategy vs dynamic spectrum allocation technique based on cognitive radio concept. It can be considered as the simplest application of cognitive radios.

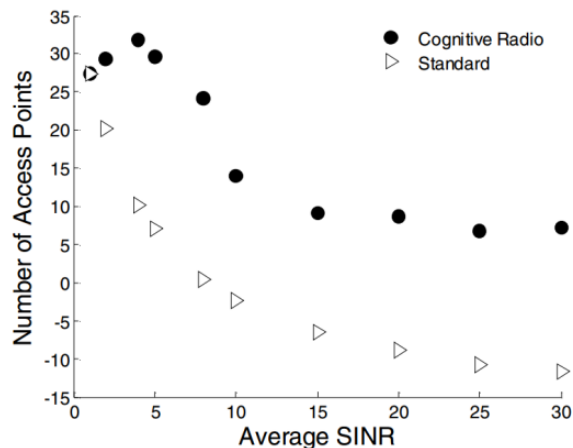


Fig. 1. Enhancement of SINR relating to standard technique and CR

B. TV Band Devices

The TV band devices (TVBDs) can be classified into two main categories: fixed and portable [7]. Maximum power radiated by Fixed TVBDs is not greater than 4W; possessing PSD of 16.7 mW/100 kHz from a fixed pre identified location. They're expected to either use geo location functionality or be appropriately setup in a predefined never moving spot and possess the ability to extract a summary of accessible channels from an authorized list of channel bank. Frequency channels which are permitted to be used for fixed TVBDs cannot exist adjacent to primary user operating channels ranging from channels between 2 and 51 apart from channels 3, 4 and 37 which are an exception case. In case of portable TVBDs, they are allowed to use channels between 21 and 51 excluding channel 37 and maximum power constraint for radiation is set to be 100 mW with the power spectral density of 1.67 mW/100 kHz in non-adjacent frequency channels while PSD constraint for adjacent frequency channels is 0.7 mW/100 kHz. Portable devices are furthermore divided into two additional modes of operation: mode-I and mode-II. Mode-I devices don't require geo location functionality or permission to access a database. Mode II devices require geo location functionality as well as the way to approach a database for listing of accessible channels.

A sensing-only device is some type of handheld TVBD, which makes use of RF spectrum detection to acquire and pull out a listing of accessible television stations. The sensing-only equipment like the one mentioned will be able to broadcast on any number of readily accessible channels within the band of frequencies ranging from 512-608 MHz (corresponding TV channels 21-36) and 614-698 MHz (corresponding TV channels 38-51), and generally are limited to an utmost transmission power of 50 mW with a power spectral density of 0.83 mW/100 kHz on non-adjacent channels and 40 mW with a power spectral density of 0.7 mW/100 kHz on adjoining channels [7]. Aside from that, a sensing-only device is required to make sure with an exceptionally higher level of assurance that it will not contribute to local radio transmissions of the primary users. The necessary power levels for detecting the signals are: NTSC Analog TV: -114 dBm, mean value across a 100 kHz frequency band; ATSC digital TV: -114 dBm, mean value across a 6MHz frequency band; Low power wireless microphone signals: -107 dBm, mean value across a 200 kHz frequency band. A TVBD might start working over a TV station when there is no TV; it takes only a time period of 30 seconds to identify the cordless microphone as well as any other below average power auxiliary equipment transmitting signals over the threshold range. A TVBD is required to accomplish in service supervision of the working station at the very least one time after every 60 seconds period. All transmissions are brought to a halt as soon as the TV, a cordless microphone or similar lower power auxiliary gadget signal is detected over the TVBD in service channel.

TABLE 1. PARAMETERS & APPLICATIONS

	Fixed device	Sensing only
Channels	Channels ranging from 2 to 51 except 3, 4 and 37. Only Non-adjoining channels	Channels 21 to 51 excluding 37
Power constraints	4 W	50 mW
Prospective applications of CR	Cellular backhaul (base station, relay stations), Smart grid stations	Public safety, Femto-cell

C. Wireless Broadband access in TV bands

Cognitive Radio (CR), a present day technology has already been prevailed as a central framework in increasing wireless access methods, including the IEEE 802.22 also known as Wireless Regional Area Networks (WRANs) [2]. An excellent utilization of IEEE 802.22 is the wireless broadband internet connection in non-urban as well as far off areas, offering results are very much similar to existing broadband access systems such as cable modems and digital subscriber line (DSL). WRAN networks are expected to take advantage of the infrequently employed ultra high frequency (UHF) TV band spectrum, providing wireless solutions including data, speech, and video traffic maintaining satisfying levels of quality of service (QoS).

D. Medical Body Area Networks

In the past few years we have seen accelerating curiosity pertaining to supervision of medical patients in hospitals for crucial indicators such as human body temperature, blood oxygen, blood pressure, and ECG. Generally most of these vitals are supervised by on-body receptors which are then hooked up to cable connections to a bedroom screen. The MBAN is an appealing substitute for getting rid of these electrical wires, consequently enabling sensors to easily and reasonably obtain a number of needed parameters immediately and communicate the observing details wirelessly which would mean that doctors can react exponentially fast.

Typically, the 2.4 GHz ISM frequency spectrum is not well suited for life-critical healthcare systems because of the interference and bottleneck caused by wireless IT systems' medical facilities. By making use of 2360 to 2400 MHz frequency band specified for body area networks on alternative basis, Quality of Service (QoS) for such life-crucial monitoring devices could perhaps be much better ensured. Furthermore, the frequency band ranging from 2360 to 2400 MHz is specifically next to the 2.4 GHz frequency band wherein a number of wireless systems are already available right now which may often be used again for MBANS like IEEE 802.15.4 standard devices [7]. This certainly will end up in cheap implementations owing to economies of scale, and finally result in larger arrangements of medical body area networks(MBAN) and as a consequence, there would be immense advancement in patient health-care.

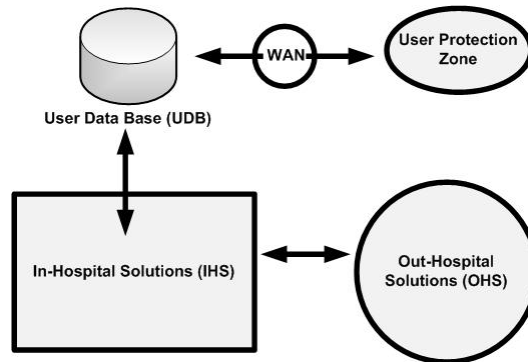


Fig. 2. MBANs Basic Architecture

Transmissions from body area network devices would likely to be of data only (without voice). It is strongly recommended that the frequency band ranging from 2360 to 2400 MHz should be classified into two categories: band-I in the frequency range 2360 to 2390 MHz and band-II in the frequency range 2390 to 2400 MHz while in the 2360-2390 MHz frequency range, body area networks operation is confined for indoor use exclusively. And for the frequency range 2390 to 2400 MHz, body area network operation is permitted pretty much anywhere [7]. A contention-based protocol, which is unrestricted, is proposed for gaining access to the medium. The maximum amount of emission of bandwidth for body area networks is allowed to be 5 MHz. The utmost transmission power should not meet or exceed 1 mW.

E. Smart Grid Networks

Remodeling of the previous century power grid right into an intelligent smart grid will probably be advocated by many nations as a means of handling electrical power self-reliance and durability, global warming and catastrophe challenges. The smart grid constitutes 3 abstract-level tiers, from a technological innovation point of view: the physical electrical power tier, communication networking tier, together with the application layer [5]. The smart grid manages the electrical power in a manner in which electric power is produced, transported, used up and charged. Putting intellect through the entire freshly networked power grid boosts grid durability, enhances demand management and responsiveness, and incorporates distributed sources of energy, and also essentially lowers expenses towards the customers and service provider.

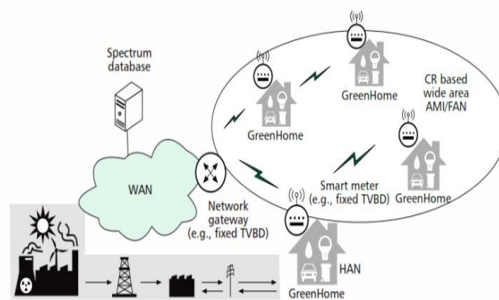


Fig. 3. Smart Grid Network

A smart grid network has normally three building blocks:

- The home area networks (HANs) which generally connect on-premise devices and intelligent meters, dispersed alternative sources and plug-in electric powered automobiles.
- The field area networks (FANs) or advanced metering infrastructure (AMI) which assists transmit data linking sites (through intelligent metering) together with a network gateway, that might be a power substation, a utility rod-fitted appliance, or just a transmission tower system.
- The wide area networks (WANs) that function as being the central resource for interaction among utility data center and the aggregation points/network gateways.

F. Cellular Networks

In the last decade, usage of the cellular networks has increased considerably, with consumers always hoping of staying connected regardless of their different locations and time. Beginning of smart phones and social networking era, increasing usage of multimedia websites which includes daily motion, facebook, YouTube, and flicker, releasing of innovative gadgets for example e-readers etc have additionally enhanced the dramatical improvement in the usage of mobile networks for conventional data services, e.g., web surfing and electronic mail. Now this offers not only new possibilities for innovative businesses but at the same time it's a real challenge for cellular operators. The increasing number of data services creates an opportunity as they add to the overall revenue. But, it becomes challenging as in some geological regions, mobile networks have become congested because of the limited bandwidth acquired by cellular operators. Recent studies indicate that the broadband internet bandwidth shortfall is anticipated to come closer to 300 MHz by 2014 [7].

For applications requiring access to the network, two scenarios are usually kept in view. Primarily are hotspots, like in airports and game stadiums, mainly because people arrive in massive numbers at majority of these spots. Let us consider the scenario of an athletic ground, participants in this modern age possess smart phones which have cameras by means of which they can easily take photographs of the proceedings of the sporting activity and share them with their friends through social media sites. This kind of video and graphic data adds massive load on mobile phone network. During a research investigation by Cisco, it is concluded that this picture and video data can cause up to 60 percent increase [7]. These days a fraction of the multimedia content could be very easily diverted to ISM (industrial, scientific, and medical) band used in WiFi networks. Nevertheless, because of the huge amount of information produced within a smaller region, both ISM band Wifi networks as well as cellular networks are likely to be jammed. If this particular type of multimedia content (images, video etc) can be side tracked to some other extra channel, for example TVWS, then the mobile network may possibly be utilized for other speech services offered by the network with a significantly

more effective manner, and as a result reaping the benefits for both the user as well as cellular operator.

Femto-cell can be seen as the second access network application. These days many cellular operators provide miniaturized base stations whose visual appearance is just like a Wi-Fi router or access point, individuals can purchase them and install them within their houses. These mini base stations also called Femto-cells which can be used in areas having bad coverage areas like basements. These femto-cells and cellular operators use the same frequency range [7].

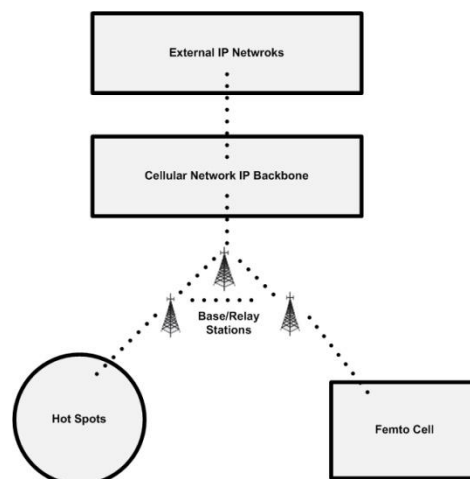


Fig. 4. Basic Architecture of Cellular Network

G. Military

The capability to improve interoperability connecting several dissimilar radio standards, combined with the ability to observe the existence of interferers, CR device has turned into a must-have technology gadget. This cutting edge technology provides you with added benefits by means of safeguarding and shielding the ongoing communications, recognizing the adversary transmissions, as well as revealing of tracks of opportunity.

The U.S. Department of Defense (DoD) has dedicated lots of energy and efforts to revolutionary state-of-the-art wireless applications over the last few years and has now developed packages for instance, Joint Tactical Radio System (JTRS), SPEAKeasy radio system, and Next Generation (XG) to make it possible for the development of an intelligent and a smart communication agent [5].

H. Public Safety Networks

General consumer protection and crisis situation feedback is nevertheless an additional sphere where exactly CRs have acquired loads of interest and attention. For quite a few years public safety and security organizations have desperately needed a whole lot more spectrum share to help ease frequency over-crowding and greatly improve interoperability. Equipped with spectrum sharing functionality, CRs can show their usefulness simply by using a portion of the pre-existing spectrum which is not frequently used at the same time help in taking care of call priority and response time. On top of that, Cognitive Radios may play a significant part in further enhancing interoperability by

allowing gadgets to bridge communications between areas by making use of separate frequencies and modulation forms.

Public safety high-risk workers have become considerably important turning out to be backed up with wifi enabled mobile computing devices, laptop systems, together with mobile camcorders to enhance most of the functionality and capability to instantaneously team up making use of centralized control, co-workers, in conjunction with other groups [7]. Specified cordless support services relating to community protection and safety stretch out ranging from web surfing, speech to text messaging, electronic mail, database accessibility, graphic transmission, video media buffering, along with other wideband features. Video monitoring spy cameras coupled with sensor devices are increasingly becoming immensely important resources to enhance the eyes and ears concerning general public protection and security organizations. Correspondingly, information rates, integrity, as well as lag time specifications differ from service to service.

In comparison, RF band frequencies designated for the consumer's safety and security purpose are increasingly becoming jam-packed, particularly in metropolitan areas. Aside from that, primary users originating from various areas and associations usually are not able to connect in the course of crisis situation. As shown in Figure 5, these kinds of cognitive devices could possibly be positioned in a number of ultra-powerful crisis responders' automobiles coupled with wireless routers or access points. This approach elevates the strain from mobile handheld devices to acquire cognitive ability to lessen the situation in which various critical responders might use several radios nowadays and most probably in the foreseeable future to a greater extent.

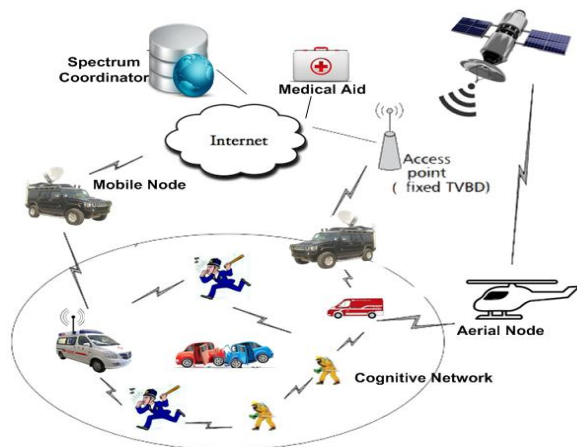


Fig. 5. Public Safety Network

CR was indeed recognized as a promising solution to supercharge effectiveness and usefulness of RF band. Equipped with Cognitive Radios, customer safety operators can make use of a whole lot more RF band for day-to-day operations from area to area and time to time. By working with the appropriate spectrum collaborating partners, public security personals are also able to get access licensed RF bands and professional operator networks. For instance, the

public protection people might possibly roam on wireless networks in 700 MHz frequency range and possibly several other frequency bands throughout the spots in which public security wireless services are inaccessible and the places where there exists at the moment a working public coverage network, however considerably more data capacity is needed to respond proficiently and resourcefully for a critical situation.

So it will remain to be witnessed the way in which Cognitive Radio concept will assist the top priority distribution and routing of data packets by means of its very own specialized network together with the general public wireless networks, consequently safeguarding time-critical priority data packets from losses or postponement caused by network over-crowding. This goes beyond the borders of spectrum recognition to content recognition, from the PHY layer towards the App layer.

III. CONCLUSION

CR technology can play an important role in order to make an excellent use of the limited spectrum to compliment the rapidly growing desires and needs pertaining to wireless applications, such as the common man basic safety, intelligent power grid, and the wireless broadband internet, mobile networks to even healthcare applications. At the same time, challenges continue to exist due to the fact that CR-enabled networks are expected to exist together with incumbents as well as cognitive users and are required to minimize interference in a manner that they will more effectively facilitate these kinds of applications from end to end.

IV. REFERENCES

- [1] S. Haykin, "Cognitive radio: Brain-empowered wireless communications," *IEEE J. Select. Areas Commun.*, vol. 23, no. 2, pp. 201-220, Feb. 2005.
- [2] Quan, Zhi, Shuguang Cui, H. Poor, and Ali Sayed. "Collaborative wideband sensing for cognitive radios," *Signal Processing Magazine, IEEE* 25, no. 6, pp. 60-73, 2008.
- [3] Mitola III, Joseph, and Gerald Q. Maguire Jr. "Cognitive radio: making software radios more personal," *Personal Communications, IEEE* 6, no. 4, pp. 13-18, 1999.
- [4] Mahonen, Petri, Marina Petrova, and Janne Riihijarvi. "Applications of topology information for cognitive radios and networks," In *New Frontiers in Dynamic Spectrum Access Networks. 2nd IEEE International Symposium on*, pp. 103-114. IEEE, 2007.
- [5] Maldonado, David, Bin Le, Akilah Hugine, Thomas W. Rondeau, and Charles W. Bostian. "Cognitive radio applications to dynamic spectrum allocation: a discussion and an illustrative example," In *New Frontiers in Dynamic Spectrum Access Networks, 2005. First IEEE International Symposium on*, pp. 597-600, 2005.
- [6] Goldsmith Andrea, Syed Ali Jafar, Ivana Maric, and Sudhir Srinivasa. "Breaking spectrum gridlock with cognitive radios: An information theoretic perspective." *Proceedings of the IEEE* 97, no. 5, pp. 894-914, 2009.
- [7] Wang, Jianfeng, Monisha Ghosh, and Kiran Challapali. "Emerging cognitive radio applications: A

survey." *Communications Magazine, IEEE* 49, no. 3, pp. 74-81, 2011.

[8] Yau, K-LA, F-AG Tan, Peter Komisarczuk, and Paul D. Teal. "Exploring new and emerging applications of Cognitive Radio systems: Preliminary insights and framework." In *Humanities, Science and Engineering (CHUSER), 2011 IEEE Colloquium on*, pp. 153-157, 2011.

On Multi-channel Opportunistic Access in Heterogeneous Cognitive Radio Networks

Said Rutabayiro Ngoga, Yong Yao and Adrian Popescu

School of Computing,
Blekinge Institute of Technology,
371 79 Karlskrona, Sweden,
Email: {srn,yya,apo}@bth.se

Abstract—In the paper, we study optimal transmission strategies in multi-channel opportunistic spectrum access (OSA) networks where one secondary user (SU) opportunistically accesses multiple orthogonal channels of primary users (PUs) under a continuous time Markov chain modeling of the channel occupancy by the PUs. Referred to as tunable threshold strategy, at a given time the SU chooses one channel of a given PU, decides if it should transmit or not and if so it protects the PU of this channel. To be operational, such a structure depends on the capability of the SU radio front-end to perform channel sensing. We consider one scenario where the SU node can simultaneously sense multiple channels and another scenario where the SU node can sense only one channel at a time. For each scenario, we develop the structure of the optimal transmission strategy and analyse the performance. We show that the optimal transmission strategy can be implemented using a simple tunable threshold algorithm.

Index Terms—Opportunistic spectrum access, MAC, multichannel, cognitive radio networks

I. INTRODUCTION

The concept of Dynamic Spectrum Access (DSA) has been envisaged in the context of secondary sharing of the spectrum, with the objective that sharing is transparent to the spectrum licensee, also called the primary user (PU). The spectrum is shared with secondary users (SU)s but absolute protection is demanded for PUs on all channels. As part of the DSA, the opportunistic spectrum access (OSA) approach encompasses operating regime in which the spectrum is shared on the interference tolerance basis: a SU has open access to the multiple channels of PUs when the PUs are not transmitting, provided that the level of interference caused by the SU is kept below a prescribed tolerance level [1]. We refer to such a regime the OSA medium access control (OSA MAC).

Following the OSA model, the OSA MAC protocol is the main element that determines the efficiency of secondary sharing of the spectrum with the PUs. The fraction of channel bandwidth used by successfully transmitted messages of a SU, also called *throughput*, gives a good indication of the efficiency of an operational OSA MAC, and the maximum value it can attain is known as the *capacity* of the protocol. However, the diverse behavior of different PUs on various channels creates spectrum opportunities having different characteristics that affects the design of the OSA MAC protocol and therefore inherently puts limitations on the capacity it can achieve [1],[2].

For an optimal design of OSA MAC, it is of interest to characterize the maximum throughput as an objective function, with optimal sensing and transmission strategies being the set of optimization variables. Here, the sensing strategy suggests which channel to sense and the transmission strategy determines whether to transmit or not.

In the paper, we study optimal transmission strategies in multi-channel OSA networks where one SU opportunistically accesses multiple orthogonal channels of PUs under a continuous time Markov chain modeling of the channel occupancy by the PUs. Referred to as tunable threshold strategy, at a given time the SU chooses one channel of a given PU, decides if it should transmit or not and if so it protects the PU of this channel. To be operational, such a structure depends on the capability of the SU radio front-end to perform channel sensing. We consider one scenario where the SU node can simultaneously sense multiple channels and another scenario where the SU node can sense only one channel at a time. For each scenario, we develop the structure of the optimal transmission strategy and analyse its performance. We show that the optimal transmission strategy can be implemented using a simple tunable threshold algorithm. The performance of this class of threshold strategies is analyzed and it characterizes the maximum throughput of a multi-channel OSA network as a function of the collision tolerance and the number of channels.

A first cognitive MAC protocol supporting secondary sharing over multiple primary channels was presented in [3]. The optimal sensing problem that governs the channel selection for opportunistic communications over multiple channels was addressed in [4]. Assuming that both PU and SU follow the same transmission structure, it was shown that the sensing policy has a simple structure that reduces the channel selection to a counting procedure and it avoids the need for knowing the channel transition probabilities. A separation principle that decouples the design of sensing and access policies was advanced in [5].

A more realistic model that characterizes the spectrum occupancy of PUs as on-off continuous time Markov processes was presented in [6]. The problem of designing cognitive MAC protocol was extended to multiple continuous time Markovian channel in [7], where the sensing policy is restricted to a periodic sensing scheme yielding to a simple and practical access strategy that satisfies interference constraints.

Interesting results were reported in [8], where it was shown that when the collision constraints are tight, a periodic sensing scheme with memoryless access is optimal compared to the case when all channels are simultaneously sensed. Different from that, we introduce an alternative way to represent the SU's limitations, which allows us the application of maximum entropy principle to construct the hopping sensing sequence, and thereby derive optimal dynamic access strategies.

The rest of the paper is organized as follow. Section II describes the system model that characterizes PU and SU activities. Section III describes operational properties of the multichannel cognitive access. Section IV presents the structural solutions of the multichannel cognitive access policies. Section V reports numerical results. Section VI concludes the paper.

II. SYSTEM MODEL

In this section, we describe the basic elements of a typical OSA system for which we derive the system protocol types and their operating procedures. Two protocols are described and analyzed, which we call multi-channel sensing capability (MCSC) and single-channel sensing capability (SCSC). These in turn serve as a mean to evaluate the OSA network performance with respect to technical and regulatory aspects.

We consider the scenario where a single SU is trying to access N independent channels by using a time slotted transmission structure. Three elements compose such a scenario: the primary networks with spectrum, a secondary network with usage and the OSA MAC responsible to carry out the sharing of spectrum among PUs and SUs.

A. PU Model

We consider a heterogeneous network with N orthogonal channels indexed by i , $i = 1, 2, \dots, N$. The index i designates a PU channel and the PU activities on different channels are independent. A channel is required to have the following attributes to be a candidate for secondary sharing.

1) *Channel occupancy*: we assume that the occupancy of each channel by PU transmissions follows a two state homogeneous continuous time Markov chain. The two states of channel i denotes the idle state(0) and the busy state(1). This is motivated by the packet-based traffic pattern for PUs activity [9]. The Markovian assumption means that the sojourn time attached to each state is exponentially distributed with parameter λ_i^{-1} for the idle state and μ_i^{-1} for the busy state, respectively. The transition rate matrix Q_i of the occupancy of PU channel i is given by

$$Q_i = \begin{pmatrix} -\lambda_i & \mu_i \\ \mu_i & -\lambda_i \end{pmatrix} \quad (1)$$

Let the probability vector $\{\eta_i(0), \eta_i(1)\}$ be the stationary distribution of the i th channel occupancy model associated with Q_i . This is given by

$$\eta_i(0) = \frac{\mu_i}{\lambda_i + \mu_i}, \quad \eta_i(1) = \frac{\lambda_i}{\lambda_i + \mu_i} \quad (2)$$

2) *Interference tolerance*: although the networks of the PUs were not designed to tolerate interference from secondary transmissions, we assume that the collision in these networks caused by a SU transmission is under control. This enables us to evaluate the effect of interference caused by the SU to a channel in terms of the capacity loss considered acceptable by the PU rather than as a reliability consideration [10]. We assume that for each candidate PU channel there is a packet collision probability denoted by ζ_i . This is defined as the maximum probability of collision for a packet on channel i that the PU can tolerate.

B. SU Model

We consider a single SU trying to opportunistically access the N channels so as to maximize its throughput, but it can transmit using only one channel at a time. The SU is cognitive radio equipped. Time is slotted into discrete time steps indexed by t , $t = 1, 2, \dots, T$, but the PUs are not synchronized to it.

For an effective usage of the spectrum by the SU communications, a spectrum opportunity is associated with two characteristics. One includes the estimate of the probability of a channel being free from PU's activity whereas the other includes the estimate of the collision rate of the service being provided on the channel. Thus, we associate the following attributes to the notion of spectrum opportunity.

1) *Opportunity identification*: the notion of spectrum opportunity is local to a pair of SU nodes. Specifically, a SU is capable of channel sensing, then a channel in the spectrum is an opportunity for secondary sharing if no primary signal is heard, and thereafter the channel is deemed idle at both the sender and receiver of the SU pair. We assume that the SU accurately executes the channel sensing operation. In this way, the performance of channel sensing over a long run provides the actual estimate of the probability that a channel is free from PU's activity at any given time.

2) *Interference constraint*: a spectrum opportunity depends on the type of collision constraint imposed by PUs, which in turn is determined by the communication activities of the PUs. Let the collision probability for PU on channel i denoted by ξ_i be the fraction of collided packets in packets fully transmitted by the particular PU. Therefore the collision constraint imposed on channel i is given by

$$0 \leq \xi_i \leq \zeta_i, \quad i = 1, 2, \dots, N \quad (3)$$

We talk of equal collision constraints if $\zeta_i = \zeta$ for all i . Also, this can be considered as the PU protection requirement in the sense that PU communications experiencing collision below ζ_i do not affect the reliability of the overall PU service being provided on channel i .

Throughout the paper, for a particular PU channel i , we refer to ξ_i as *capacity cost*, and ζ_i as *capacity limit*. We assume that the SU has the estimate of the PUs traffic parameters (λ_i, μ_i) whose values are integer multiples of the SU slot length. Also the stationary probabilities $\{\eta_i(0), \eta_i(1)\}$ and the capacity constrains are known a priori.

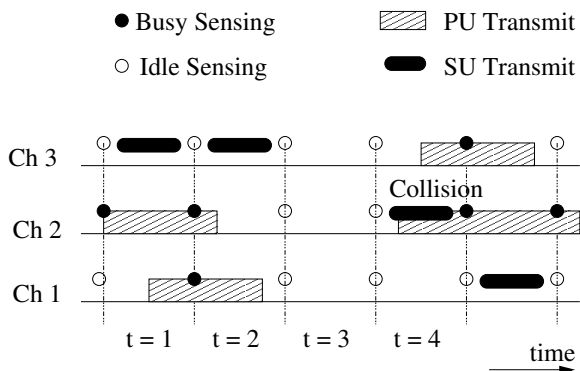


Figure 1. Illustration of the SCSC protocol. All channels are simultaneously sensed. Each SU slot consists of a sensing period and a transmission period. Open circles denote idle sensing result. Filled circles denote busy sensing result. An idle slot happens when the protocol decides so ($t = 3$). A collision happens when the SU starts transmission and PU returns before the end of the SU transmission period ($t = 4$).

C. Modeling of OSA MAC

Here we describe the system protocols, their underlying algorithms and basic assumptions.

A typical OSA MAC protocol operates by sensing the spectrum at the beginning of each slot, then it uses the sensing results to decide if and in which channel to transmit during the remainder of this particular slot. Since a collision with PUs can occur, it uses an acknowledgment scheme to be informed of its success or failure.

The various protocols considered defer by the spectrum sensor ability to carry out spectrum sensing. However, in all cases the SU senses the N channels and operates as follows.

We first describe the multi-channel sensing capability (MCSC) as is illustrated in Figure 1. The assumption here is that the SU node is equipped with an additional radio dedicated for sensing. In this case if the spectrum sensor has a broadband sensing capability the N channels can be sensed simultaneously in each time slot. This gives rise to the MCSC.

- i) if the selected channel i is observed idle, with probability ω_i the SU transmits and with probability $(1 - \omega_i)$ the SU delays this transmission until the next slot;
- ii) if the selected channel i is observed busy, with probability 1 the SU does not transmit.

Next we describe the single-channel sensing capability (SCSC) as is illustrated in Figure 2. Here the assumption is that a single radio is shared by both the sensing operation and the transmission operation. In this case the spectrum sensor is limited to sensing one of the N channels at a time, while the remaining channels are hidden. This gives rise to the SCSC.

III. MULTICHANNEL COGNITIVE ACCESS PROPERTIES

In this section, we analyze the performance of the MSSC protocol and SCSC protocol, respectively. This provides the foundation for analytical characterizations of the capacity of the system for these access protocols.

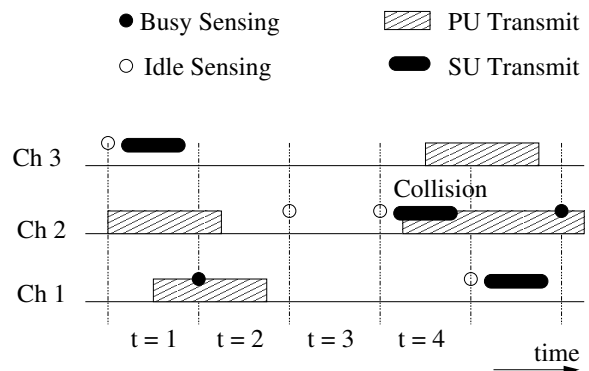


Figure 2. Illustration of the SCSC protocol. One channel is sensed at a time. Each SU slot consists of a sensing period and a transmission period. Open circles denote the idle sensing result. Filled circles denote the busy sensing result. An idle slot happens when the protocol decides so ($t = 3$). A collision happens, when the SU starts transmission and PU returns before the end of the SU transmission period ($t = 4$).

A. Preliminaries

Prior to developing on the performance of the access protocols, we characterize the throughput of the system and the capacity costs as follows. We have assumed that each packet of SU is of constant length requiring t time for transmission. Let π be a method used to select a channel in each time slot t , and with probability ω_i the SU has access to the selected channel. By using π , if the transmission of SU packet has no overlap with the transmission of a PU packet, we consider the SU to have a successful access to the channel i for t time. Further, let $P_{succ,i}$ be the probability that channel i contains a success transmission of a SU for t time. This happens if the channel i is observed idle and also remains idle for the duration t . The throughput of this policy is given by

$$J(\pi) = \sum_i^N \omega_i P_{succ,i} \quad (4)$$

$$P_{succ,i} = \eta_i(0) \exp(-\lambda_i t) \quad (5)$$

Besides, the SU is considered to be penalized of the interference mitigation attempt failures. Now, let us define π such that the SU keeps transmitting on a particular channel until a collision happens. Under the assumption that a SU slot is no greater than the maximum of PU packet lengths, and also that the sensing outcome of the SU is perfect, we observe that there may be at most one PU packet collision that may occur whenever the PU returns and after a SU has already sensed the channel to be idle and started a transmission. Therefore the collision probability of PU for a packet experiencing collision on channel i , also referred to as the capacity cost ξ_i under this policy, is given by

$$\xi_i = \frac{E[N_i^c]}{E[N_i]}, \quad \forall i \quad (6)$$

$$E[N_i^c] = 1 - \exp(-\lambda_i t) \quad (7)$$

$$E[N_i] = 1 - \eta_i(0) \exp(-\lambda_i t) \quad (8)$$

where N_i^c and N_i are random variables representing the number of collided and transmitted PU packets, respectively. Also $E[\cdot]$ denotes the expectation of a random variable.

B. Multi-Channel Sensing Capability (MCSC)

We assume that the SU has the capability to simultaneously sense all channels, but it can use at most one channel at a time to execute its transmission. However, over time its transceiver device can switch among different channels.

Let $s_i(t) \in \{0, 1\}$ be the state of channel i such that a SU executes sensing at time t and then it observes the channel being idle(0) or busy(1). For clarity purposes, we denote the outcome of channel sensing as the true state because we assume the channel sensing to be error free.

The process $\{s_i(t), t \in T\}$ characterizes the occupancy of channel i and it is assumed to have a discrete-time Markovian structure. Let $\mathbf{S}(t) = [s_1(t), s_2(t), \dots, s_N(t)]$ be the actual system state under MCSC such that the process $\{\mathbf{S}(t), t \in T\}$ characterizes the actual occupancy of the N channels. We assume that all $\{s_i(t)\}$ are independent Markov chains, so that $\{\mathbf{S}(t)\}$ has also a Markovian structure. This is completely specified by the state space $\mathcal{S} = \{\mathbf{s}, \mathbf{s} \in \{0, 1\}^N$. Let $F(\mathbf{s})$ be the probability of state \mathbf{s} . It can be evaluated by using $\{\eta_i(0), \eta_i(1)\}, \forall i$. As such, the SU maintains the actual state of the system at the beginning of each time slot t , $\mathbf{S}(t) = \mathbf{s}$.

Consider an arbitrary time slot t , then a status vector $\mathbf{s} = [s_1, s_2, \dots, s_N]$ indicates which channels have been already sensed and also the state of each channel. In this time slot, when channel i is idle, we use $X_i(t)$ to denote a state that indicates the number of channels currently idle including the channel i . $X_i(t)$ takes its values in the set $\{1, 2, \dots, N\}$. Let $[X_i = x] = \{\mathbf{s} | X(\mathbf{s}) = x, s_i = 0\}$ be the set of idle channels at state x , $x \in \{1, 2, \dots, N\}$. The probability of X_i gives, respectively, the PMF($p_{X_i}(x)$) and CDF($F_{X_i}(x)$) denoted by

$$\begin{aligned} p_{X_i}(x) &= \sum_{[X_i=x]} \frac{F(\mathbf{s})}{x} \\ F_{X_i}(x) &= \sum_{j=1}^x p_{X_i}(j), \quad 1 \leq x \leq N \end{aligned} \quad (9)$$

where $F_{X_i}(x)$ denotes the probability of state x given that channel i is idle.

Let Π denote the set of all MCSC policies. We characterize an access mode $\pi_{\text{MC}} \in \Pi$ as follows. In each time slot, a SU maintains its transmission probability $\omega_i(x, \mathbf{s})$ with which it decides to transmit on channel i at state x given \mathbf{s} or not.

The maximization of the system throughput for the MCSC protocol can be done by specifying:

- The normalization, which is given by

$$\sum_{i=1}^N \omega_i(x, \mathbf{s}) \leq 1, \quad \omega_i(x, \mathbf{s}) \geq 0 \quad (10)$$

- The capacity cost $\xi_{i,N}(\pi_{\text{MC},X})$ of using channel i , which

is given by:

$$\xi_{i,N}(\pi_{\text{MC}}) = \sum_{x=1}^N F_{X_i}(x) \omega_i(x, \mathbf{s}) \frac{1 - \exp(-\lambda_i t)}{1 - \eta_i(0) \exp(-\lambda_i t)} \quad \forall i \quad (11)$$

- The capacity constraints, which is given by

$$\xi_{i,N}(\pi_{\text{MC}}) \leq \zeta_i, \quad i = 1, \dots, N \quad (12)$$

C. Single Channel Sensing Capability (SCSC)

We assume that the SU can sense at most one channel at a time. Let $\{D_i\}, i = 1, \dots, N$, be the set of system states under SCSC such that the system is at state $D_i(t)$ when the SU senses the i -th channel in slot t and it observes the channel i being idle. The state probabilities $\{p_i\}, i = 1, \dots, N$, with the entropy function H given by

$$H(p_1, \dots, p_N) = - \sum_i p_i \ln(p_i) \quad (13)$$

denotes how likely it is that the channel i is idle(0) before sensing starts at any time slot t . We assume p_i are independent and without loss of generality we also assume that $p_1 \geq p_2 \geq \dots \geq p_N$.

Let $\hat{\Pi}$ denote the set of all SCSC. We characterize an access mode $\pi_{\text{SC}} \in \hat{\Pi}$ as follows. In each time slot, a SU maintains its transmission probability $\omega_i(s_i)$ with which it decides to transmit on channel i at state D_i given s_i or not.

The maximization of the system throughput for the SCSC protocol is done as follows.

1) *Prior Information*: we assume that we know about the state probabilities $\{p_i\}, i = 1, 2, \dots, N$:

- The normalization

$$\sum_{i=1}^N p_i = 1 \quad (14)$$

- The capacity cost ξ_i^{SC} on each channel i , and the average capacity limit $\bar{\zeta}$ over all channels

$$\xi_i^{\text{SC}} = \omega_i \eta_i(0) \frac{1 - \exp(-\lambda_i t)}{1 - \eta_i(0) \exp(-\lambda_i t)} \quad (15)$$

$$\bar{\zeta} \geq \sum_{i=1}^N p_i \xi_i^{\text{SC}} \quad (16)$$

2) *Maximum Entropy*: The maximization of the system's entropy function subject to the prior information expressed by (14)-(15) can be done by Lagrangian's method after specifying the "Lagrangian multipliers" α and β . Thus, this leads to the solutions:

$$p_i = \exp[-(\xi_i^{\text{SC}} \beta + \alpha + 1)], \quad \forall i \quad (17)$$

where

$$\alpha = \ln \left[\sum_{i=1}^N \exp(-\xi_i^{\text{SC}} \beta) \right] - 1 \quad (18)$$

$$g(\beta) = \sum_{i=1}^N (\bar{\zeta} - \xi_i^{\text{SC}} \exp[(\bar{\zeta} - \xi_i^{\text{SC}}) \beta]), \quad \beta \geq 0 \quad (19)$$

The structure of the hopping sequence is provided by the parameter β .

IV. MULTICHANNEL COGNITIVE ACCESS POLICIES

Simple structural solutions are presented as optimal algorithms for the MCSC protocol and the SCSC protocol, respectively.

A. MCSC Structure

The setting of the optimal MCSC algorithm is as follows. Let K , $1 \leq K \leq N$, be the threshold of the MCSC algorithm such that for each channel i the following conditions are met.

- Given $\{\xi_{i,K}\}$, $1 \leq K \leq N$, for each channel i , we find the threshold K by using $\zeta_i \in [\xi_{i,K-1}, \xi_{i,K}]$
- For the channel i currently observed busy,

$$\omega_i(x, \mathbf{s}) = 0$$

- For the channel i currently idle at state x , there are tree subcases.

- For the states x such that $x = K$ and $K \geq 1$

$$\omega_i(x, \mathbf{s}) = \frac{\zeta_i - \xi_{i,K-1}}{x [\xi_{i,K} - \xi_{i,K-1}]}, \quad \xi_{i,0} = 0$$

- For the states x such that $x < K$ and $K > 1$

$$\omega_i(x, \mathbf{s}) = \frac{1}{x}$$

- For the states x such that $x > K$

$$\omega_i(x, \mathbf{s}) = 0$$

Therefore, the throughput of the MCSC is given by

$$J(\pi_{MC}) = \sum_{i=1}^N \sum_{x=1}^N \omega_i(x, \mathbf{s}) \eta_i(0) \exp(-\lambda_i t) \quad (20)$$

B. SCSC Structure

The setting of the optimal MCSC algorithm is as follows. Let G , $1 \leq G \leq N$, be the threshold of the SCSC algorithm such that for all channels N the following conditions are met.

- Given $\{\xi_G\}$, $1 \leq G \leq N$, for the N channels, we find G by using $\bar{\zeta} \in [\xi_{G-1}, \xi_G]$, $\xi_0 = 0$.
- For the case that either $G = 1$ or $G > N$, then β , $\{p_i\}$ and $\{\omega_i\}$ are given respectively by

$$\beta = 0, \quad p_i = \frac{1}{N}, \quad \omega_i = \min \left(1, \frac{\bar{\zeta}}{\xi_i} \right), \quad \forall i$$

- For the case that $G > 1$, then β , $\{p_i\}$ and $\{\omega_i\}$ are given respectively by

$$\beta > 0, \quad p_i = \exp[-(\xi_i \beta + \alpha + 1)], \quad \omega_i = 1, \quad \forall i$$

Therefore, the throughput of the SCSC is given by

$$J(\pi_{SC}) = \sum_{i=1}^N p_i \omega_i \eta_i(0) \exp(-\lambda_i t) \quad (21)$$

V. NUMERICAL RESULTS

In this section we report two numerical results: one on the performance of the MCSC approach and the other on the performance of the SCSC approach. In particular, the throughput performance for both MCSC and SCSC defines, for a given set of PUs channels characteristics, the capacity of a multi-channel opportunistic system with multi-channel sensing and single-channel sensing, respectively.

For the purpose of performance comparison, we use the periodic sensing with memoryless access (PSMA) approach optimized for strict collision constraints regime [7],[8]. This means that the collision probability on individual channels must be small.

In calculations, the slot duration t is chosen to be $t = 0.25ms$. The selection of the channel parameters are motivated from the experiments conducted in [6]. For the operating environments, we use examples of network configurations with $N = 2, 3$ parallel primary channels, and the channels parameters being:

- For $N = 2$, $\lambda = [1/4.20, 1/3.23] \text{ ms}^{-1}$ and $\mu = [1/2.32, 1/1.11] \text{ ms}^{-1}$.
- For $N = 3$, $\lambda = [1/6.23, 1/4.20, 1/3.23] \text{ ms}^{-1}$ and $\mu = [1/3.12, 1/2.32, 1/1.11] \text{ ms}^{-1}$.

A. Performance of the MCSC Structure

We study the throughput of the MCSC approach in comparison to the throughput of PSMA approach. In Figure 3 we plot the throughputs of MCSC approach and the PSMA approach for the two network configurations and the capacity limit on each channel ζ_i ranging in $[0.01, 0.15]$.

It is observed that, for each network configuration, MCSC gives poor performance similar to PSMA when the constraints are strict. This happens when $\zeta \in [0, 0.0475]$ in the figure marked MCSC($N = 2$) with $K_1 = 2$, $K_2 = 1$ obtained through computation, and also when $\zeta \in [0, 0.025]$ in the figure marked MCSC($N = 3$) with $K_1 = 3$, $K_2 = K_3 = 2$ obtained through computation. However, the throughput of MCSC substantially improves compared to the throughput of PSMA until the constraints relax on each channel. This happens when $\zeta \in [0.1225, 0.15]$ in the figure marked MCSC($N = 2$) with $K_1 = K_2 = 2$ obtained through computation, and also when $\zeta \in [0.0875, 0.15]$ in the figure marked MCSC($N = 3$) with $K_1 = K_2 = K_3 = 3$ obtained through computation. This reflects the threshold nature of MCSC. In particular, when N is fixed, a strict capacity constraint is achieved with the reduction in the number of channels, requiring the SU to use a small set of channels. In case the capacity constraints relax, only the SU with advanced cognitive radio capabilities can use all spectrum, resulting in substantial throughput improvement.

B. Performance of the SCSC Structure

Similarly, we study the throughput of the SCSC approach in comparison to the throughput of the PSMA approach. In Figure 4 we plot the throughputs of the SCSC approach and

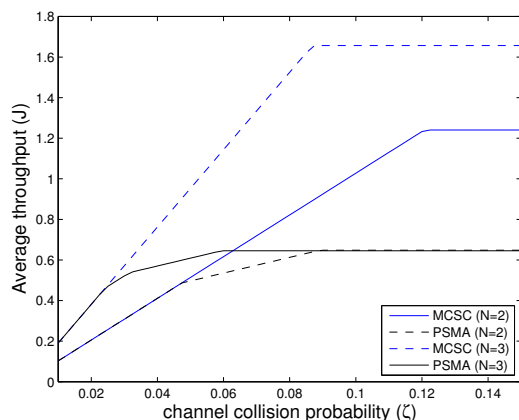


Figure 3. Comparison of the throughputs of the MCSC and PSMA approaches

the PSMA approach for the two network configurations and the average capacity limit $\bar{\zeta}$ over all channels ranging in $[0.01, 0.2]$.

It is observed that, for each network configuration, SCSC gives poor performance similar to PSMA approach when the constrains are strict. This happens when $\bar{\zeta} \in [0, 0.09]$ in the figure marked SCSC($N = 2$) with $\beta = 0$ obtained through computation. The throughput of SCSC saturates when the constraint on each channel relaxes. This happens when $\bar{\zeta} \in [0, 0.14]$ in the figure marked SCSC($N = 2$) with $\beta = 0$ obtained through computation. Similarly, this reflects the threshold nature of SCSC. In particular, $\beta = 0$ features the case where the channels exhibit equal opportunities, therefore it is likely that the SU can use the spectrum without sophisticated learning techniques.

However, the spectrum opportunities depart from being uniform when $\bar{\zeta} = 0.095$ in the figure marked SCSC($N = 2$) with $\beta = 64.229$ obtained through computation, and also when $\bar{\zeta} = 0.075$ in the figure marked SCSC($N = 3$) with $\beta = 99.05$ obtained through computation. In this case, the SCSC makes it possible to resort to more structured sensing patterns, consequently it improves its throughput substantially compared to the PSMA approach.

We also note that the protocol threshold decreases with the increase in the number of channels, thus adding more channels provides for additional opportunities for secondary exploitation.

VI. CONCLUSION

Optimal transmission strategies in multi-channel opportunistic spectrum access (OSA) networks have been studied where one secondary (SU) opportunistically accesses multiple orthogonal channels of primary users (PUs) under a continuous time Markov chain modeling of the channel occupancy by the PUs. Optimal access strategies for a single user under the assumption that the SU has perfect knowledge on all channels

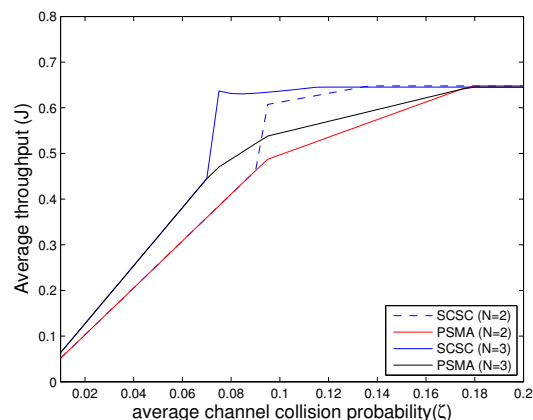


Figure 4. Comparison of the throughputs of the SCSC and PSMA approaches

have been analysed. A special case has been considered with limited sensing capability in which we first constructed a hopping sequence using the principle of maximum entropy. This hopping sequence is then used to devise the access strategy for the SU. We have shown that the channel selection strategy that maximizes the system entropy function subject to capacity constrains induces a hopping sequence with optimal access. Future work is about access policies with multiple users.

REFERENCES

- [1] D. F. Marshall, "Dynamic spectrum access as a mechanism for transition to interference tolerant systems," in *IEEE New Frontiers in Dynamic Spectrum (DySPAN'10)*, Singapore, Apr. 2010, pp. 1–12.
- [2] Q. Zhao, "Spectrum opportunity and interference constraint in opportunistic spectrum access," in *2007 IEEE International Conference on Acoustics, Speech and Signal Processing, ICASSP '07*, Honolulu, HI, Apr. 2007, pp. III605–III608.
- [3] Q. Zhao, L. Tong, A. Swami, and Y. Chen, "Decentralized cognitive mac for opportunistic spectrum access in ad hoc networks: A pomdp framework," *IEEE Trans. Inf. Theory*, vol. 25, no. 3, pp. 589–600, May 2007.
- [4] Q. Zhao, B. Krishnamachari, and K. Liu, "On myopic sensing for multi-channel opportunistic access: structure, optimality, and performance," *IEEE Trans. Wireless Commun.*, vol. 7, no. 12, pp. 5431 – 5440, Dec. 2008.
- [5] Y. Chen, Q. Zhao, and A. Swami, "Joint design and separation principle for opportunistic spectrum access in the presence of sensing errors," *IEEE Trans. Inf. Theory*, vol. 54, no. 5, pp. 2053–2071, May 2008.
- [6] S. Geirhofer, L. Tong, and B. Sadle, "Cognitive medium access: Constraining interference based on experimental models," *IEEE J. Sel. Areas Commun.*, vol. 26, no. 1, pp. 95–101, Jan. 2008.
- [7] Q. Zhao, S. Geirhofer, L. Tong, and B. Sadler, "Opportunistic spectrum access via periodic channel sensing," *IEEE Trans. Signal Process.*, vol. 56, no. 2, pp. 785–796, Jan. 2008.
- [8] X. Li, Q. Zhao, X. Guan, and L. Tong, "Optimal cognitive access of markovian channels under tight collision constraints," vol. 29, no. 4, pp. 746–756, Apr. 2011.
- [9] D. Willkomm, S. Machiraju, J. Bolot, and A. Wolisz, "Primary users in cellular networks: A large-scale measurement study," in *IEEE New Frontiers in Dynamic Spectrum (DySPAN'08)*, Singapore, Oct. 2008, pp. 1–11.
- [10] A. P. Jardosh, K. N. Ramachandran, K. C. Almeroth, and E. M. Belding-Royer, "Understanding congestion in ieee 802.11b wireless networks," in *Proc. ACM SIGCOMM Workshops Conf. Comput. Commun.*, Philadelphia, PA, Aug. 2005, pp. 11–16.

Wireless Deterministic Medium Access: A Novel Concept Using Cognitive Radio

Dimitri Block

inIT, Institute of Industrial Information Technologies
Ostwestfalen-Lippe University of Applied Sciences
Lemgo, Germany
e-mail: dimitri.block@hs-owl.de

Uwe Meier

inIT, Institute of Industrial Information Technologies
Ostwestfalen-Lippe University of Applied Sciences
Lemgo, Germany
e-mail: uwe.meier@hs-owl.de

Abstract—The growing demand for coexistence of wireless systems in industrial automation applications must be met by a implementation of a deterministic medium access. Therefore, we propose a novel concept which is based on inter-system communication. It optimizes spectrum efficiency by handling resource reservations in the frequency and time domain. It is also aware of its environment by cooperatively mitigating interferences. Further, it requires only minor modifications of existing wireless solutions.

Keywords—deterministic medium access, cognitive radio, control channel, inter-system protocol

I. INTRODUCTION

The demand for wireless devices has been continuously growing in the last decades. Especially license-free bands such as the 2.4 GHz ISM band become more and more crowded. The range of application fields rises for wireless devices, too. Some application fields are mobile telephones, remote control, monitoring, notification services, Internet access and multimedia streaming. Many high data rate application demands will arise in the near future due to trends like the so called smart-phones. It creates a need for the coexistence of license-free bands.

The growing demand in consumer applications decreases the costs of standard components such as wireless transceivers. Thus, the number of wireless solutions increases also for industrial automation (IA) applications. Wireless solutions enable monitoring and controlling tasks for long distances and hard-to-reach locations. They also decrease the dependence on expensive, failure-prone wired connections and replace outwearing sliding contacts.

Wireless solutions are also enablers of new IA applications with even more challenging requirements for coexisting license-free bands. They require a deterministic medium access and data transmission behavior. However, currently the license-free bands do not guarantee any specific medium access.

In this work-in-progress paper, we propose a novel cognitive radio approach focusing on IA. The approach has mainly three goals:

- 1) To provide a deterministic medium access,
- 2) To apply only minor modifications to existing wireless solutions especially to all slave nodes, and

- 3) To be aware of its environment.

The first goal is necessary for IA applications to ensure real-time performance and reliable communication. In addition to IA applications, a deterministic medium access improves security application.

The second goal focuses on low implementation requirements. While only few devices require the usage of a new protocol, most devices do not need any additional functionality. They use their protocol-specific interference reporting functionality such as packet loss notification in a specific time slot and channel. Hence, most of the existing and widely used wireless systems only require an adaption of the master device such as an access point in case of an IEEE 802.11 system [1].

Finally, the approach targets environmental awareness – the third goal. Hence, it does not interfere with other detectable and predictable wireless systems but protects itself from being interfered. The interference mitigation is performed for several dimensions such as time, frequency and space.

The paper is structured as follows: Section II discusses the three categories of medium access methods: non-adaptive, adaptive and cognitive. In Section III the novel medium access method and its three components (the supervisor, the clients and the control channel) are introduced. Finally, Section IV discusses open issues and Section V concludes the paper.

II. MEDIUM ACCESS METHODS

The coexistence requirements for wireless communication raised the number of medium access methods (MAMs). There are

- Non-adaptive MAMs,
- Adaptive MAMs and
- Cognitive MAMs.

These are described in the following sections.

A. Non-adaptive Medium Access Methods

Non-adaptive MAMs are for example multiple access methods such as time-, frequency- and code-division multiple-access (TDMA, FDMA and CDMA) [2]. They do not include any mechanism to mitigate interference

but rely on central planning by a dedicated device or on manual configuration. Due to their synchronous structure, non-adaptive MAMs require only a little overhead of communication. In consequence, it is easy to implement and to provide a deterministic MAM. However, they do not adapt to the environment by ignoring interference but interfere with others. Due to such drawbacks it is advisable to use adaptive MAMs.

B. Adaptive Medium Access Methods

While non-adaptive MAMs represent straight forward approaches, adaptive MAMs are aware of the radio environment. They react to a feedback from the radio environment to mitigate packet loss. Such methods are for example ALOHA [3], carrier sense multiple access with collision avoidance (CSMA/CA e.g., applied in IEEE 802.11 DCF [1]) and adaptive frequency hopping (AFH e.g., applied in Bluetooth [4]).

Adaptive MAMs mitigate interference with others and ensure error-free transmission. On the other hand they have no deterministic behavior. Thus, adaptive MAMs require an overhead of communication and/or synchronization. For example in CSMA/CA the receiver has to wait for an unknown and random period of time for packet transmission.

Further, adaptive MAMs can be distinguished with respect to the moment of feedback: Listen before talk (LBT) and listen after talk (LAT) MAMs. LBT requires feedback before transmission. Such a MAM is for example CSMA/CA. It senses the channel before transmitting. Hence, if the channel is classified as idle a permission for packet transmission is provided. The adaption of LBT MAMs is based on the current state of the channel. If no new interference appears during transmission, LBT MAMs will ensure error-free transmission.

While LBT MAMs react on feedback before transmission, LAT MAMs adapt to new situations. This can be concluded from the evaluation of previous transmissions. In this context AFH is a good case in point. AFH is based on the spectrum spreading technique FHSS, which switches – called hopping – between multiple non-overlapping narrow-band frequency channels in a (pseudo) random manner. If there is a packet loss in a specific channel, AFH will block the channel for future use. The adaption of LAT MAMs basically depends on the state of the channel for previous transmissions. Therefore, LAT MAMs are not able to guarantee error-free transmission, even if no new interferences appear during data transmission.

C. Cognitive Medium Access Methods

Although adaptive MAMs improve the quality of transmission by mitigating interference, they suffer from the system centric approach and missing abilities to collaborate in any way with different systems. In consequence, adaptive

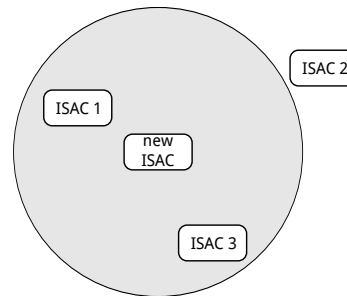


Figure 1. Example coverage range of the system "new ISAC"

MAMs are suboptimal for inhomogeneous radio environments. Collaboration would improve the efficient usage of spectrum, time and space. Further, collaboration reduces overlapping resource allocation.

MAMs which are aware of their environment – more than only by adaption – can be called cognitive MAMs. They are not limited to collaborative approaches. Cognitive MAMs in general adapt to the environment by sensing channels, predicting channel occupancy, negotiating sensing information and transmission parameters, and adequate tuning. Further, cognitive MAMs are able to adapt themselves flexibly in more than one dimension (e. g. time, frequency and space).

III. INTER-SYSTEM AUTOMATIC CONFIGURATION METHOD

We propose a novel MAM called inter-system automatic configuration MAM (ISAC MAM). The approach is operating between systems. A system is for example a wireless network based on IEEE 802.11 with one access point and several stations. For proper operation ISAC has to be supported by each system operating in the same frequency band.

Each system consists of several types of devices. From the ISAC MAM point of view, system devices are either ISAC supervisors or ISAC clients. An ISAC supervisor is a dedicated device which performs processes and negotiations. An ISAC client includes only minor supporting and adapting tasks. Each system must have one ISAC supervisor while having an unspecified number of ISAC clients. The communication between ISAC supervisors is done via a dedicated channel called ISAC control channel.

A. Supervisor

The most important device in an ISAC MAM system is the ISAC supervisor. It has two main tasks: (i) to handle resource allocation and (ii) to mitigate interferences. Resource allocation is performed by *resource allocation negotiation* and by *resource reversion negotiation*. In the following we discuss the tasks of an ISAC supervisor for an IEEE 802.11 (WLAN) system as example.

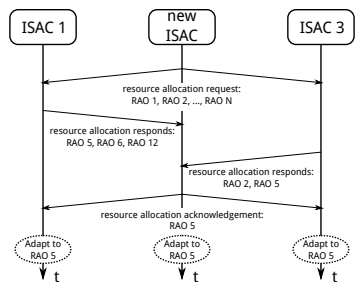


Figure 2. ISAC resource allocation negotiation

Table I
EXAMPLES OF RESOURCE ALLOCATION OPPORTUNITIES

Opportunity No.	Dimension	Unit	Type	Value
1	Frequency	MHz	Minimum	2402
	Frequency	MHz	Maximum	2422
	Time	%	Duty cycle	100
2	Frequency	MHz	Minimum	2407
	Frequency	MHz	Maximum	2427
	Time	%	Duty cycle	100

...

Resource Allocation Negotiation: If a new ISAC supervisor requires resources, it has to initiate a *resource allocation negotiation*. The negotiation principle is illustrated in Fig. 2.

First, the initiating ISAC supervisor has to broadcast a *resource allocation request*. This message also contains a list of resource allocation opportunities (RAO). The RAOs are limited in each dimension (see Table I). Each RAO is associated with a specific operation mode of that particular system. Hence, the RAO 1 is associated with WLAN channel 1 and RAO 2 with WLAN channel 2.

All ISAC supervisors in the coverage range (see Fig. 1) participate in the negotiation. After receiving the request, they check which RAOs are not conflicting with their own operation or to which RAOs their operation is able to adapt while proper operation will be guaranteed. The identifiers of the coexistence capable RAOs are sent to the initiating ISAC supervisor with the *resource allocation responds*.

After receiving all responds, the initiating ISAC supervisor has to choose the optimal RAO. An optimal RAO is permitted by all ISAC supervisors. The initiating ISAC supervisor broadcasts a *resource allocation acknowledgement* containing the identifier of the optimal RAO.

Finally, the initiating ISAC supervisor informs its own system about the optimal operation mode. If necessary, the other ISAC systems also adapt their operation mode. The chosen optimal RAO is considered allocated until it is reverted or until the associated ISAC supervisor is no longer accessible.

Resource Reversion Negotiation: If some resource allocation is no longer needed, an ISAC supervisor can revert the

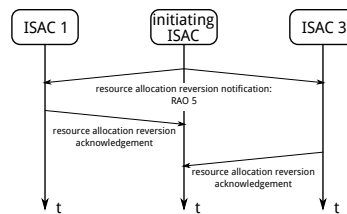


Figure 3. ISAC resource reversion negotiation

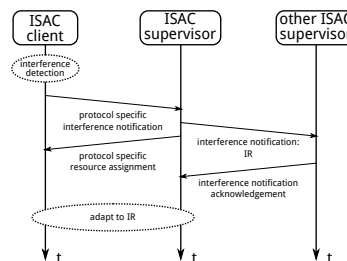


Figure 4. ISAC interference notification

allocation by performing a *resource reversion negotiation*. The principle is illustrated in Fig. 3.

The initiating ISAC supervisor broadcasts a *resource allocation reversion notification* containing the concerned RAO. The ISAC supervisors in the coverage range acknowledge the notification with a *resource allocation reversion acknowledgement*. Then the resource allocation is canceled and it is no longer considered allocated.

Interference Notification: The second main task of an ISAC supervisor is to mitigate interferences. The source of an interference may be an unknown wireless system. It may also be an ISAC system which is out of the ISAC supervisor’s coverage range, but close enough to disturb the communication of the ISAC system (see ISAC 2 in Fig. 1). An interference can be observed by the ISAC supervisor or even by an arbitrary ISAC client due to its cognitive features.

If an interference is observed, an ISAC system mitigates the interference and its ISAC supervisor informs other ISAC supervisors about the interference. This principle is displayed in Fig. 4. In case the ISAC client observes an interference, it informs the ISAC supervisor. This is done in the specific protocol used by the particular ISAC system (e. g. IEEE 802.11). The ISAC supervisor may detect an interference. Then the ISAC supervisor broadcasts an *interference notification*. The notification contains the interfered resources specification (IRS). IRSs use the same structure as RAOs but represent interfered resource specifications, which are also called black holes [5]. The notification is responded by an *interference notification acknowledgement*. Thus, if the informed ISAC supervisors want to allocate resources later on, they know the IRSs.

Additionally, the ISAC supervisors have to take care of their own system. Therefore the protocol specific adaptive

MAM is used. In our example the ISAC clients shall take care of the IRs by using CSMA/CA. In case some IRSs cannot be mitigated by protocol-specific adaptive MAMs, the ISAC supervisor has to initiate a *resource allocation negotiation*.

B. Client

An ISAC system contains one ISAC supervisor and an arbitrary number of ISAC clients. The ISAC clients do not use the control channel. Owing to the fact that they only have to communicate with the ISAC supervisor, the communication protocol is system-specific and therefore not part of this paper. Hence, in a WLAN ISAC system an arbitrary client communicates with its supervisor using IEEE 802.11 packet frames.

In order to detect interferences, ISAC clients should also be equipped with cognitive features. ISAC clients mainly have two tasks: (i) to adapt to resource assignment instructed by their ISAC supervisor and (ii) to inform their ISAC supervisor about interferences. While the first task is mandatory, the second one may be optional. These tasks have already been discussed in detail in the previous section.

C. Control Channel

The ISAC control channel is used for the communication between ISAC supervisors. Using a control channel is a well-known cognitive radio approach (see [6]). Therefore, the control channel is commonly reserved for ISAC supervisor communication. To guarantee proper operation the control channel always has to be available.

We consider that the ISAC control channel is in itself a specific wireless technology, although it is not necessary. In contrast to the conditions given in the context of wired communication, it is easy to setup such systems. They also allow for temporary radio systems such as adhoc inter-vehicular communication systems. However, the disadvantage is that the control channel might be temporarily not available, as in the case of non-deterministic interferences or due to degradation of radio propagation conditions. This problem can be solved by data redundancy and packet retransmissions.

While an ISAC system itself may use any specific protocol, the ISAC control channel uses a common protocol. The control channel also has to be a-priori known to avoid time-consuming discovery and synchronization techniques. Hence, the ISAC control channel cannot use cognitive MAMs.

Further, to enable fast varying network scenarios, the control channel itself cannot be managed in a centralized manner. For this reason, an optimal MAM is distributed and non-cooperative. Therefore, we suggest an adaptive MAM. To realize a non-cooperative approach LAT cannot be used. Thus, the optimal control channel is based on an adaptive MAM using LBT.

IV. CONCLUSION

In this paper, the growing demand for coexistence of wireless technologies, especially in license-free frequency bands, is met by the introduction of a new approach. The approach focuses on the requirements of industrial automation to ensure a deterministic medium access.

The approach handles inter-system reservation of resources such as frequency and time. In other words, it ensures efficient usage of available resources. In addition to resource reservation, it handles interference mitigation, cooperatively. Therefore, it is aware of the radio environment. Further, the approach brings only minor modifications to existing wireless solutions. Hence, the approach is also easy to implement.

The inter-system communication itself is performed via a fixed control channel. This control channel is also based on wireless communication. The control channel has to be constantly available. In some scenarios this could be a challenge. Further, we conclude that the optimal control channel shall use an adaptive medium access method of listen-before-talk type.

V. FUTURE WORK

This paper discusses a novel approach, which requires some future work. Most importantly, the protocol for the wireless communication of the control channel has to be specified. Further, sample implementations have to be provided and appropriate simulations have to be performed. The results shall be verified by measurements.

REFERENCES

- [1] "IEEE Standard for Information technology—Telecommunications and information exchange between systems Local and metropolitan area networks—Specific requirements Part 11: Wireless LAN Medium Access Control (MAC) and Physical Layer (PHY) Specifications," *IEEE Std 802.11-2012 (Revision of IEEE Std 802.11-2007)*, 29 2012.
- [2] T. Rappaport, *Wireless communications: principles and practice*. Publishing House of Electronics Industry, 2004.
- [3] N. Abramson, "The ALOHA System: Another Alternative for Computer Communications," in *Proceedings of the November 17-19, 1970, fall joint computer conference*. ACM, 1970, pp. 281–285.
- [4] "Bluetooth Core Specification v1.2," 2003.
- [5] S. Haykin *et al.*, "Cognitive radio: brain-empowered wireless communications," *IEEE journal on selected areas in communications*, vol. 23, no. 2, pp. 201–220, 2005.
- [6] J. Marinho and E. Monteiro, "Cognitive radio: survey on communication protocols, spectrum decision issues, and future research directions," *Wireless Networks*, vol. 18, no. 2, pp. 147–164, 2012.

Analytical Evaluation of Proactive Routing Protocols with Route Stabilities under two Radio Propagation Models

M. Umar khan, Imad Siraj, Nadeem Javaid
 Center for Advanced Studies in Telecommunication
 (CAST), COMSATS Institute of Information Technology
 Islamabad, Pakistan
 umar_khan, imadsiraj, njaved @comsats.edu.pk

Abstract— This paper contributes to modeling links and route stabilities in three diverse wireless routing protocols. For this purpose, we select three extensively utilized proactive protocols; Destination-Sequenced Distance Vector (DSDV), Optimized Link State Routing (OLSR) and Fish-eye State Routing (FSR). We also enhance the performance of these protocols by modifying default parameters. Optimization of these routing protocols are done via performance metrics, i.e., average Throughput, End to End Delay (E2ED) and Normalized Routing Load (NRL) achieved by them. Default routing protocols DSDV, OLSR and FSR are compared and evaluated with modified versions named as M-DSDV, M-OLSR and M-FSR using Network Simulator (NS2). Numerical Computations for Route Stabilities of these routing protocols through a mathematical modeled equation is determined and compared with simulation results. Moreover, all-inclusive evaluation and scrutiny of these proactive routing protocols are done under the MAC layer standards 802.11 DCF and 802.11e EDCF. In this way both Network and MAC layer exploration has been done under the performance metrics which gives overall performance and tradeoff with respect to full utilization of the available resources of Ad-hoc network high scalability scenario. Routing latency effects with respect to route stabilities and MAC layer standards 802.11 and 802.11e are compared and scrutinized with the tradeoff observed in throughput and in overhead (NRL) generated.

Keywords-802.11;802.11e;DCF;EDCF;MANETs;Ad-Hoc

I. INTRODUCTION

IEEE standard 802.11, at present, is a significant and trendy access methodology used in wireless communication. It enables speedy and straightforward design of network communication as a *de facto* MAC standard for LANs, WANs in Small Office Home Office (SOHO) or open-places and to the highest degree facilitated wireless access to the internet. Growing esteem of 802.11 standard, numerous services also improved and requirement for Quality of Service (QoS) become obvious. Hence, therapy to QoS setback in 802.11, enhanced version, i.e., 802.11e was anticipated [1]. IEEE standard 802.11e, i.e., EDCF (Enhanced Distributed Channel Function) defines numerous QoS parameters to IEEE standard 802.11 Distributed Coordination Function (DCF).

Conferring to 802.11 DCF, every station with a fresh data packet equipped to access transmission observers channel activity while waiting for an unused period comparable to a Distributed Inter- Frame Space (DIFS) is sensed and at that point the station transmits. Else, when channel is intuited busy, station initializes its back off timer and delays the

transmission access for arbitrarily chosen back off interval so to lessen aggregate of collisions.

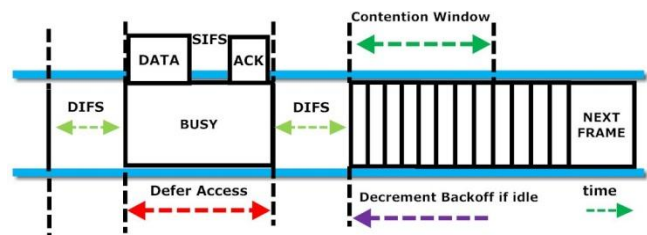


Figure 1. Basic Access Mechanism 802.11

The basic access mechanism is illustrated in the Fig.1. The EDCF, 802.11e standard announces service differentiation compared to the DCF standard 802.11 DCF by launching four access categories or classes (ACs) for data priorities [2,3]. Presuming QoS Stations (QSTAs) work under saturated or congested traffic, i.e., each QSTA has a data unit called as MAC Protocol Data Unit (MPDU) to correspond later while closing all succeeded transmissions [4]. Standard 802.11e methodology is formulated on four Access Categories (ACs); 1. Voice, 2. Video, 3. Best Effort, 4. Background.

Rest of the paper is organized as follows. Section II contains brief description of proactive protocols in ad-hoc networks. Related work and shortcomings from previous work can be found in Section III. Section IV determines the route scalabilities with the proposed mathematical equation. Simulation result analysis has been done in Section V and finally conclusion with some insight of future work is discussed in Section VI.

II. PROACTIVE PROTOCOLS IN AD-HOC NETWORK

DSDV [5], FSR [6] and OLSR [9] which are proactive in nature are table driven protocols. They update their routing table periodically without demand, so issue of extra band width utilization occurs. Several methods are designed to compensate this problem. In the Low Scalability region, all three protocols perform well, but when we take a look at Medium Scalability region OLSR has better performance. This makes this standard efficient by checking the medium state more rapidly than 802.11. In this way, time consumed for accessing the medium is decreased and more enhanced Throughput is achieved in shorter time than

that in 802.11 DCF. The enhanced version 802.11e EDCF provides small Contention Window (CW) size which helps to access the medium more immediately than in 802.11e EDCF.

A. Proactive Protocols in Brief

The three extensively utilized protocols in Ad-hoc Networks that we considered Destination Sequenced Distance Vector (DSDV) [5], Fish-eye State Routing (FSR) [6], [7] and Optimized Link State Routing (OLSR) [8], [9], are proactive in nature. Altogether, these three proactive protocols practice hop-by-hop routing scheme designed for packet forwarding. In DSDV, packets are disseminated and then path is calculated by Distributed Bellman Ford (DBF) algorithm. In FSR, DBF algorithm is utilized for path calculation. The nodes keep up a table carrying link state information constructed on fresh statistics acknowledged via adjacent nodes. In addition, nodes occasionally interchange it with confined neighbors. Path calculation mechanism in OLSR is carried out through Dijkstra’s algorithm [9]. Proactive routing protocols in brief with their features are given below in Table I.

TABLE I. PROACTIVE FEATURES IN BRIEF

Features	DSDV	OLSR	FSR
Path Calculation	DBF Algo	Dijkstra’s Algo	DBF Algo
Flooding Control Mechanism	Exchange topology info with neighbors	Broadcast via selected MPRs	Graded Frequency mechanism
Overhead Reduction	Incremental updates	MPRs	Fish-eye technique
Packet Forwarding	Hop by Hop routing	Hop by Hop routing	Hop by Hop routing
Special Features	Route Settling Time	MPRs	Multi-Scope Routing

III. RELATED WORK AND SHORTCOMINGS

After the extensive research concerning to our contribution, we have summarized the previously done work and its shortcomings with the help of Tables VI and VII.

IV. MODELING ROUTE STABILITIES

Modeling Route Stabilities of these three proactive routing protocols are determined depending upon their broadcast time interval T_{Bi} . Numerical computation is carried out for each proactive routing protocols. Route stabilities are determined using the following equation (1). Suppose, we have two nodes na and nb . Node na transmits a packet at time t_j which is received by nb at time t_k . Link stability at node nb , for link l , at time t_k , for a particular broadcast interval T_{Bi} with respect to certain routing protocol parameters, $Stability_{nb}^l(t_k)$ can be defined as follows:

$$Stability_{nb}^l(t_k) = \frac{t_k(na) - t_j(na)}{T_{Bi}} \quad (1)$$

The above equation is accompanied by the following constraints:

- (i) $\forall k > 0$
- (ii) $T_{Bi} \neq 0$
- (iii) $0 < T_{Bi} < 1$ (Ideal Situation)
- (iv) $Stability_{nb}^l(t_k) < T_h$, where T_h is a threshold value defined through specific parameter which varies from protocol to protocol.

A. DSDV Route Stabilities

In case of Trigger Updates between active links, T_{Bi}^{DSDV} varies according to state of the link. When link breaks, trigger messages are sent by the respective node by increasing NRL.

For $T_{Bi} = 0.01$, $T_h \leq 5$ and for $T_{Bi} = 0.07$, $T_h \leq 0.71$, so $0.1 \leq T_{Bi} \leq 0.7$

TABLE II. NUMERICAL COMPUTATIONS FOR DSDV

Parameters	Default Value	Modified Value
$T_{Bi}(s)$.0588	0.1176
$T_h \leq$	0.85	0.425
Stability	0.017	0.0085

B. OLSR Route Stabilities

TABLE III. NUMERICAL COMPUTATIONS FOR OLSR

Parameters	Inner Scope		Outer Scope	
	Default Value	Modified Value	Default Value	Modified Value
TTL	2	2	255	255
$T_{Bi}(s)$	5s	1s	15s	3s
$T_h \leq$	0.01	0.05	0.0033	0.016
Stability	0.00002	0.001	0.00006	0.003

C. FSR Route Stabilities

TABLE IV. NUMERICAL COMPUTATIONS FOR FSR

Parameters	TC Messages		Hello Messages	
	De-fault Value	Modified Value	De-fault Value	Modified Value
$T_{Bi}(s)$	5s	3s	2s	1s
$T_h \leq$	0.01	0.016	0.025	0.05
Stability	0.0002	0.0003	0.0005	0.001

TABLE V. SIMULATION PARAMETERS

Parameters	Values	Parameters	Values
Bandwidth	2Mb	Simulation Time	900 sec
Packet size	1000 B	Interface Queue	50
Speed	15 m/s	Channel Type	Wireless
Traffic type	UDP, CBR	Nodes	10 - 100

TABLE VI. RELATED WORK AND SHORTCOMINGS

Related Work	Scalability (Nodes)	Performance Metrics	MAC Layer Standard Reasoning	Modified Parameters and Modeling Route Stabilities
In [10] Samar R Das <i>et al</i>	30 & 60	Throughput, E2ED, NRL	Not Considered	NOT CONSIDERED
In [11] Bianchi <i>et al</i>	50	other	Not Considered	
In [12] Daneshgram <i>et al.</i>	20	Throughput, E2ED, NRL	802.11	
D. Malone <i>et al.</i> [2] & Engelstad <i>et al.</i> [3]	20	other	802.11/802.11e	

TABLE VII. RESULTS AND MODIFICATIONS

Our Work	Scalability (Nodes)	Performance Metrics	MAC Layer Standard Reasoning	Modified Parameters and Modeling Route Stabilities
	10 to 100	Throughput, E2ED, NRL	802.11/802.11e	Modification in Default Parameters of Protocols and Mathematical Modeling is done

V. SIMULATIONS AND RESULTS

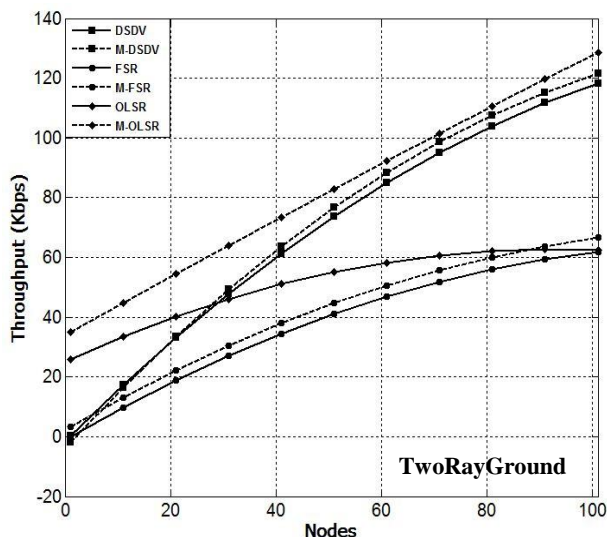


Figure 2. Throughput 802.11 DCF

In high scalabilities, (Fig. 2 and Fig. 3) MPR techniques achieve more optimization and efficiency, therefore both OLSR and M-OLSR overall produce high throughput among selected proactive protocols. After modification in all of three chosen protocols, OLSR produces the highest throughput both in DCF and EDCF. It is because of the frequent updating of routing messages that results in stabilized MPRs. DSDV achieves the second highest average throughput in DCF and EDCF as compared to the rest of two selected routing protocols. The reason for high efficiency of DSDV is due to incremental updates which are generated in case of any change in links of active routes.

But in high scalabilities it fails to converge because the exchange of routing messages through flooding cause more overhead, and in high densities the rate of change is increased, thus causes more drop rates. On the other hand, OLSR’s throughput is more in high scalabilities of 80 nodes, 90 nodes and 100 nodes because MPRs provide more optimizations in high densities.

However, FSR use only periodic updates for link status monitoring and route updating. It is more suitable for hundreds and thousands of nodes, because fish-eye scopes with graded frequency mechanisms are best suited in very high densities. Frequent routing updating in FSR by reducing inner-scope and outer-scope intervals augments more throughputs in FSR-M as compared to FSR, but FSR-M fails to converge in EDCF comparative to that of FSR. Whereas, increasing the interval of triggered update generation in DSDV-M increase throughput in EDCF while in DCF.

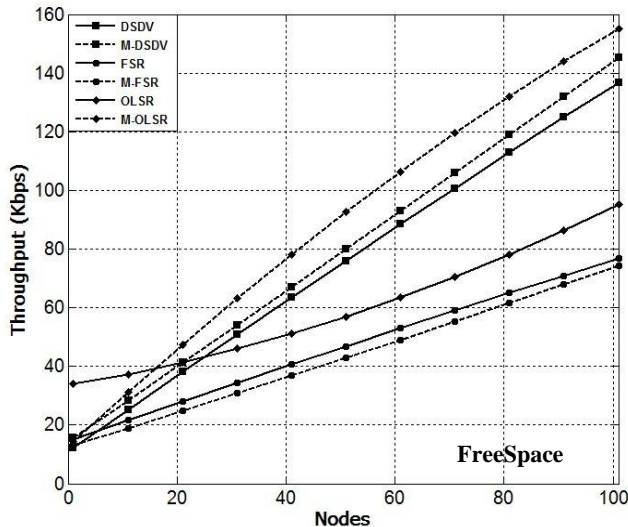


Figure 3 Throughput 802.22 EDCF

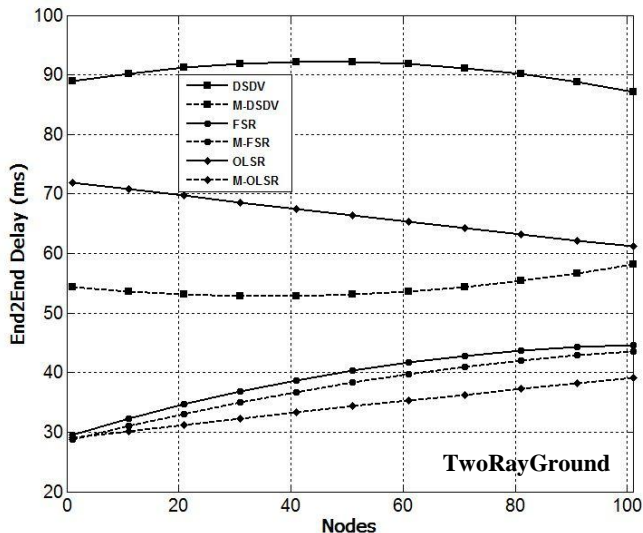


Figure 4. End2End Delay 802.11 DCF

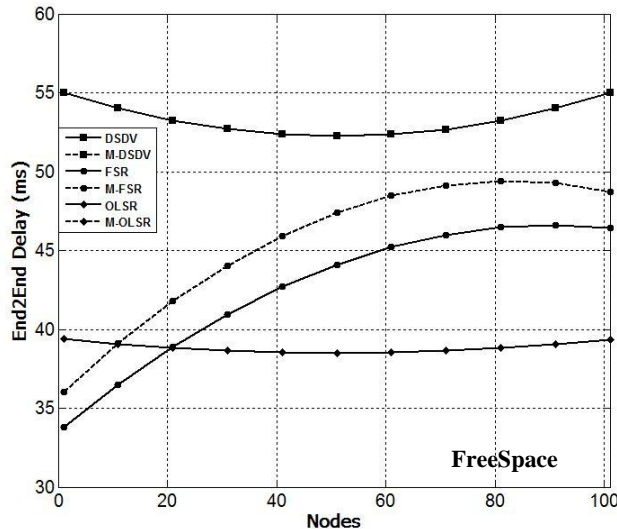


Figure 5. End2End Delay 802.11 EDCF

In Fig. 4 and Fig. 5, E2ED of selected routing protocols is less in EDCF as compared to DCF due to efficient stability checking of link in EDCF comparative to DCF. FSR attains the lowest routing latency in DCF as compared to DSDV and OLSR. Pure proactive approach route updating keeps overall routing latency low in FSR. Although in DSDV data remains for the time required for route settling to maintain correct information of routes before sending it to the destination, but this route settling time augments the delay. Whereas, DSDV produces the highest delay, moreover, it does not optimize network wise broadcasting (in DSDV exchange of routing messages is only performed through flooding, as compared to MPRs of OLSR which reduce number of retransmissions and scope updates of FSR by using graded frequency mechanism).

DSDV-M has less routing latency as compared to DSDV in case of DCF. While DSDV-M and DSDV possess equal routing delay in EDCF, because efficient mechanism of 802.11e EDCF helps to reduce E2ED. Same is the case of OLSR, where OLSR-M achieves lowest delay as compared to OLSR in EDCF, while this delay is more in DCF. As FSR-M's periodic intervals for scope routing are reduced, therefore it attains low E2ED in both DCF and EDCF. Moreover it does not update routing information instantly after detection of any change in the network unlike DSDV and OLSR; therefore, EDCF mechanism does not effect too much to improve its performance.

All selected routing protocols have attained high NRL referring to Fig. 6 and Fig. 7 after modifications. The rate for successive routing messages exchange is highest in OLSR as compared to the rest of the protocols (clearly mentioned in the table), therefore it generates high routing load. As FSR does not trigger any routing messages in case of link breakage and relies only on periodic updating, thus it produces lowest NRL in DCF. Furthermore, DSDV produces lowest routing messages in case of EDCF as compared to OLSR and FSR as shown in Fig. 6, because the efficient information of link connectivity reduces incremental updates. TTL value in ring search algorithm increases while increase in network density is observed, this leads to increase in broadcast routing packets during route discovery as increasing NRL behavior in FSR.

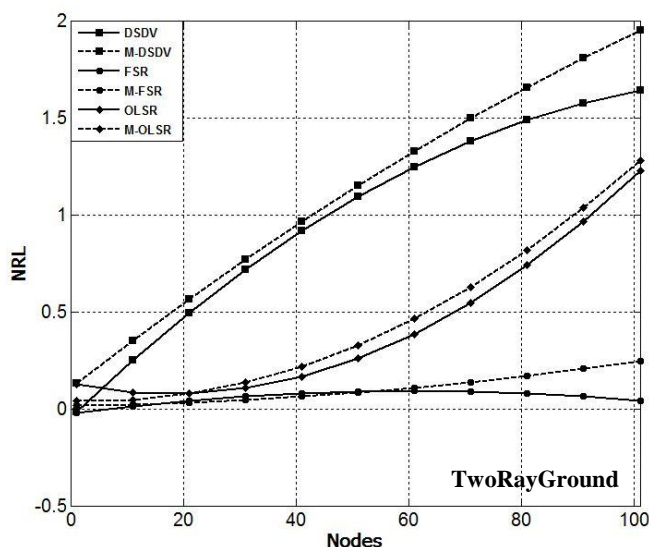


Figure 6. NRL 802.11 DCF

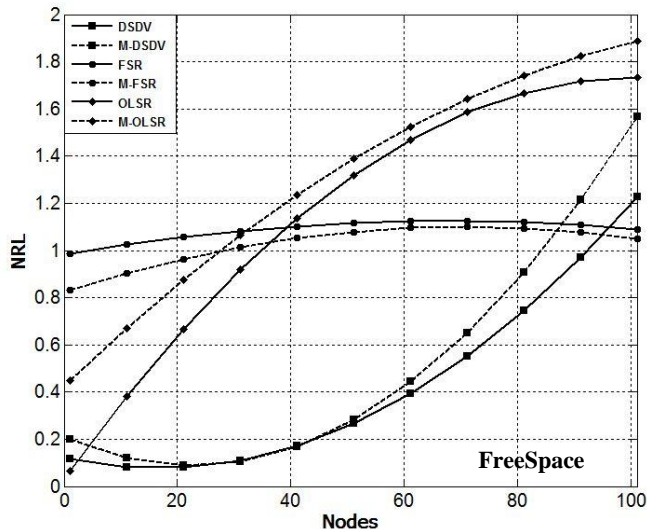


Figure 7. NRL 802.11 EDCF

TABLE VII. DEFAULT AND MODIFIED PARAMETERS

Protocols	Default Parameters	Modified Parameters
DSDV	$T_{bi} = 15 \text{ s}$ or $8/15 = .0588 \text{ s}$	$T_{bi} = 10 \text{ s}$ or $.1176 \text{ s}$
OLSR	TC_Messages = 5 s Hello_Messgaes = 2 s	TC_Messages = 3 s Hello_Messgaes = 1 s
FSR	$T_{bi} = 5 \text{ s}$	$T_{bi} = 1 \text{ s}$

Performance Trade-offs of three proactive routing protocols; DSDV, OLSR and FSR as shown in Fig. 7 according to three performance metrics carried out on the basis of simulation results analysis. DSDV achieves enhanced and high throughput with trade-off between E2ED but reduction in routing overhead is observed using incrementals. OLSR outperforms as concerned to its lowest E2ED observed with the increase in throughput and normalized routing load. FSR produces more normalized routing load with a minimum trade-off between other two performance metrics, i.e., throughput and E2ED.

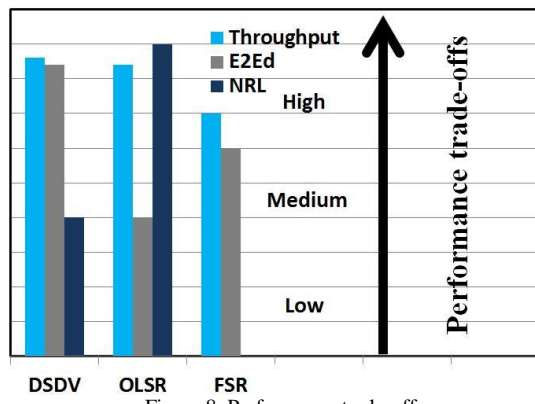


Figure 8. Performance trade-offs

VI. CONCLUSION AND FUTURE WORK

In this paper, we have estimated and matched the performance of three extensively utilized proactive protocols; DSDV, OLSR and FSR. Total normalized routing load achieved by a protocol which is centered upon two changing aspects; control traffic produced by control packets and data traffic accelerated over and done with routes of non-optimal path lengths. Consequently, for evaluating the route stabilities of these protocols in dense networks and with different broadcast intervals of each routing protocol; we have varied different scalability scenarios. In lieu of analysis, three performance parameters; E2ED, NRL and throughput are worked out by using NS-2. In conclusion, we perceived that OLSR is additionally scalable for the reason of bargain in routing overhead due to MPRs and lowest E2ED, as OLSR permits retransmission via MPRs. On the other influence, FSR is supplementary appropriate for extraordinary network loads owed to scope routing over GF (no flooding), that decreases broadcasting storm, as a result it saves additional bandwidth and accomplishes high throughput when data traffic upturns in high scalabilities.

In the future, we are concerned to evaluate reactive routing protocols under same scalability scenarios, but with varying mobilities and under route stabilities computed using the equation proposed in (1).

REFERENCES

- [1] Peter Clifford, et al., "Modeling 802.11e for data traffic parameter design," Hamilton Institute, Ireland, 2008.
- [2] D. Malone, et al., "Modeling the 802.11 distributed coordination function in non-saturated heterogeneous conditions," IEEE/ACM Transactions on Networking, 2007.
- [3] P.E. Engelstad, et al., "Non-saturation and saturation analysis of IEEE 802.11e EDCA with starvation prediction," ACM International Symposium, 2005.
- [4] J. Hu, et al., "A comprehensive analytical model for IEEE 802.11e QoS differentiation schemes under unsaturated traffic loads, in: Proceedings of the ICC08," 2008.
- [5] C. E. Perkins and P. Bhagwat, "Highly dynamic Destination-Sequenced Distance-Vector routing (DSDV) for mobile computers," SIGCOMM Comput. Commun. Rev, vol. 24, pp. 234-244, 1994.
- [6] G. Pei, et al., "Fisheye State Routing in Mobile Ad Hoc Networks," in ICDCS Work-shop on Wireless Networks and Mobile Computing, 2000, pp. D71-D78.
- [7] M. Gerla, et al., IETF Draft-01, "Fisheye State Routing Protocol (FSR) for Ad Hoc Networks," 2000.
- [8] T. Clausen and P. Jacquet, "Optimized Link State Routing Protocol (OLSR)," 2003.
- [9] T. Clausen and P. Jacquet, IETF RFC-3626, "Optimized Link State Routing Protocol OLSR," The Internet Society <http://www.ietf.org/rfc/rfc3626.txt>, 2003.
- [10] Samir R. Das, et al., "Simulation-based performance evaluation of routing protocols for mobile ad hoc networks".
- [11] G. Bianchi, Performance analysis of the IEEE 802.11 distributed coordination function, IEEE Journal on Selected Areas in Communications 18 (3) (2000).
- [12] F. Daneshgaran, et al., "Unsaturated throughput analysis of IEEE 802.11 in presence of non-ideal transmission channel and capture effects," IEEE Transactions on Wireless Communications 7 (4) (2008) 12761286

A Quantization Scheme based on Kullback-Leibler Divergence for Cooperative Spectrum Sensing in Cognitive Radio

Hiep Vu-Van
The School of Electrical Engineering
University of Ulsan
Ulsan, Republic of Korea
Email: vvhiep@gmail.com

Insoo Koo
The School of Electrical Engineering
University of Ulsan
Ulsan, Republic of Korea
Email: iskoo@ulsan.ac.kr

Abstract—Cognitive radio (CR) is one of the most promising next-generation communication systems due to its ability to improve spectrum utilization by the detection and the use of vacant channels of licensed users. Reliable detection of the licensed user signal is a pre-requirement for avoiding interference to the licensed user in a CR network. Cooperative spectrum sensing (CSS) is able to offer AN improved sensing performance compared to individual sensing. However, in CSS transmission of raw data from cognitive user (CU) to the fusion center (FC) requires large bandwidth of control channel, long latency and high consumption power. A quantization scheme, in which the raw data can be quantized with few bits at the CU and then be reported to the FC, can solve these problems of raw data transmission. In this paper, we proposed a quantization scheme based on Kullback-Leibler (KL) Divergence for reducing the number of quantization bits while keeping the similar sensing performance to the case that raw sensing data are used. Through simulation, it shown that the proposed scheme can achieve better sensing performance than that of uniform quantization scheme.

Keywords-cognitive radio; quantization; Kullback-Leibler Divergence; cooperative spectrum sensing.

I. INTRODUCTION

Recently, additional bandwidth and higher bitrates have been required in order to meet the users demands in wireless communication systems. As a result, available frequency bands have become a scarce resource. However, according to the Federal Communications Commissions spectrum policy task force report [1], actual utilization of the licensed spectrum varies from 15% to 80%. Cognitive radio technology [2] has been proposed to solve the problem of ineffective utilization of spectrum bands. The scarcity of spectrum bands can be relieved by allowing some CUs to opportunistically access the spectrum assigned to the Primary user (PU) whenever the channel is free. However, CUs must vacate their frequency when the presence of a PU is detected. Therefore, reliable detection of the PU signal is an essential requirement of CR networks.

To ascertain the presence of a PU, CUs can use one of several common detection methods, such as matched filter, feature, and energy detection methods [2], [3]. Energy

detection is the optimal method if the CR user has limited information about a PU signal (e.g., only the local noise power is known) [3]. With energy detection, the frequency energy in the sensing channel is received in a fixed bandwidth, W , over an observation time window, T , in order to compare with the energy threshold and determine whether or not the channel is being utilized. However, the received signal energy may severely fluctuate due to multipath fading and shadowing effects; therefore, it is difficult to obtain reliable detection with only one CR user. Fortunately, improved usage detection can be obtained by allowing some CR users to perform Cooperative Spectrum Sensing (CSS) [4].

In CSS, a quantization scheme can help to reduce the overhead in the control channels which is mainly due to transmission of raw data from CUs and the FC. KL-divergence theory often uses as a measure of the (dis)similarity between two distributions [5]. Subsequently, KL-divergence can be used to measure reliability of sensing information in CSS. In this paper, therefore we proposed a quantization scheme based on KL-divergence theory for CSS in CR network, in which KL-divergence is used as a reliable level of sensing data to decide boundary points for quantization scheme.

In particular, in Section II, we describe system model of the proposed scheme. In Section III, we present detail of the proposed quantization scheme based on KL-divergence. In Section IV, simulation results are shown for evaluating performance of the proposed scheme. Finally, we conclude the paper in Section V.

II. SYSTEM MODEL

We consider a CR network composed of N CR users and one PU. All of the CR users use energy detectors to detect the presence of the PU signal. In order to perform CSS, sensing information will be quantized at CUs and after that they will be reported to the Fusion Center (FC) through a control channel. At the FC, all quantization levels obtained from the CUs will be combined to make a global decision concerning about the presence or absence of the PU signal by using equal gain combination (EGC) rule.

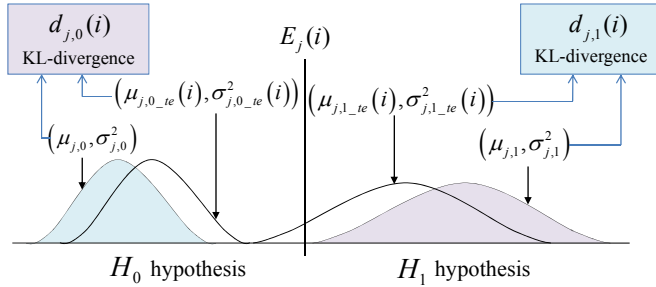


Figure 1. KL-divergences according to the presence or absence hypothesis of PU signal.

The received signal of a CU under absence and presence hypothesis of PU signal can be formulated as follows:

$$\begin{cases} H_0 : x_j(k) = n_j(k) \\ H_1 : x_j(k) = h_j s(k) + n_j(k) \end{cases} \quad (1)$$

where H_0 and H_1 correspond to the hypothesis of the absence and presence, respectively, of the PU signal, $x_j(k)$ represents the signal received by the j^{th} CU, h_j denotes the amplitude gain of the channel, $s(k)$ is the signal transmitted from the PU, and $n_j(k)$ is the additive white Gaussian noise.

At the i^{th} sensing interval for the j^{th} CU, the received signal energy, $E_j(i)$, is given as

$$E_j(i) = \begin{cases} \sum_{k=k_i}^{k_i+M-1} |n_j(k)|^2, & H_0 \\ \sum_{k=k_i}^{k_i+M-1} |h_j x(k) + n_j(k)|^2, & H_1 \end{cases} \quad (2)$$

where M is the number of samples over one sensing interval, and k_i is the time slot at which the i^{th} sensing interval begins. When M is relatively large (e.g. $M > 200$), E_j can be closely approximated as a Gaussian random variable under both hypotheses such that

$$E_j \sim \begin{cases} N(M, 2M), & H_0 \\ N(M(\gamma_j + 1), 2M(2\gamma_j + 1)), & H_1 \end{cases} \quad (3)$$

where γ_j is the SNR of the channel between the PU and the j^{th} CU.

III. THE PROPOSED QUANTIZATION SCHEME BASED ON KULLBACK-LEIBLER DIVERGENCE FOR COOPERATIVE SPECTRUM SENSING

A. Kullback-Leibler Divergence

The KL-divergence [5] is also known as the relative entropy between two probability density functions, $f(x)$ and $g(x)$, such that

$$D(f \| g) = \int f(x) \log \left[\frac{f(x)}{g(x)} \right] dx \quad (4)$$

It is obvious that the KL-divergence is always non-negative. Also, it is zero if and only if the two distributions coincide. KL-divergence is often used as a measure

of the (dis)similarity between two distributions. The KL-divergence between two normal distributions with means and variance as $f \sim (\mu_f, \sigma_f^2)$ and $g \sim (\mu_g, \sigma_g^2)$ respectively, can be obtained such that [6]

$$\begin{aligned} D(f \| g) &= D(\mu_f, \mu_g, \sigma_f^2, \sigma_g^2) \\ &= \frac{1}{2} \left[\log \left(\frac{\sigma_g^2}{\sigma_f^2} \right) - 1 + \frac{\sigma_f^2}{\sigma_g^2} + \frac{(\mu_f - \mu_g)^2}{\sigma_g^2} \right] \end{aligned} \quad (5)$$

B. The Proposed Quantization Scheme based on Kullback-Leibler Divergence

Since KL-divergence is a useful tool to measure the (dis)similarity between two distributions, it can be a suitable measurement for reliability of sensing information (e.g. received signal energy) in spectrum sensing. Subsequently, KL-divergence will be utilized to decide quantization boundary for sensing information in CU.

Firstly, based on current received signal energy, the “temporary mean” and “temporary variance” of received signal energy under H_0 , $\mu_{j,0-te}(i)$ and $\sigma_{j,0-te}^2(i)$, or H_1 , $\mu_{j,1-te}(i)$ and $\sigma_{j,1-te}^2(i)$, hypothesis of the PU signal will be calculated as follows, respectively:

$$\begin{cases} \mu_{j,0-te}(i) = \frac{m-1}{m} \mu_{j,0} + \frac{1}{m} E_j(i) \\ \sigma_{j,0-te}^2(i) = \frac{m-1}{m} \sigma_{j,0}^2 + \frac{m-1}{m^2} [E_j(i) - \mu_{j,0}]^2, \end{cases} \quad (6)$$

$$\begin{cases} \mu_{j,1-te}(i) = \frac{m-1}{m} \mu_{j,1} + \frac{1}{m} E_j(i) \\ \sigma_{j,1-te}^2(i) = \frac{m-1}{m} \sigma_{j,1}^2 + \frac{m-1}{m^2} [E_j(i) - \mu_{j,1-te}]^2, \end{cases} \quad (7)$$

where $\mu_{j,0}$, $\sigma_{j,0}^2$ and $\mu_{j,1}$, $\sigma_{j,1}^2$ are the means and variances of the received signal energy of the j^{th} CR user under H_0 and H_1 hypothesis of the PU signal respectively, and m is the pre-defined constant that represents the “effecting level” of the current received signal energy to its mean and variance. Based on numerical experiments, it is observed that the value of m should be chosen from 20 to 50 for keeping the accuracy of the sensing performance.

The KL-divergences will be calculated between the PDF and temporary PDF (with temporary mean and variance) of the received signal energy of each CR user under the presence or absence hypothesis of the PU signal, denoted as $d_{j,1}(i)$ and $d_{j,0}(i)$, respectively. Base on Eqn. (5), we are able to define

$$\begin{aligned} d_{j,0}(i) &= D[\mu_{j,0-te}(i), \mu_{j,0}, \sigma_{j,0-te}^2(i), \sigma_{j,0}^2] \\ d_{j,1}(i) &= D[\mu_{j,1-te}(i), \mu_{j,1}, \sigma_{j,1-te}^2(i), \sigma_{j,1}^2] \end{aligned} \quad (8)$$

Fig. 1 shows an example of KL-divergence calculations of a CU.

Here, we define the “extended KL-divergence” as follows

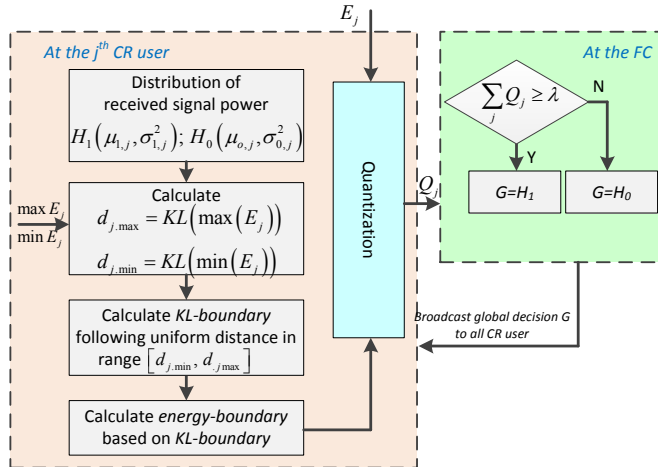


Figure 2. Flow-chart of the proposed scheme.

$$\begin{aligned} d_j(i) &= d_{j,0}(i) - d_{j,1}(i) \\ &= KL[E_j(i), \mu_{j,0}, \sigma_{j,0}^2, \mu_{j,1}, \sigma_{j,1}^2] \end{aligned} \quad (9)$$

It can be seen that $d_j(i)$ can obtain higher value when the value of $d_{j,1}(i)$ is smaller and the value of $d_{j,0}(i)$ is higher. It means that if the value of $d_j(i)$ is higher, the current received signal energy $E_j(i)$ will “near” H_1 distribution than H_0 distribution. In contrary, if the value of $d_j(i)$ is smaller, the current received signal energy $E_j(i)$ will “near” H_0 distribution than H_1 distribution. Subsequently, $d_j(i)$ can represent for reliable level of the sensing information, e.g. with higher absolute value of $d_j(i)$, we have more reliable sensing information.

We propose a quantization scheme based on the “extended KL-divergence” of which flow-chart is shown in Fig. 2.

At the first state, the values range of $d_j [d_{j,\min}, d_{j,\max}]$ will be splitted into 2^{Nb} equal parts by $(2^{Nb} + 1)$ “KL-boundary” poits, Bd_j , as

$$Bd_j(n) = d_{j,\min} + \frac{n-1}{Nb} (d_{j,\max} - d_{j,\min}) \quad (10)$$

where $n = 1, \dots, 2^{Nb} + 1$, Nb is number of quantization bits, $d_{j,\max} = KL(\max E_j)$ and $d_{j,\min} = KL(\min E_j)$. At the first sensing interval, the maximum value, $\max E_j$, and minimum value, $\min E_j$, of received signal energy of the j^{th} CU can be set as $(\mu_{j,1} + \sigma_{j,1})$ and $(\mu_{j,0} - \sigma_{j,0})$ respectively. After that, they are updated based on the real received signal energy, that is, if the current received signal energy is higher than $\max E_j$, $\max E_j$ will be set to be equal to the current received signal energy. On the other hand, if the current received signal energy is smaller than $\min E_j$, $\min E_j$ will be set to be equal to the current received signal energy.

For the next state, the “energy-boundary” will be calculated according to the values of “KL-boundary” as follows:

$$BE_j(n) = KL^{-1}(Bd_j(n)) \quad (11)$$

Based on “energy-boundary”, each CU quantizes the received signal energy and reports quantization level to the FC. We define $u_j(i)$ as the quantization decision and $E_j(i)$ as the quantization input. The quantization process $Q(\cdot)$ can be expressed as

$$\begin{aligned} u_j(i) &= Q(E_j(i)) \\ &= m \text{ if } E_j(i) \in \Delta_j(m), m = 1, 2, \dots, 2^{Nb} \end{aligned} \quad (12)$$

where $\Delta_j(m) = [BE_j(m), BE_j(m+1))$.

At the FC, all quantization levels received from CUs will be combined to make a global decision concerning about the presence or absence of the PU signal by using equal gain combination rule (EGC) as

$$\begin{cases} G(i) = 1, & \text{if } \sum_j u_j(i) \geq \lambda \\ G(i) = 0, & \text{if otherwise} \end{cases} \quad (13)$$

where λ is the threshold for global decision.

IV. SIMULATION RESULTS

We consider a CR network with $N = 20$ CUs, in which all CUs have the same SNR = -15dB. As references, sensing performances of following CSS scheme are provided: EGC with raw sensing information (denoted as EGC-raw data), EGC with the proposed quantization scheme (denoted as EGC-the proposed scheme) and EGC with the uniform quantization scheme (denoted as EGC-uniform quantization).

Fig. 3 illustrates the ROC curves of the proposed scheme and the considered comparison schemes. The figure shows that EGC-the proposed scheme with 3bits can obtain the similar sensing performance to EGC-raw data. On the other

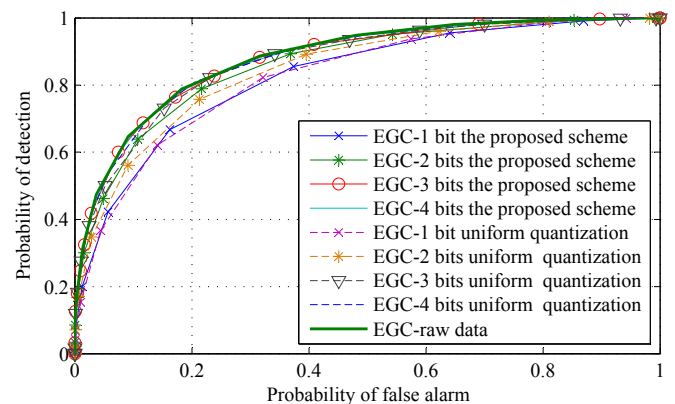


Figure 3. ROC curves of cooperative spectrum sensing when SNR of all CUs are given as -15dB.

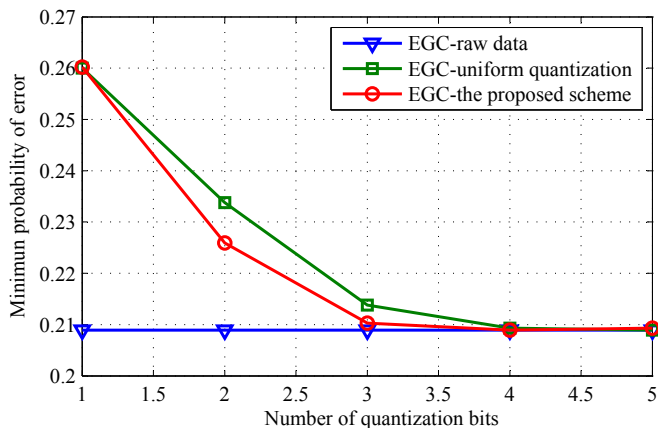


Figure 4. Minimum probability of error of cooperative spectrum sensing when SNR of all CUs are given as -15dB.

hand, EGC-uniform quantization needs 4 bits to achieve the similar performance.

Fig. 4 shows the minimum probability of error of the proposed scheme and above reference schemes, where probability of error is defined as:

$$P_e(\lambda) = P_f(\lambda) \Pr(H_0) + P_m(\lambda) \Pr(H_1) \quad (14)$$

where $P_f(\lambda)$ and $P_m(\lambda)$ are probability of false alarm and probability of miss detection of the global decision, respectively. Since $P_f(\lambda)$ and $P_m(\lambda)$ are function of λ , $P_e(\lambda)$ is also a function of λ . We define λ_{opt} as the optimal threshold at the FC with which probability of error of global decision is minimized. Subsequently, minimum probability of error can be given as $P_{e.min} = P_e(\lambda_{opt})$. Fig. 4 shows the effect of the quantization bits on the minimum probability of error. From Fig. 4, we can observe that the EGC-the proposed scheme can achieve same performance to that of EGC-raw data with more than 3 quantization bits while the EGC-uniform quantization requires more than 4 quantization bits to achieve same performance.

V. CONCLUSION

In this paper, we have proposed a quantization scheme based on KL-divergence for cooperative spectrum sensing in CR network. The proposed scheme can reduce the necessary quantization bits comparison with the uniform quantization scheme while still keeping the same sensing performance with the raw data.

ACKNOWLEDGEMENT

“This research was supported by Basic Science Research Program through the National Research Foundation of Korea (NRF) funded by the Ministry of Education, Science and Technology (NRF-2012R1A1A2038831)”

REFERENCES

- [1] *Spectrum Policy Task Force report*, technical report 02-135, Federal Communications Commission, 2002.
- [2] Y. Hur, J. Park, W. Woo, K. Lim, C. H. Lee, H. S. Kim, and J. Laskar, “A wideband analog multi-resolution spectrum sensing (MRSS) technique for cognitive radio (CR) systems,” in Proc. IEEE Int. Symp., Circuit and System, Greece, pp.4090-4093, 2006.
- [3] A. Sahai, N. Hoven, and R. Tandra, “Some fundamental limits on cognitive radio,” in Proc. Allerton Conf. on Communications, control and computing, Monticello, pp.1-11, 2004.
- [4] G. Ganesan and Y. G. Li, “Cooperative spectrum sensing in cognitive radio networks,” in Proc. IEEE Symp., New Frontiers in Dynamic Spectrum Access Networks (DySPAN05), Baltimore, USA, pp.137-143, 2005.
- [5] F. Mosteller and J. W. Tukey, *Data Analysis and Regression: A Second Course in Statistics*. Reading, MA: Addison-Wesley.
- [6] J. R. Hershey and P. A. Olsen “Approximating the kullback leibler divergence between gaussian mixture models,” In IEEE International Conference on Acoustics, Speech and Signal Processing, volume 4, pp.IV317-IV320, 2007.